IN VIVO NONINVASIVE MOUSE MODEL OF LOAD INDUCED OSTEOARTHRITIS

A Dissertation

Presented to the Faculty of the Graduate School

of Cornell University

In Partial Fulfillment of the Requirements for the Degree of

Doctor of Philosophy

by

Frank Changburm Ko

May 2014

IN VIVO NONINVASIVE MOUSE MODEL OF LOAD-INDUCED OSTEOARTHRITIS

Frank Changburm Ko, Ph.D.

Cornell University 2014

Osteoarthritis (OA) is the leading cause of disability among the elderly population, affecting approximately 27 millions Americans and costing $60 billion in related-health care costs. Mouse models of OA have been developed to study the mechanisms of OA and therapeutic interventions. However, traditional animal models induce OA pathology through traumatic surgeries, which only represent 10% of human OA patients. Thus, in this thesis, a novel noninvasive OA mouse model was developed, characterized, and applied to transgenic mice. The changes in articular cartilage and subchondral bone were analyzed by histology, immunohistochemistry, and microcomputed tomography.

To develop a noninvasive OA mouse model, an *in vivo* tibial loading model was used to investigate the adaptive responses of cartilage and bone to mechanical loading and to assess the influence of load level and duration. Peak cyclic compression of 4.5 and 9.0N was applied to the left tibia via the knee joint of adult (26-week-old) male mice for 1, 2, and 6 weeks at 1200 cycles/day. In addition, 9.0N loading was utilized in young (10-week-old) mice. Loading promoted cartilage damage, cartilage thinning, and subchondral cortical bone thickening in both age groups. Both age groups developed periarticular osteophytes at the tibial plateau in response to the 9.0N load, but no osteophyte formation occurred in adult mice subjected to 4.5N load.

Development of a novel noninvasive loading model was followed by investigating the traumatic vs. nontraumatic nature of cyclic loading of the mouse knee joint. To differentiate traumatic tissue damage versus cell-mediated processes in the development of OA pathology, a

single nondestructive 5-minute loading session was applied to the left tibia of adult (26-week-old) mice at a peak load of 9.0N. Knee joints were subsequently analyzed at 0, 1 and 2 weeks after loading. At T = 0, no change was evident in cartilage or subchondral bone. However, cartilage pathology demonstrated by localized thinning, proteoglycan loss, and inhibition of chondrocyte autophagy occurred at 1 and 2 weeks after the single session of loading. Transient cancellous bone loss was evident at 1 week, associated with increased osteoclast number, reversed at 2 weeks.

Finally, the *in vivo* tibial loading model was implemented to study the role of Dickkopf-1, an inhibitor of the Wnt pathway, in the development of load-induced OA. To identify the role of Dickkopf-1 protein in OA, novel viable mice with Dickkopf-1 knockout and Wnt3 knockdown (Dkk1-/-;Wnt3+/-) were used. The left tibia of 10-week-old Dkk1-/-;Wnt3+/- and respective control groups, littermate control (Dkk1+/+;Wnt3+/+) and Wnt3 knockdown (Dkk1+/+;Wnt3+/-) mice, underwent cyclic compression at a peak load of 9.0N for 2 weeks. As a result of loading, both Dkk1-/-;Wnt3+/- and Dkk1+/+;Wnt3+/+ mice demonstrated cartilage erosion, subchondral cancellous bone loss, and osteophyte formation. However, Dkk1+/+;Wnt3+/- mice did not undergo cartilage degeneration and showed limited osteophyte formation, indicating knockdown of Wnt3's potential chondroprotection against an altered joint loading environment.

In summary, an altered joint loading environment caused by *in vivo* tibial loading repeatedly and robustly produced OA pathology in mouse joints. This loading modality was nontraumatic as evidenced by the absence of physical damage and presence of biological events that led to OA. In addition, the *in vivo* tibial loading model can be applied to investigate potential chondroprotection from genetic or pharmacological interventions. The novel *in vivo* tibial

loading model presents tremendous opportunities to study the etiology of OA from patients without a history of traumatic joint injury and will be an excellent platform to develop therapeutic interventions.

BIOGRAPHICAL SKETCH

Frank Changburm Ko was born in Norman, Oklahoma. He graduated from Ohyun High School in Jeju, South Korea in 2004. In 2008, he graduated from William Marsh Rice University with a Bachelor of Science Degree in Bioengineering. While at Rice, he was involved in biomechanics research developing and testing a false pedicle screw that stabilized spine after spinal fusion. He also participated in an NSF REU summer research program in 2006, he was at the University of Missouri, Columbia to investigate the conditioning of lateral amygdala via computational modeling and in 2007, he was at the University of Minnesota, Twin Cities to develop nonmetallic piezoelectric/pneumatic devices that can be used inside an MRI machine. In 2012, he received his Master of Science degree in Mechanical Engineering at Cornell University. In January 2014, he received his Doctor of Philosophy degree in Mechanical Engineering with a minor in Functional Structural Biology. While at Cornell, he received an NSF Graduate Research Fellowship, ASBMR Young Investigator Award, and ORS Kappa Delta Travel Award.

I dedicate this work to my wife and Alexis

ACKNOWLEDGEMENTS

I have received funding from agencies and foundations that allowed me to pursue my work in musculoskeletal diseases: NSF who provided me a Graduate Research Fellowship, NIH for their research support (R01-AG028664, P30-AR46121, S10-RR024547), and travel grants from the Burroughs Wellcome Fund and an ORS Kappa/Delta Travel Award.

I would like to acknowledge my committee members who have guided and trained me to become not only a scientist with techniques and scientific knowledge, but also an independent thinker and creative problem solver when facing challenging problems in research. My committee chair, Dr. Marjolein van der Meulen, has inspired me to become a scientist who is always thirsting for knowledge and willing to challenge the existing paradigm to become a creative solver. Also I would like to acknowledge my committee members Drs. Cornelia Farnum, Tim Wright, and Christopher Hernandez who greatly assisted me with my research and my career.

I am greatly thankful for my mentors and colleagues who have contributed significantly in training and helping me to successfully complete my dissertation. I would like to thank Drs. Mathias Bostrom, Mary Goldring, and Adele Boskey who have kindly provided their laboratory space and offered advice during my stint at the Hospital for Special Surgery. Also my mentors Drs. Russell Main, Maureen Lynch, Darren Plumb, and Cecilia Dragomir, who despite their busy schedule, always gladly discussed troubleshooting of experiments, appropriate next steps, and career advice. I am also thankful for the students and my colleagues who have assisted in the experiment along the way. I would like to thank Kirk Gunsallus, Dan Brooks, Kirsten Stoner, Funmi Adebayo, Allison Hsia, Dan Loeffler, and Stephen Hong for their participation and

assistance in various loading studies and experiments. In addition, without help from Judy Thoroughman and Marcia Sawyer, my graduate school experience would not have been as smooth as it had been. Last but not least, I would like to thank the Cornell Center for Animal Resources and Education staff members, Kevin Yager, Cherie Brown, Denny Totman, and Cheryl Pribulick, who have greatly assisted in animal experiments.

I am greatly thankful for the feedback and support I received from my colleagues and professors along the way. My former and current group members Eve Donnelly, Russ Main, Marueen Lynch, Dan Brooks, Jayme Burket, Garry Brock, Katie Melville, Natalie Kelly, and Funmi Adebayo provided critical input and guidance during preparation for my experiments, talks, presentations, or any other issues that I ran into. I am also thankful for my colleagues at HSS: Lyuda Lukashova, Bettina Willie, Kate Meyers, Xu Yang, Anna Fahlgren, Cesare Ciani, Miguel Otero, Dr. Stephen Doty, Dr. Paddy Ross, and Dr. Carl Blobel.

I would not have been here without the support and caring from my family and parents: my wife, Dr. Erica Eunjung Jung, who continues to support and love me despite my inability to reciprocate, my father, who also as a professor is always willing to challenge my existing views and discuss my progress, my mother from whom I learned organization skills, my sister always being with my parents in Korea during holidays, which I unfortunately cannot do, and last but not least, our daughter Alexis who on a good day, can sleep 6 hours straight. Thank you all.

TABLE OF CONTENTS

List of Figures

List of Tables

CHAPTER 1

INTRODUCTION

1.1. Osteoarthritis

Osteoarthritis (OA) is the leading cause of musculoskeletal disability, disrupting diarthroidal joints such as the wrist, hip, or knee and impairing functional activities among the affected individuals. Approximately 27 million Americans suffer from OA and $60 billion related-healthcare costs are spent annually for treatment and management of OA [1, 2]. With increasing life expectancy, better management of overall health care, and increased level of athletic activities, the number of people suffering from OA is expected to rise sharply, which will dramatically increase the burden among health care professionals and caregivers. Currently no Disease Modifying OA Drugs (DMOADs) are available, which results in limited treatment options to alleviate pain or slow the progression of OA: non-steroidal anti-inflammatory drugs (NSAIDs), moderate physical exercise, weight loss, and ultimately, total joint replacement. A detailed understanding of pathomechanisms of OA can provide opportunities to develop not only chemical or biological DMOADs, but also novel therapeutic interventions to prevent the development of OA that will ultimately enhance the quality of life within the population highly susceptible to OA.

1.2. Alterations in the Osteoarthritic Joint

Diarthroidal joints are composed of articular cartilage, subchondral bone, synovial membrane, meniscus, and ligaments (Figure 1.1a). The articular cartilage and meniscus provide lubrication and shock absorption during locomotion, subchondral bone maintains joint structural

integrity, ligaments stabilize the joint, and the synovial membrane provides synovial fluid for maintaining functional lubrication and nutrients to avascular cartilage. Development and progression of OA are accompanied by significant changes in each of the diarthroidal joint components, resulting in pain and inability to maintain functional range of motion (Figure 1.1b).

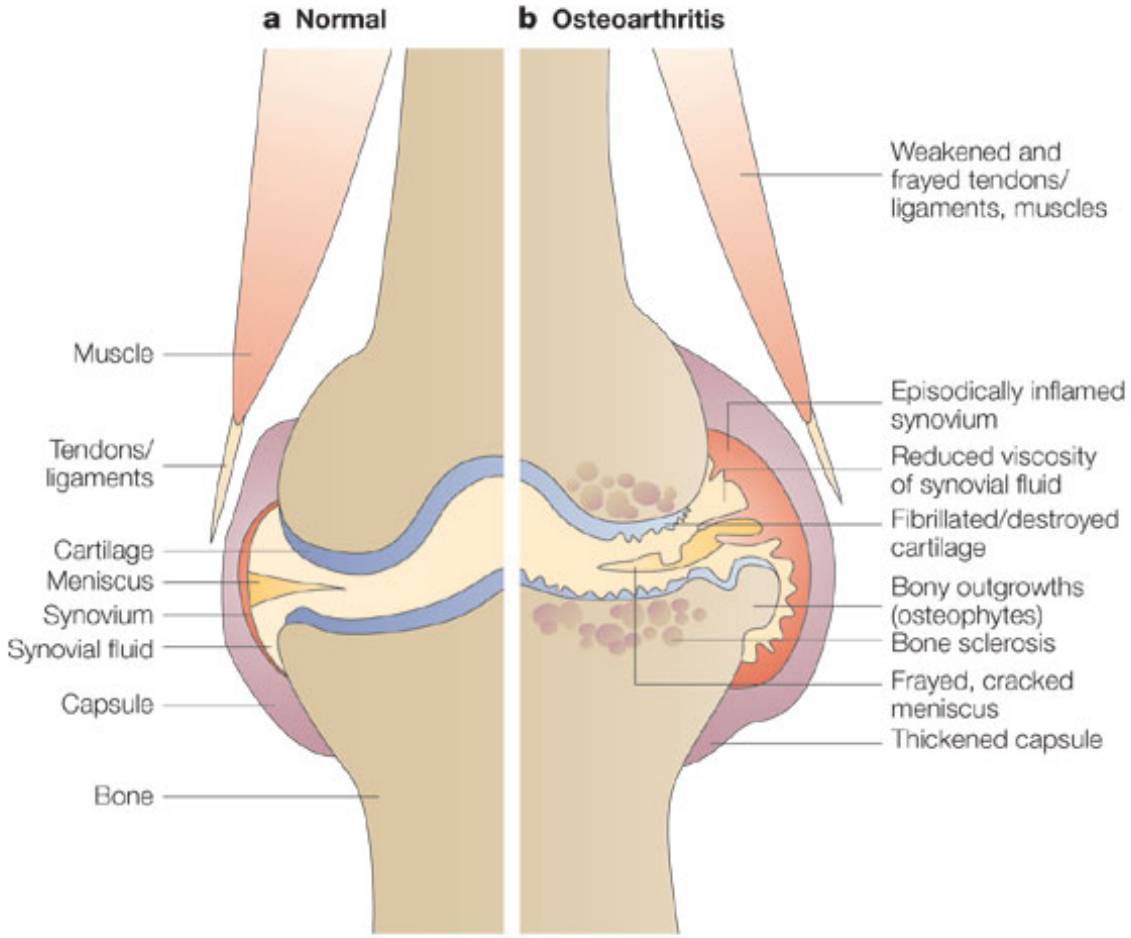

Figure 1.1 (a) Healthy joint without structural damage or inflammation at any of the joint components and (b) osteoarthritic joint with focal degeneration, bone spurs, and synovial inflammation [3].

1.2.1. Articular Cartilage

Articular cartilage is the lubricating surface on the joint and prevents bone-bone contact that results in significant pain and reduced range of motion. Avascular in nature, articular cartilage is

composed of resident cells (chondrocytes) and surrounding extracellular matrices composed of water, collagen, proteoglycan, and noncollagenous proteins (Figure 1.2). Articular cartilage can be separated in three different zonal layers: superficial, middle, and deep zones (Figure 1.3). These zonal layers resemble the growth plate chondrocyte morphology; superficial zone chondrocytes resemble the reserved zone of the growth plate; and the deep zone resembles the hypertrophic zone with enlarged chondrocytes.

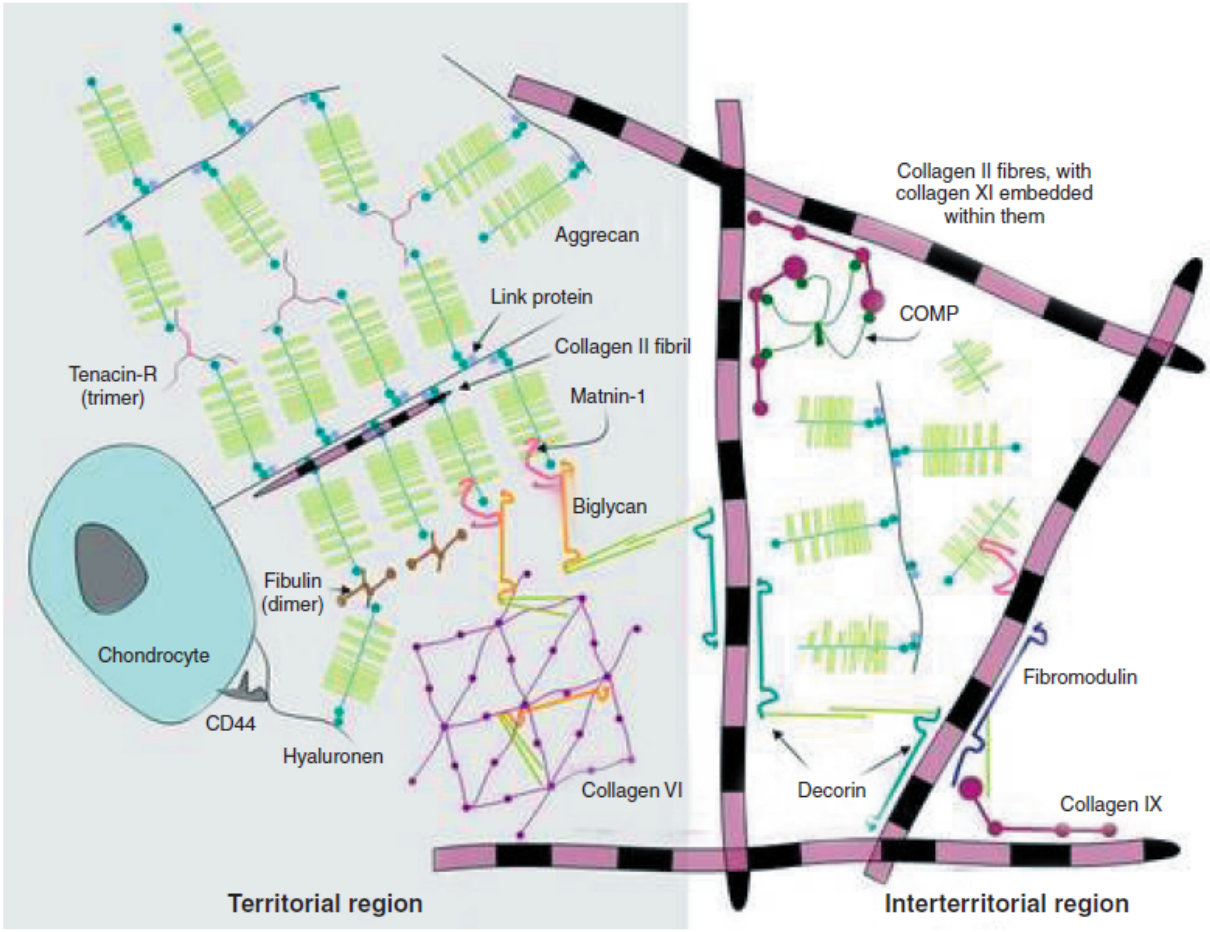

Figure 1.2 Chondrocyte and its interaction with surrounding extracellular matrices within articular cartilage [4].

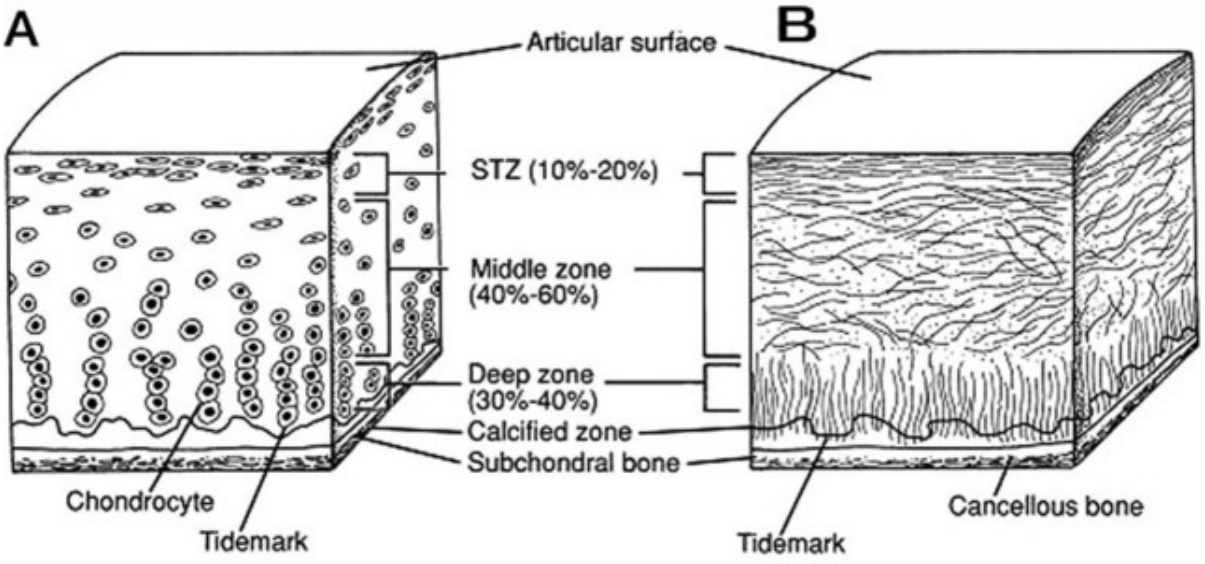

Figure 1.3 Chondrocyte morphology in different zonal layers of articular cartilage (A) and collagen orientation within each layer (B) [5]. Deep zone chondrocytes are enlarged with surrounding collagen oriented vertically whereas in the superficial zone, chondrocytes are surrounded by collagen oriented horizontally.

Partial or complete erosion of articular cartilage is common among late-stage OA patients. Instead of a smooth articulating surface at the superficial zone, late-stage OA cartilage is characterized by a roughened surface and significant fissures penetrating into the deep zone, chondrocyte proliferation and hypertrophy, and loss of proteoglycan (Figure 1.4). These morphological alterations lead to resistance to articulating movement and increased friction at the joint.

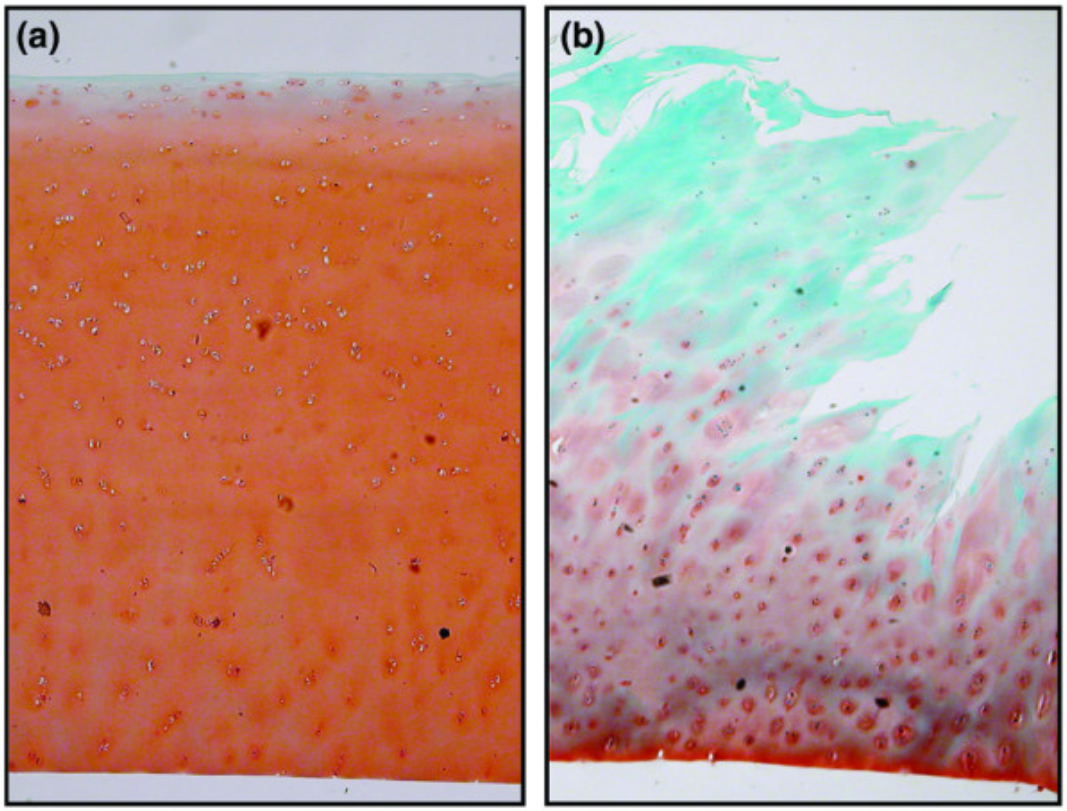

Figure 1.4 Healthy (a) and osteoarthritic (b) articular cartilage stained by Safranin O/Fast green [6]. Proteoglycan loss and surface erosion are common features in osteoarthritic cartilage. Also, the deep zone of osteoarthritic cartilage contains a high percentage of enlarged chondrocytes compared to healthy cartilage.

1.2.2. Subchondral Bone

Subchondral bone, which consists of subchondral cortical and cancellous bone, maintains structural integrity at the joint. Composed predominantly of collagen and hydroxyapatite mineral, subchondral bone can withstand significantly higher loads than any other surrounding joint tissue. Subchondral cortical bone (alternatively referred to as the subchondral plate) is located directly adjacent to the calcified zone of articular cartilage, followed by subchondral cancellous bone (Figure 1.5). Unlike articular cartilage in which chondrocytes show limited activity due to their avascular environment, resident bone cells such as osteoblasts, osteoclasts, and osteocytes are continuously active (bone remodeling) via nutrients from bone marrow and

the vascular network in the bone matrix.

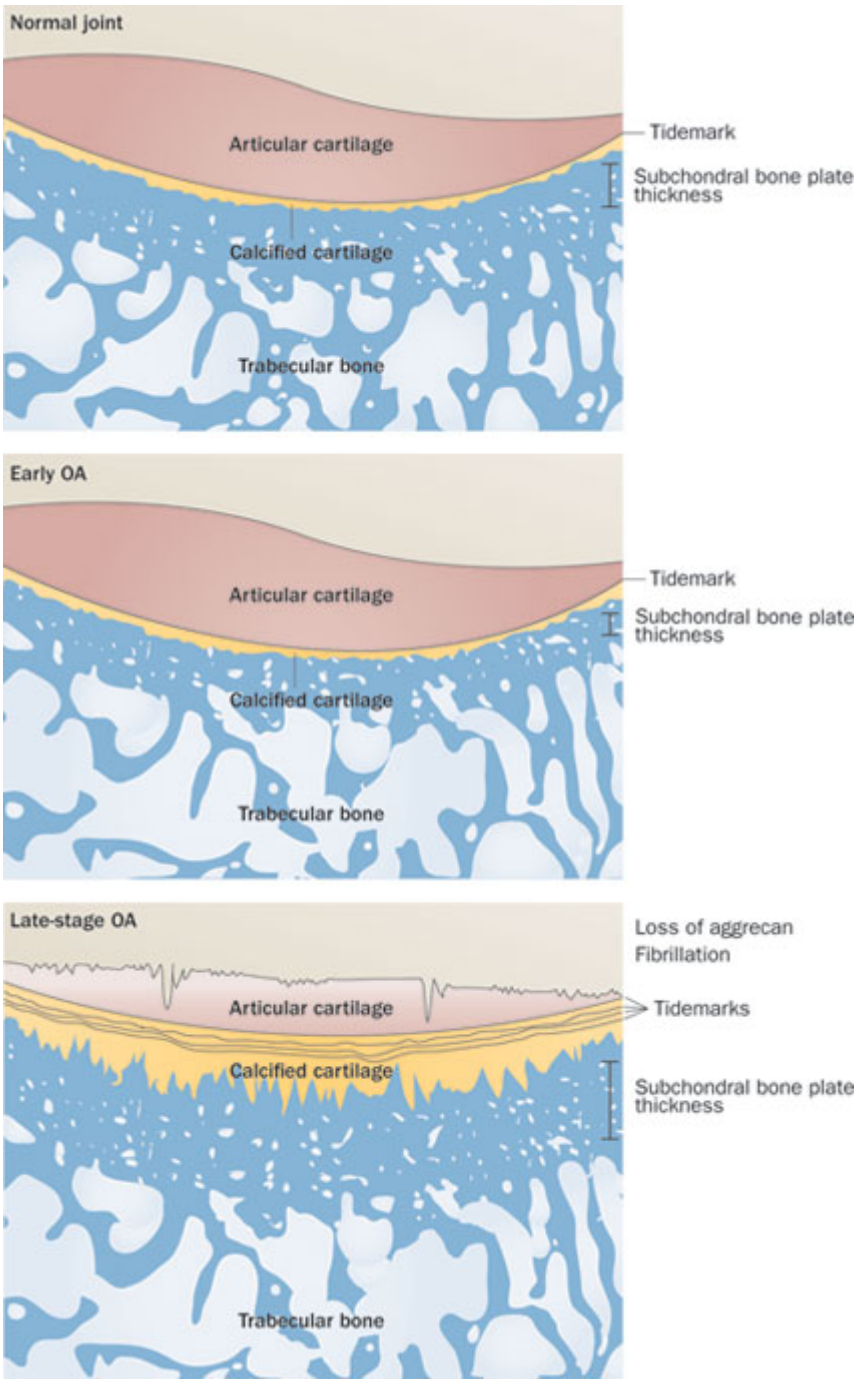

Figure 1.5 Progressive changes in articular cartilage, calcified cartilage, and subchondral cortical and cancellous bone over the course of OA development [7].

Subchondral cortical and cancellous bones undergo several changes over the course of OA

development. During the onset and early stages of OA, subchondral cortical bone thins due to increases in bone resorption. Thinning of subchondral cortical bone increases porosity that allows the transport of solutes and mediators that promote expansion of calcified cartilage [8]. As the disease progresses to the late stage, subchondral cortical bone thickens while subchondral cancellous bone becomes thinner due to stress shielding from the cortical bone (Figure 1.5) [7].

1.2.3. Synovial Membrane

The synovial membrane is the thin layer surrounding the joint that supplies and maintains the synovial fluid within the joint capsule. Synovial fluid allows lubrication at the joint and also transports necessary nutrients to maintain healthy avascular articular cartilage. Synoviocytes produce lubricin and hyaluronic acid that allow efficient lubrication at the diarthroidal joint [9].

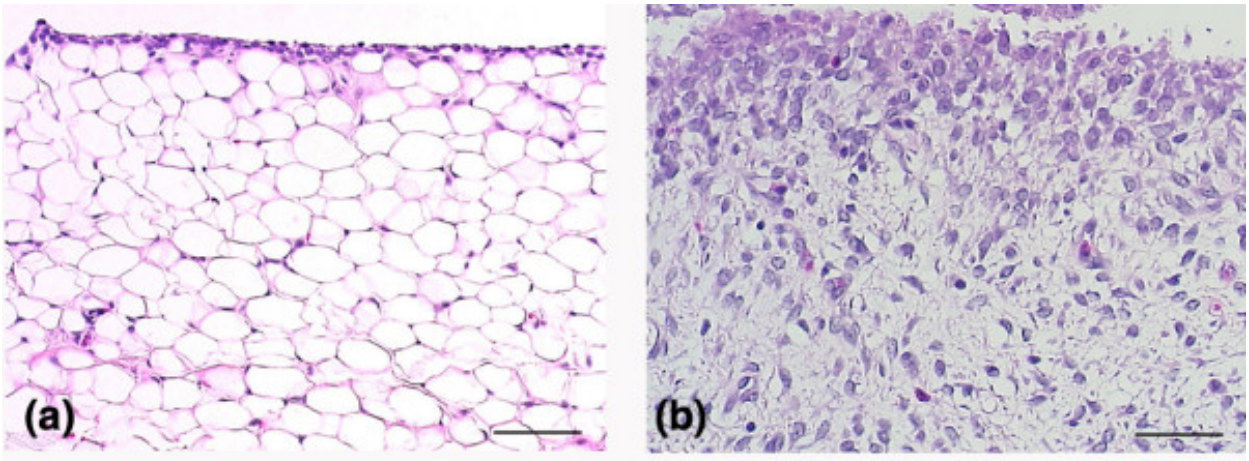

Figure 1.6 Healthy (a) and osteoarthritic (b) synovial membrane stained by H&E. Osteoarthritic synovial membranes display significant hyperplasia of synovial cells and infiltration of inflammatory cells [10]

At the onset and during the development of OA, the synovial membrane undergoes significant morphological changes characterized by hyperplasia of the synovial lining, fibrosis, and infiltration of lymphocytes and macrophages (Figure 1.6) [9]. These changes not only result

in secretion of inflammatory mediators that promote secretion of collagenase in articular chondrocytes, but also are suggested to play a crucial role in pain sensitivity [9].

1.2.4. Meniscus

The meniscus resides between femoral and tibial surfaces of the knee joint to provide both lubrication and load-bearing capacity. Primarily composed of collagen and proteoglycans, the unique horn-like anatomical shape (knee meniscus) and biochemical composition allow the meniscus to withstand a variety of forces such as shear, tension, and compression (Figure 1.7). Unlike articular cartilage, which only consists of chondrocytes, cells in the meniscus are composed of fibroblast- and chondrocyte-like cells.

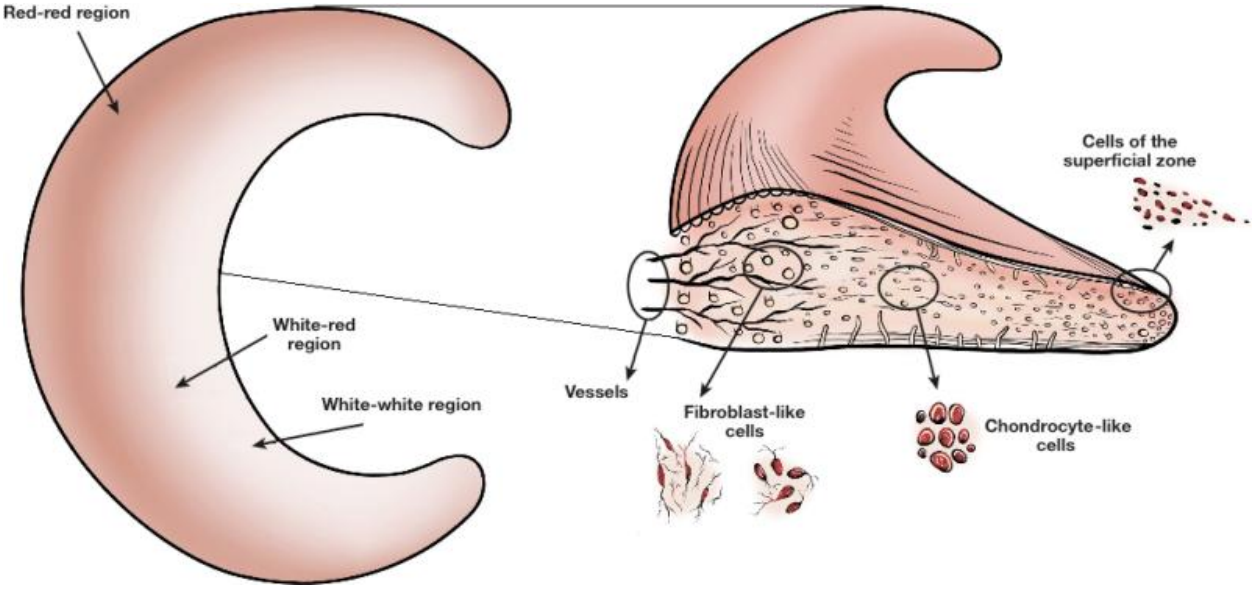

Figure 1.7 Overall meniscus morphology and resident cell population [11]

While articular cartilage and subchondral bone undergo changes during the onset and development of OA, the meniscus is responsible for initiating those changes by destabilizing the mechanical environment at the joint while also disrupting its own structural integrity. Partial or

complete meniscectomy increases the likelihood of developing OA in animal models and patients who underwent such surgeries.

1.2.5. Ligaments

Ligaments exist in the joint to provide stability during movement. For example, in the knee, four primary ligaments, lateral and medial ligaments and anterior and posterior cruciate ligaments (ACL and PCL), allow the tibiofemoral joint to extend and flex and provide optimal distribution of stress across the tibial plateau. Similar to the meniscus, removal or injury of any of the ligaments alters the biomechanical environment at the joint, which initiates changes in articular cartilage and subchondral bone pathology leading to OA.

1.3. Pathomechanisms of Osteoarthritis due to Joint Loading Alterations

The complex anatomical structure of the joint leads to multiple contributing factors that initiate the development of OA. Since a diarthroidal joint provides articulating surfaces during locomotion and bears mechanical loads, OA can develop due to alterations in the joint loading environment and subsequent changes in biological response.

The joint loading environment can be altered by increasing the amount of load being transmitted, the frequency and duration of loading, and characteristic motions occurring at the joint. Clinical studies show strong associations between obesity and incidence of OA, indicating that increased joint load due to increases in body weight can be an important risk factor in the development of OA [12]. In addition, workers who require daily heavy lifting are more susceptible in developing hip OA [13, 14]. While evidence is conflicting among amateur long distance runners, professional athletes who were exposed to strenuous training regimens and

competitions developed OA prematurely [15-19]. In addition to being exposed to a competitive loading environment, athletes with histories of joint injuries such as an anterior cruciate ligament tear, meniscectomy, or intraarticular tibial plateau fracture are at a higher risk of developing post-traumatic OA [20-22]. Joint injuries and post-operative surgeries often lead to altered gait patterns, which substantially shift joint contact locations and stress patterns on the joint [23-25]. As a result, reducing body weight, lessening the daily workload, providing a moderate exercise program, or gait modification have been recommended to alleviate or potentially prevent symptoms of OA among patients [26-29]. For example, lowering body mass by 5kg led to a 50% reduction in the odds of developing OA [30].

In vitro and preclinical models of OA also corroborate findings from clinical studies that alterations in the joint loading environment can promote changes similar to OA seen in humans. These models provide further insights into mechanical and biological processes responsible for OA development. Overloading at high strain rates or repeated compressive cyclic loading decreased stiffness and chondrocyte viability and increased cellular expression of catabolic factors in cartilage explants [31-36]. In response to an altered loading environment, chondrocytes initially undergo proliferation and hypertrophy, and then secrete catabolic factors such as MMP-13 and ADAMTS-5 [37-39]. These catabolic factors degrade articular cartilage components such as collagen and glycosaminoglycan and also promote chondrocyte apoptosis and ossification of the cartilage deep zone [40]. Preclinical animal models that underwent surgical joint instability showed similar biological changes in articular cartilage [40-42]. Also, whole joint analysis of *in vivo* OA models revealed potential cross-talk between articular cartilage and subchondral bone, in which the early thinning of subchondral bone may promote vasculature that transports cytokines and mediators to the deep zone of cartilage, leading to chondrocyte hypertrophy and

ossification [8, 43-45].

1.4. *In Vivo* Models of Osteoarthritis

Animal models of OA have been used extensively to characterize the disease mechanism and develop therapeutic interventions. With the ability to study multiple joint components simultaneously, animal models will continue to be extraordinary research tools that will greatly benefit OA research community. Animal models can be broadly classified as non-rodent and rodent models, in which OA can be promoted via traumatic or non-traumatic interventions at the joint.

1.4.1. Non-rodent Models

Rabbits are the most widely used non-rodent models of OA, due to their relative ease of handling and cost of care compared to larger animals. Rabbits that underwent ACL transection or meniscectomy surgery developed OA pathology similar to humans, including articular cartilage erosion and osteophyte formation [46-50]. To alleviate or treat these changes in rabbits and demonstrate translatability of rabbit OA models to clinical settings, investigators have administered intra-articular injection of potential therapeutic agents that demonstrated improvements in rabbit joints [51-53]. Nonsurgical OA induction has been attempted by noninvasive mechanical loading of the knee or intra-articular injection of collagenase or papain [54-57]. While the nonsurgical nature is an advantage to study OA population cohorts without prior joint injuries, intra-articular injection of proteases does not consistently replicate the traditional OA pathology seen in humans.

Canine models are also widely studied due to a high incidence of naturally occurring joint

dysplasia and subsequent development of OA among larger breeds such as Labrador retrievers and Shepherd dogs [58, 59]. In addition to the large body weight that the joint needs to resist during activities, increases in joint laxity and distraction are often observed in larger breeds of dogs, further altering the joint loading environment that can lead to OA [58]. OA can be artificially-induced in canine models by surgically destabilizing the joint or by strenuous exercise [60-64]. Similar to rabbit OA models, canine models have also been used as a therapeutic testing platform for OA and demonstrated translatability of the model to the clinical scenario [65-68].

Ovine and equine models have also been developed and implemented to study OA. Sheep with increased joint instability due to either ligament transection or meniscectomy developed similar OA pathology to humans [69, 70]. Unlike sheep and other mammals used for OA studies, horses have unique limb structure in that their functional "knees" correspond to the anatomical locations of wrists or ankles in human. Despite the anatomical differences, equine OA models of osteochondral defects are commonly used, and treatments strategies for such defects have been developed, including bone-marrow aspirate concentrate, cytokines, or exercise [71-75].

1.4.2. Rodent Osteoarthritis Models

Easily accessible, relatively lower costs of care compared to larger mammals, and advances in transgenic mouse techniques attract investigators to use rodent models of OA to investigate mechanisms responsible for joint degeneration and to develop novel therapeutic interventions. Mice and rats are commonly implemented for preclinical non-traumatic or traumatic OA models, and guinea pigs have also been used due to the spontaneous occurrence of joint degeneration [76-79]. Rodents undergo varying degrees of surgical or nonsurgical interventions to promote the development of OA to address specific OA patient cohorts.

1.4.2.1. Traumatic Rodent Osteoarthritis Models

Similar to non-rodent OA models, creating joint instability through surgical removal of the meniscus or ligament can lead to OA in rodents. Destabilization of the medial meniscus (DMM), by transecting the meniscotibial ligament, resulted in cartilage degeneration and limited osteophyte formation in mice and rats [80, 81]. In addition to articular cartilage degeneration, thinning of the subchondral plate was evident in rodents that underwent DMM surgery [82, 83]. These changes were observed over the course of 8 weeks. At 4 weeks, only mild surface fibrillation occurred, but at 8 weeks, complete articular cartilage erosion occurred with osteophytes at the joint margins.

Joint instability in rodents can also be achieved by surgically transecting ligaments that maintain joint articulation. In the knee joint, transection of the ACL, PCL, or both led to significant articular cartilage degeneration, subchondral plate thinning, and osteophyte formation [41, 84-87]. The extent of joint alterations was significantly greater than mice that underwent DMM surgery. Not only articular cartilage fibrillation occur in the ACL model, but also ectopic bone formation, complete loss of epiphyseal bone, and significant periosteal reactions. At 4 and 8 weeks following ACL transection, the extent of joint alterations was indistinguishable, indicating the surgery results in rapid joint reactions and remains constant for extended periods. These results indicate ACL transection may activate additional biological responses that lead to strong reactions at the joint margins [80].

Closed intraarticular fracture in the mouse knee also leads to development of OA phenotypes in cartilage and bone [88]. Following fracture, joint changes include synovial inflammation, decrease in chondrocyte viability, heterotopic bone formation, and thinning of subchondral bone

[89]. The severity of these changes were significantly increased when mice became obese from a high-fat diet [90].

Traumatic rodent models of OA provide great insights in potential management of care and development of DMOADs for OA patients who had histories of traumatic joint injuries such as an ACL tear, tibial osteotomy, or meniscectomy. However, given that the majority of patients developing OA do not have histories of joint injuries, other non-traumatic risk factors such as genetics, diet, and repetitive nontraumatic joint loading need to be addressed by rodent models [91, 92]

1.4.2.2. Non-traumatic Rodent Osteoarthritis Models

Since the complete sequencing of the mouse genome and rapid advances of transgenic mouse technology, a detailed mechanistic understanding of OA progression can now be investigated at the whole joint level using genetically modified mice. Mice with partial or complete inactivation of genes that are important in producing the collagen matrix of cartilage such as COL2A1, COL9A1, or COL11A1 exhibit OA phenotypes similar to humans [93-95]. Also, increases in cartilage turnover enzymes such as MMP-13 or ADAMTS-5 have been shown to expedite the development of OA in mice [96-98]. In addition to transgenic models, certain strains of mice are naturally more susceptible to developing OA. For example, the STR/Ort mouse spontaneously develops OA compared to the CBA strain [99, 100]. Also, when C57BL/6 and BALB/c mice reach 2 years of age, spontaneous OA develops as evidenced by type II collagen degradation epitopes [101].

In addition to generating unique transgenic mice to investigate molecular mechanisms governing OA development, the strong association between increases in body weight and high

incidence of OA led to the development of mouse models of obesity with different diets. Obese mice that were chow-fed with impaired leptin-signaling did not develop OA, but mice fed a high-fat diet had a higher incidence of OA development [102, 103]. This result suggests that while not all obesity may result in OA, the combination of poor diet and other systemic factors could trigger development of OA. In contrast, exercising of obese mice fed the high-fat diet slowed the progression of OA, indicating these systemic risk factors of OA are preventable through physical interventions [104].

However, not all exercise is beneficial. Mice that underwent lifelong moderate running, which started at 2 months of age with 1,000m/day running until the age of 18 months, had increased the incidence and severity of OA [105]. However, OA symptoms were alleviated by voluntary running exercise in mice with high risk of developing OA [95, 104]. Appropriate physical intervention needs to be carefully considered as OA severity is related to the increase in the amount of exercise [106].

1.5. Thesis Aims

Traditional preclinical OA models have shed light on the mechanisms governing initiation and progression of OA. However, the majority of traditional preclinical OA models involve surgical induction of significant joint instability, despite only a small portion of OA patients being represented by these models. In addition, surgical procedures not only destabilize the joint, but also promote inflammation and local tissue reactions that confound the outcome of a study. As a result, developing, characterizing, and applying a noninvasive OA model that does not create traumatic injury are the goals for this thesis.

1.5.1. Aim 1: Development of a Noninvasive In Vivo Mouse Loading Model of OA

In humans, the strong correlation between the loading environment and the risk for development of OA suggests that a preclinical model with loading could recapitulate pathological changes seen in osteoarthritic human joints. With only limited studies investigating the controlled loading environment at a noninvasive level, the goal of this aim was to develop a noninvasive *in vivo* mouse tibial loading model with detailed characterization of tissue pathology development at the whole joint level [107, 108]. To alter the loading environment in the mouse knee joint, a tibial loading model that was implemented previously to study bone adaptation was used [109, 110]. Young (10 week old) and adult (26 week old) male C57Bl/6 mice underwent daily cyclic compression of the left tibiae at two load levels (4.5N and 9.0N) for 1, 2, and 6 weeks. Alterations in epiphyseal and metaphyseal bone, articular cartilage, and periarticular regions were analyzed by microcomputed tomography (microCT) and histology.

1.5.2. Aim 2: Characterize Mouse Joint Alterations Following Single Dose of In Vivo Loading

Daily cyclic compression of mouse tibiae promoted alterations in the knee joint that recapitulated hallmarks of human OA including cartilage erosion, subchondral bone sclerosis, and osteophyte formation [108]. However, the mechanism initiated by loading the joint was unclear; distinguishing whether the compressive loading created traumatic damage at the joint or promoted biological events that initiated signaling cascades leading to changes in joint morphology was unclear. Thus, in this second aim the response to a single dose (5 min) of cyclic loading was examined. Following loading, mice were euthanized immediately, and 1- and 2-weeks after the single session of loading. Tissue morphology and cellular responses in the knee

joint were assayed by microCT, histology, and immunohistochemistry using antibodies specific for osteoclasts, autophagy, and apoptosis markers.

1.5.3. Aim 3: Investigate the Roles of Dickkopf-1 Ablation and Noninvasive In Vivo Loading in Mouse Knee Joints

Noninvasive *in vivo* loading of the mouse knee resulted in concurrent changes in articular cartilage and subchondral bone over the course of loading, indicating that any interventions to treat OA need to target multiple tissue compartments simultaneously. The Wnt pathway is a critical regulator of whole joint development and homeostasis, and alterations in the pathway lead to severe musculoskeletal phenotypes [45, 111-114]. As a result, attenuating the Wnt pathway could lead to potent therapeutics to alter the progression and development of OA [112, 115]. Using a novel genetic knockout of a key component of wnt signaling, the role of this pathway in OA development was examined [116-119]. Mice underwent daily cyclic compressive loading of left tibiae for 2 weeks as in Aims 1 and 2. Alterations in the joint compartments were analyzed by microCT, histology, and immunohistochemistry using antibodies specific for MMP-13 and β-catenin.

1.6 REFERENCES

1. Lawrence RC, Felson DT, Helmick CG, Arnold LM, Choi H, Deyo RA, Gabriel S, Hirsch R, Hochberg MC, Hunder GG, Jordan JM, Katz JN, Kremers HM, Wolfe F. Estimates of the prevalence of arthritis and other rheumatic conditions in the United States. Part II. Arthritis Rheum. 2008 Jan;58(1):26-35.
2. Yelin E, Murphy L, Cisternas MG, Foreman AJ, Pasta DJ, Helmick CG. Medical care expenditures and earnings losses among persons with arthritis and other rheumatic conditions in 2003, and comparisons with 1997. Arthritis Rheum. 2007 May;56(5):1397-407.
3. Wieland HA, Michaelis M, Kirschbaum BJ, Rudolphi KA. Osteoarthritis - an untreatable disease? Nat Rev Drug Discov. 2005 Apr;4(4):331-44.
4. Dudhia J. Aggrecan, aging and assembly in articular cartilage. Cell Mol Life Sci. 2005 Oct;62(19-20):2241-56.
5. Buckwalter JA, Mow VC, Ratcliffe A. Restoration of Injured or Degenerated Articular Cartilage. The Journal of the American Academy of Orthopaedic Surgeons. 1994 Jul;2(4):192-201.
6. Mastbergen SC, Jansen NW, Bijlsma JW, Lafeber FP. Differential direct effects of cyclo-oxygenase-1/2 inhibition on proteoglycan turnover of human osteoarthritic cartilage: an in vitro study. Arthritis Res Ther. 2006;8(1):R2.
7. Burr DB, Gallant MA. Bone remodelling in osteoarthritis. Nat Rev Rheumatol. 2012 Nov;8(11):665-73.

8. Botter SM, van Osch GJ, Clockaerts S, Waarsing JH, Weinans H, van Leeuwen JP. Osteoarthritis induction leads to early and temporal subchondral plate porosity in the tibial plateau of mice: an in vivo microfocal computed tomography study. Arthritis Rheum. 2011 Sep;63(9):2690-9.

9. Scanzello CR, Goldring SR. The role of synovitis in osteoarthritis pathogenesis. Bone. 2012 Aug;51(2):249-57.

10. Uchii M, Tamura T, Suda T, Kakuni M, Tanaka A, Miki I. Role of fibroblast growth factor 8 (FGF8) in animal models of osteoarthritis. Arthritis Res Ther. 2008;10(4):R90.

11. Makris EA, Hadidi P, Athanasiou KA. The knee meniscus: structure-function, pathophysiology, current repair techniques, and prospects for regeneration. Biomaterials. 2011 Oct;32(30):7411-31.

12. Felson DT, Anderson JJ, Naimark A, Walker AM, Meenan RF. Obesity and knee osteoarthritis. The Framingham Study. Ann Intern Med. 1988 Jul 1;109(1):18-24.

13. Sulsky SI, Carlton L, Bochmann F, Ellegast R, Glitsch U, Hartmann B, Pallapies D, Seidel D, Sun Y. Epidemiological evidence for work load as a risk factor for osteoarthritis of the hip: a systematic review. Plos One. 2012;7(2):e31521.

14. Cameron KL, Hsiao MS, Owens BD, Burks R, Svoboda SJ. Incidence of physician-diagnosed osteoarthritis among active duty United States military service members. Arthritis Rheum. 2011 Oct;63(10):2974-82.

15. Chakravarty EF, Hubert HB, Lingala VB, Zatarain E, Fries JF. Long distance running and knee osteoarthritis. A prospective study. American journal of preventive medicine. 2008 Aug;35(2):133-8.

16. Kujala UM, Kettunen J, Paananen H, Aalto T, Battie MC, Impivaara O, Videman T, Sarna S. Knee osteoarthritis in former runners, soccer players, weight lifters, and shooters. Arthritis Rheum. 1995 Apr;38(4):539-46.

17. Lane NE, Bloch DA, Jones HH, Marshall WH, Jr., Wood PD, Fries JF. Long-distance running, bone density, and osteoarthritis. JAMA : the journal of the American Medical Association. 1986 Mar 7;255(9):1147-51.

18. Marti B, Knobloch M, Tschopp A, Jucker A, Howald H. Is excessive running predictive of degenerative hip disease? Controlled study of former elite athletes. BMJ. 1989 Jul 8;299(6691):91-3.

19. Spector TD, Harris PA, Hart DJ, Cicuttini FM, Nandra D, Etherington J, Wolman RL, Doyle DV. Risk of osteoarthritis associated with long-term weight-bearing sports: a radiologic survey of the hips and knees in female ex-athletes and population controls. Arthritis Rheum. 1996 Jun;39(6):988-95.

20. Buckwalter JA, Lane NE. Athletics and osteoarthritis. Am J Sports Med. 1997 Nov-Dec;25(6):873-81.

21. Englund M, Lohmander LS. Risk factors for symptomatic knee osteoarthritis fifteen to twenty-two years after meniscectomy. Arthritis Rheum. 2004 Sep;50(9):2811-9.

22. Papagelopoulos PJ, Partsinevelos AA, Themistocleous GS, Mavrogenis AF, Korres DS, Soucacos PN. Complications after tibia plateau fracture surgery. Injury. 2006 Jun;37(6):475-84.

23. Andriacchi TP, Koo S, Scanlan SF. Gait mechanics influence healthy cartilage morphology and osteoarthritis of the knee. J Bone Joint Surg Am. 2009 Feb;91 Suppl 1:95-101.

24. Chaudhari AM, Briant PL, Bevill SL, Koo S, Andriacchi TP. Knee kinematics, cartilage morphology, and osteoarthritis after ACL injury. Med Sci Sports Exerc. 2008 Feb;40(2):215-22.

25. Noyes FR, Schipplein OD, Andriacchi TP, Saddemi SR, Weise M. The anterior cruciate ligament-deficient knee with varus alignment. An analysis of gait adaptations and dynamic joint loadings. Am J Sports Med. 1992 Nov-Dec;20(6):707-16.

26. Jordan KM, Arden NK, Doherty M, Bannwarth B, Bijlsma JW, Dieppe P, Gunther K, Hauselmann H, Herrero-Beaumont G, Kaklamanis P, Lohmander S, Leeb B, Lequesne M, Mazieres B, Martin-Mola E, Pavelka K, Pendleton A, Punzi L, Serni U, Swoboda B, Verbruggen G, Zimmerman-Gorska I, Dougados M, Standing Committee for International Clinical Studies Including Therapeutic Trials E. EULAR Recommendations 2003: an evidence based approach to the management of knee osteoarthritis: Report of a Task Force of the Standing Committee for International Clinical Studies Including Therapeutic Trials (ESCISIT). Ann Rheum Dis. 2003 Dec;62(12):1145-55.

27. Zhang W, Doherty M, Arden N, Bannwarth B, Bijlsma J, Gunther KP, Hauselmann HJ, Herrero-Beaumont G, Jordan K, Kaklamanis P, Leeb B, Lequesne M, Lohmander S, Mazieres B, Martin-Mola E, Pavelka K, Pendleton A, Punzi L, Swoboda B, Varatojo R, Verbruggen G, Zimmermann-Gorska I, Dougados M, Therapeutics ESCfICSI. EULAR evidence based recommendations for the management of hip osteoarthritis: report of a task force of the EULAR Standing Committee for International Clinical Studies Including Therapeutics (ESCISIT). Ann Rheum Dis. 2005 May;64(5):669-81.

28. Ettinger WH, Jr., Afable RF. Physical disability from knee osteoarthritis: the role of exercise as an intervention. Med Sci Sports Exerc. 1994 Dec;26(12):1435-40.

29. Fregly BJ, Reinbolt JA, Rooney KL, Mitchell KH, Chmielewski TL. Design of patient-specific gait modifications for knee osteoarthritis rehabilitation. IEEE transactions on bio-medical engineering. 2007 Sep;54(9):1687-95.

30. Felson DT, Zhang Y, Anthony JM, Naimark A, Anderson JJ. Weight loss reduces the risk for symptomatic knee osteoarthritis in women. The Framingham Study. Ann Intern Med. 1992 Apr 1;116(7):535-9.

31. Kurz B, Jin M, Patwari P, Cheng DM, Lark MW, Grodzinsky AJ. Biosynthetic response and mechanical properties of articular cartilage after injurious compression. J Orthop Res. 2001 Nov;19(6):1140-6.

32. Thibault M, Poole AR, Buschmann MD. Cyclic compression of cartilage/bone explants in vitro leads to physical weakening, mechanical breakdown of collagen and release of matrix fragments. J Orthop Res. 2002 Nov;20(6):1265-73.

33. Lee JH, Fitzgerald JB, Dimicco MA, Grodzinsky AJ. Mechanical injury of cartilage explants causes specific time-dependent changes in chondrocyte gene expression. Arthritis Rheum. 2005 Aug;52(8):2386-95.

34. Morel V, Berutto C, Quinn TM. Effects of damage in the articular surface on the cartilage response to injurious compression in vitro. J Biomech. 2006;39(5):924-30.

35. Natoli RM, Athanasiou KA. P188 reduces cell death and IGF-I reduces GAG release following single-impact loading of articular cartilage. J Biomech Eng. 2008 Aug;130(4):041012.

36. Backus JD, Furman BD, Swimmer T, Kent CL, McNulty AL, Defrate LE, Guilak F, Olson SA. Cartilage viability and catabolism in the intact porcine knee following

transarticular impact loading with and without articular fracture. J Orthop Res. 2011 Apr;29(4):501-10.

37. Dreier R. Hypertrophic differentiation of chondrocytes in osteoarthritis: the developmental aspect of degenerative joint disorders. Arthritis Res Ther. 2010;12(5):216.

38. van der Kraan PM, van den Berg WB. Chondrocyte hypertrophy and osteoarthritis: role in initiation and progression of cartilage degeneration? Osteoarthritis Cartilage. 2012 Mar;20(3):223-32.

39. Goldring MB. Chondrogenesis, chondrocyte differentiation, and articular cartilage metabolism in health and osteoarthritis. Therapeutic advances in musculoskeletal disease. 2012 Aug;4(4):269-85.

40. Kawaguchi H. Endochondral ossification signals in cartilage degradation during osteoarthritis progression in experimental mouse models. Mol Cells. 2008 Feb 29;25(1):1-6.

41. Kamekura S, Hoshi K, Shimoaka T, Chung U, Chikuda H, Yamada T, Uchida M, Ogata N, Seichi A, Nakamura K, Kawaguchi H. Osteoarthritis development in novel experimental mouse models induced by knee joint instability. Osteoarthritis Cartilage. 2005 Jul;13(7):632-41.

42. Kamekura S, Kawasaki Y, Hoshi K, Shimoaka T, Chikuda H, Maruyama Z, Komori T, Sato S, Takeda S, Karsenty G, Nakamura K, Chung UI, Kawaguchi H. Contribution of runt-related transcription factor 2 to the pathogenesis of osteoarthritis in mice after induction of knee joint instability. Arthritis Rheum. 2006 Aug;54(8):2462-70.

43. Goldring MB, Goldring SR. Articular cartilage and subchondral bone in the pathogenesis of osteoarthritis. Ann N Y Acad Sci. 2010 Mar;1192:230-7.

44. Intema F, Sniekers YH, Weinans H, Vianen ME, Yocum SA, Zuurmond AM, DeGroot J, Lafeber FP, Mastbergen SC. Similarities and discrepancies in subchondral bone structure in two differently induced canine models of osteoarthritis. J Bone Miner Res. 2010 Jul;25(7):1650-7.

45. Lories RJ, Luyten FP. The bone-cartilage unit in osteoarthritis. Nat Rev Rheumatol. 2011 Jan;7(1):43-9.

46. Yoshioka M, Coutts RD, Amiel D, Hacker SA. Characterization of a model of osteoarthritis in the rabbit knee. Osteoarthritis Cartilage. 1996 Jun;4(2):87-98.

47. Vignon E, Bejui J, Mathieu P, Hartmann JD, Ville G, Evreux JC, Descotes J. Histological cartilage changes in a rabbit model of osteoarthritis. J Rheumatol. 1987 May;14 Spec No:104-6.

48. Chang DG, Iverson EP, Schinagl RM, Sonoda M, Amiel D, Coutts RD, Sah RL. Quantitation and localization of cartilage degeneration following the induction of osteoarthritis in the rabbit knee. Osteoarthritis Cartilage. 1997 Sep;5(5):357-72.

49. Batiste DL, Kirkley A, Laverty S, Thain LM, Spouge AR, Holdsworth DW. Ex vivo characterization of articular cartilage and bone lesions in a rabbit ACL transection model of osteoarthritis using MRI and micro-CT. Osteoarthritis Cartilage. [Research Support, Non-U.S. Gov't]. 2004 Dec;12(12):986-96.

50. Colombo C, Butler M, O'Byrne E, Hickman L, Swartzendruber D, Selwyn M, Steinetz B. A new model of osteoarthritis in rabbits. I. Development of knee joint pathology following lateral meniscectomy and section of the fibular collateral and sesamoid ligaments. Arthritis Rheum. 1983 Jul;26(7):875-86.

51. Moreland LW. Intra-articular hyaluronan (hyaluronic acid) and hylans for the treatment of osteoarthritis: mechanisms of action. Arthritis Res Ther. 2003;5(2):54-67.

52. Elmali N, Esenkaya I, Harma A, Ertem K, Turkoz Y, Mizrak B. Effect of resveratrol in experimental osteoarthritis in rabbits. Inflammation research : official journal of the European Histamine Research Society [et al]. 2005 Apr;54(4):158-62.

53. Goldberg VM, Buckwalter JA. Hyaluronans in the treatment of osteoarthritis of the knee: evidence for disease-modifying activity. Osteoarthritis Cartilage. 2005 Mar;13(3):216-24.

54. Kikuchi T, Sakuta T, Yamaguchi T. Intra-articular injection of collagenase induces experimental osteoarthritis in mature rabbits. Osteoarthritis Cartilage. 1998 May;6(3):177-86.

55. Bentley G. Papain-induced degenerative arthritis of the hip in rabbits. J Bone Joint Surg Br. 1971 May;53(2):324-37.

56. Radin EL, Martin RB, Burr DB, Caterson B, Boyd RD, Goodwin C. Effects of mechanical loading on the tissues of the rabbit knee. J Orthop Res. 1984;2(3):221-34.

57. Roemhildt ML, Beynnon BD, Gardner-Morse M, Badger G, Grant C. Changes induced by chronic in vivo load alteration in the tibiofemoral joint of mature rabbits. J Orthop Res. 2012 Sep;30(9):1413-22.

58. Smith GK, Mayhew PD, Kapatkin AS, McKelvie PJ, Shofer FS, Gregor TP. Evaluation of risk factors for degenerative joint disease associated with hip dysplasia in German Shepherd Dogs, Golden Retrievers, Labrador Retrievers, and Rottweilers. Journal of the American Veterinary Medical Association. 2001 Dec 15;219(12):1719-24.

59. Clements DN, Carter SD, Innes JF, Ollier WE. Genetic basis of secondary osteoarthritis in dogs with joint dysplasia. American journal of veterinary research. 2006 May;67(5):909-18.

60. Rogachefsky RA, Dean DD, Howell DS, Altman RD. Treatment of canine osteoarthritis with insulin-like growth factor-1 (IGF-1) and sodium pentosan polysulfate. Osteoarthritis Cartilage. 1993 Apr;1(2):105-14.

61. Ratcliffe A, Billingham ME, Saed-Nejad F, Muir H, Hardingham TE. Increased release of matrix components from articular cartilage in experimental canine osteoarthritis. J Orthop Res. 1992 May;10(3):350-8.

62. Wyland DJ, Guilak F, Elliott DM, Setton LA, Vail TP. Chondropathy after meniscal tear or partial meniscectomy in a canine model. J Orthop Res. 2002 Sep;20(5):996-1002.

63. Oettmeier R, Arokoski J, Roth AJ, Helminen HJ, Tammi M, Abendroth K. Quantitative study of articular cartilage and subchondral bone remodeling in the knee joint of dogs after strenuous running training. J Bone Miner Res. 1992 Dec;7 Suppl 2:S419-24.

64. Intema F, Hazewinkel HA, Gouwens D, Bijlsma JW, Weinans H, Lafeber FP, Mastbergen SC. In early OA, thinning of the subchondral plate is directly related to cartilage damage: results from a canine ACLT-meniscectomy model. Osteoarthritis Cartilage. 2010 May;18(5):691-8.

65. Smith GN, Jr., Myers SL, Brandt KD, Mickler EA. Effect of intraarticular hyaluronan injection in experimental canine osteoarthritis. Arthritis Rheum. 1998 Jun;41(6):976-85.

66. Kiviranta I, Tammi M, Jurvelin J, Saamanen AM, Helminen HJ. Moderate running exercise augments glycosaminoglycans and thickness of articular cartilage in the knee joint of young beagle dogs. J Orthop Res. 1988;6(2):188-95.

67. Impellizeri JA, Tetrick MA, Muir P. Effect of weight reduction on clinical signs of lameness in dogs with hip osteoarthritis. Journal of the American Veterinary Medical Association. 2000 Apr 1;216(7):1089-91.

68. Yu LP, Jr., Smith GN, Jr., Brandt KD, Myers SL, O'Connor BL, Brandt DA. Reduction of the severity of canine osteoarthritis by prophylactic treatment with oral doxycycline. Arthritis Rheum. 1992 Oct;35(10):1150-9.

69. Little C, Smith S, Ghosh P, Bellenger C. Histomorphological and immunohistochemical evaluation of joint changes in a model of osteoarthritis induced by lateral meniscectomy in sheep. J Rheumatol. 1997 Nov;24(11):2199-209.

70. Funakoshi Y, Hariu M, Tapper JE, Marchuk LL, Shrive NG, Kanaya F, Rattner JB, Hart DA, Frank CB. Periarticular ligament changes following ACL/MCL transection in an ovine stifle joint model of osteoarthritis. J Orthop Res. 2007 Aug;25(8):997-1006.

71. Kold SE, Hickman J, Melsen F. An experimental study of the healing process of equine chondral and osteochondral defects. Equine veterinary journal. 1986 Jan;18(1):18-24.

72. Brommer H, van Weeren PR, Brama PA, Barneveld A. Quantification and age-related distribution of articular cartilage degeneration in the equine fetlock joint. Equine veterinary journal. 2003 Nov;35(7):697-701.

73. Fortier LA, Potter HG, Rickey EJ, Schnabel LV, Foo LF, Chong LR, Stokol T, Cheetham J, Nixon AJ. Concentrated bone marrow aspirate improves full-thickness cartilage repair compared with microfracture in the equine model. J Bone Joint Surg Am. 2010 Aug 18;92(10):1927-37.

74. Frisbie DD, Ghivizzani SC, Robbins PD, Evans CH, McIlwraith CW. Treatment of experimental equine osteoarthritis by in vivo delivery of the equine interleukin-1 receptor antagonist gene. Gene therapy. 2002 Jan;9(1):12-20.

75. Todhunter RJ, Minor RR, Wootton JA, Krook L, Burton-Wurster N, Lust G. Effects of exercise and polysulfated glycosaminoglycan on repair of articular cartilage defects in the equine carpus. J Orthop Res. 1993 Nov;11(6):782-95.

76. Little CB, Zaki S. What constitutes an "animal model of osteoarthritis"--the need for consensus? Osteoarthritis Cartilage. 2012 Apr;20(4):261-7.

77. Bendele AM, Hulman JF. Spontaneous cartilage degeneration in guinea pigs. Arthritis Rheum. 1988 Apr;31(4):561-5.

78. Wang T, Wen CY, Yan CH, Lu WW, Chiu KY. Spatial and temporal changes of subchondral bone proceed to microscopic articular cartilage degeneration in guinea pigs with spontaneous osteoarthritis. Osteoarthritis Cartilage. [Research Support, Non-U.S. Gov't]. 2013 Apr;21(4):574-81.

79. Muraoka T, Hagino H, Okano T, Enokida M, Teshima R. Role of subchondral bone in osteoarthritis development: a comparative study of two strains of guinea pigs with and without spontaneously occurring osteoarthritis. Arthritis Rheum. 2007 Oct;56(10):3366-74.

80. Glasson SS, Blanchet TJ, Morris EA. The surgical destabilization of the medial meniscus (DMM) model of osteoarthritis in the 129/SvEv mouse. Osteoarthritis Cartilage. 2007 Sep;15(9):1061-9.

81. Bove SE, Laemont KD, Brooker RM, Osborn MN, Sanchez BM, Guzman RE, Hook KE, Juneau PL, Connor JR, Kilgore KS. Surgically induced osteoarthritis in the rat results in

the development of both osteoarthritis-like joint pain and secondary hyperalgesia. Osteoarthritis Cartilage. 2006 Oct;14(10):1041-8.

82. Moodie JP, Stok KS, Muller R, Vincent TL, Shefelbine SJ. Multimodal imaging demonstrates concomitant changes in bone and cartilage after destabilisation of the medial meniscus and increased joint laxity. Osteoarthritis Cartilage. 2011 Feb;19(2):163-70.

83. Botter SM, Glasson SS, Hopkins B, Clockaerts S, Weinans H, van Leeuwen JP, van Osch GJ. ADAMTS5-/- mice have less subchondral bone changes after induction of osteoarthritis through surgical instability: implications for a link between cartilage and subchondral bone changes. Osteoarthritis Cartilage. 2009 May;17(5):636-45.

84. McErlain DD, Appleton CT, Litchfield RB, Pitelka V, Henry JL, Bernier SM, Beier F, Holdsworth DW. Study of subchondral bone adaptations in a rodent surgical model of OA using in vivo micro-computed tomography. Osteoarthritis Cartilage. 2008 Apr;16(4):458-69.

85. Hayami T, Pickarski M, Zhuo Y, Wesolowski GA, Rodan GA, Duong le T. Characterization of articular cartilage and subchondral bone changes in the rat anterior cruciate ligament transection and meniscectomized models of osteoarthritis. Bone. 2006 Feb;38(2):234-43.

86. Hayami T, Zhuo Y, Wesolowski GA, Pickarski M, Duong le T. Inhibition of cathepsin K reduces cartilage degeneration in the anterior cruciate ligament transection rabbit and murine models of osteoarthritis. Bone. 2012 Jun;50(6):1250-9.

87. Christiansen BA, Anderson MJ, Lee CA, Williams JC, Yik JH, Haudenschild DR. Musculoskeletal changes following non-invasive knee injury using a novel mouse model of post-traumatic osteoarthritis. Osteoarthritis Cartilage. 2012 Jul;20(7):773-82.

88. Furman BD, Strand J, Hembree WC, Ward BD, Guilak F, Olson SA. Joint degeneration following closed intraarticular fracture in the mouse knee: a model of posttraumatic arthritis. J Orthop Res. 2007 May;25(5):578-92.

89. Lewis JS, Hembree WC, Furman BD, Tippets L, Cattel D, Huebner JL, Little D, DeFrate LE, Kraus VB, Guilak F, Olson SA. Acute joint pathology and synovial inflammation is associated with increased intra-articular fracture severity in the mouse knee. Osteoarthritis Cartilage. 2011 Jul;19(7):864-73.

90. Louer CR, Furman BD, Huebner JL, Kraus VB, Olson SA, Guilak F. Diet-induced obesity significantly increases the severity of posttraumatic arthritis in mice. Arthritis Rheum. 2012 Oct;64(10):3220-30.

91. Arden N, Nevitt MC. Osteoarthritis: epidemiology. Best Pract Res Clin Rheumatol. 2006 Feb;20(1):3-25.

92. Felson DT, Zhang Y, Hannan MT, Naimark A, Weissman B, Aliabadi P, Levy D. Risk factors for incident radiographic knee osteoarthritis in the elderly: the Framingham Study. Arthritis Rheum. 1997 Apr;40(4):728-33.

93. Hu K, Xu L, Cao L, Flahiff CM, Brussiau J, Ho K, Setton LA, Youn I, Guilak F, Olsen BR, Li Y. Pathogenesis of osteoarthritis-like changes in the joints of mice deficient in type IX collagen. Arthritis Rheum. 2006 Sep;54(9):2891-900.

94. Xu L, Flahiff CM, Waldman BA, Wu D, Olsen BR, Setton LA, Li Y. Osteoarthritis-like changes and decreased mechanical function of articular cartilage in the joints of mice with the chondrodysplasia gene (cho). Arthritis Rheum. 2003 Sep;48(9):2509-18.

95. Lapvetelainen T, Hyttinen M, Lindblom J, Langsjo TK, Sironen R, Li SW, Arita M, Prockop DJ, Puustjarvi K, Helminen HJ. More knee joint osteoarthritis (OA) in mice after inactivation of one allele of type II procollagen gene but less OA after lifelong voluntary wheel running exercise. Osteoarthritis Cartilage. [Research Support, Non-U.S. Gov't]. 2001 Feb;9(2):152-60.

96. Neuhold LA, Killar L, Zhao W, Sung ML, Warner L, Kulik J, Turner J, Wu W, Billinghurst C, Meijers T, Poole AR, Babij P, DeGennaro LJ. Postnatal expression in hyaline cartilage of constitutively active human collagenase-3 (MMP-13) induces osteoarthritis in mice. J Clin Invest. 2001 Jan;107(1):35-44.

97. Stanton H, Rogerson FM, East CJ, Golub SB, Lawlor KE, Meeker CT, Little CB, Last K, Farmer PJ, Campbell IK, Fourie AM, Fosang AJ. ADAMTS5 is the major aggrecanase in mouse cartilage in vivo and in vitro. Nature. 2005 Mar 31;434(7033):648-52.

98. Glasson SS, Askew R, Sheppard B, Carito B, Blanchet T, Ma HL, Flannery CR, Peluso D, Kanki K, Yang Z, Majumdar MK, Morris EA. Deletion of active ADAMTS5 prevents cartilage degradation in a murine model of osteoarthritis. Nature. 2005 Mar 31;434(7033):644-8.

99. Mason RM, Chambers MG, Flannelly J, Gaffen JD, Dudhia J, Bayliss MT. The STR/ort mouse and its use as a model of osteoarthritis. Osteoarthritis Cartilage. 2001 Feb;9(2):85-91.

100. Chambers MG, Cox L, Chong L, Suri N, Cover P, Bayliss MT, Mason RM. Matrix metalloproteinases and aggrecanases cleave aggrecan in different zones of normal cartilage but colocalize in the development of osteoarthritic lesions in STR/ort mice. Arthritis Rheum. 2001 Jun;44(6):1455-65.

101. Stoop R, van der Kraan PM, Buma P, Hollander AP, Billinghurst RC, Poole AR, van den Berg WB. Type II collagen degradation in spontaneous osteoarthritis in C57Bl/6 and BALB/c mice. Arthritis Rheum. 1999 Nov;42(11):2381-9.

102. Griffin TM, Huebner JL, Kraus VB, Guilak F. Extreme obesity due to impaired leptin signaling in mice does not cause knee osteoarthritis. Arthritis Rheum. 2009 Oct;60(10):2935-44.

103. Griffin TM, Fermor B, Huebner JL, Kraus VB, Rodriguiz RM, Wetsel WC, Cao L, Setton LA, Guilak F. Diet-induced obesity differentially regulates behavioral, biomechanical, and molecular risk factors for osteoarthritis in mice. Arthritis Res Ther. 2010;12(4):R130.

104. Griffin TM, Huebner JL, Kraus VB, Yan Z, Guilak F. Induction of osteoarthritis and metabolic inflammation by a very high-fat diet in mice: effects of short-term exercise. Arthritis Rheum. 2012 Feb;64(2):443-53.

105. Lapvetelainen T, Nevalainen T, Parkkinen JJ, Arokoski J, Kiraly K, Hyttinen M, Halonen P, Helminen HJ. Lifelong moderate running training increases the incidence and severity of osteoarthritis in the knee joint of C57BL mice. Anat Rec. 1995 Jun;242(2):159-65.

106. Galois L, Etienne S, Grossin L, Watrin-Pinzano A, Cournil-Henrionnet C, Loeuille D, Netter P, Mainard D, Gillet P. Dose-response relationship for exercise on severity of

experimental osteoarthritis in rats: a pilot study. Osteoarthritis Cartilage. 2004 Oct;12(10):779-86.

107. Poulet B, Hamilton RW, Shefelbine S, Pitsillides AA. Characterizing a novel and adjustable noninvasive murine joint loading model. Arthritis Rheum. 2011 Jan;63(1):137-47.

108. Ko FC, Dragomir C, Plumb DA, Goldring SR, Wright TM, Goldring MB, van der Meulen MC. In vivo cyclic compression causes cartilage degeneration and subchondral bone changes in mouse tibiae. Arthritis Rheum. 2013 Jun;65(6):1569-78.

109. Fritton JC, Myers ER, Wright TM, van der Meulen MC. Loading induces site-specific increases in mineral content assessed by microcomputed tomography of the mouse tibia. Bone. 2005 Jun;36(6):1030-8.

110. Lynch ME, Main RP, Xu Q, Walsh DJ, Schaffler MB, Wright TM, van der Meulen MC. Cancellous bone adaptation to tibial compression is not sex dependent in growing mice. J Appl Physiol. 2010 Sep;109(3):685-91.

111. Guo X, Day TF, Jiang X, Garrett-Beal L, Topol L, Yang Y. Wnt/beta-catenin signaling is sufficient and necessary for synovial joint formation. Genes Dev. 2004 Oct 1;18(19):2404-17.

112. Luyten FP, Tylzanowski P, Lories RJ. Wnt signaling and osteoarthritis. Bone. 2009 Apr;44(4):522-7.

113. Li J, Sarosi I, Cattley RC, Pretorius J, Asuncion F, Grisanti M, Morony S, Adamu S, Geng Z, Qiu W, Kostenuik P, Lacey DL, Simonet WS, Bolon B, Qian X, Shalhoub V, Ominsky MS, Zhu Ke H, Li X, Richards WG. Dkk1-mediated inhibition of Wnt signaling in bone results in osteopenia. Bone. 2006 Oct;39(4):754-66.

114. Gong Y, Slee RB, Fukai N, Rawadi G, Roman-Roman S, Reginato AM, Wang H, Cundy T, Glorieux FH, Lev D, Zacharin M, Oexle K, Marcelino J, Suwairi W, Heeger S, Sabatakos G, Apte S, Adkins WN, Allgrove J, Arslan-Kirchner M, Batch JA, Beighton P, Black GC, Boles RG, Boon LM, Borrone C, Brunner HG, Carle GF, Dallapiccola B, De Paepe A, Floege B, Halfhide ML, Hall B, Hennekam RC, Hirose T, Jans A, Juppner H, Kim CA, Keppler-Noreuil K, Kohlschuetter A, LaCombe D, Lambert M, Lemyre E, Letteboer T, Peltonen L, Ramesar RS, Romanengo M, Somer H, Steichen-Gersdorf E, Steinmann B, Sullivan B, Superti-Furga A, Swoboda W, van den Boogaard MJ, Van Hul W, Vikkula M, Votruba M, Zabel B, Garcia T, Baron R, Olsen BR, Warman ML. LDL receptor-related protein 5 (LRP5) affects bone accrual and eye development. Cell. 2001 Nov 16;107(4):513-23.

115. Diarra D, Stolina M, Polzer K, Zwerina J, Ominsky MS, Dwyer D, Korb A, Smolen J, Hoffmann M, Scheinecker C, van der Heide D, Landewe R, Lacey D, Richards WG, Schett G. Dickkopf-1 is a master regulator of joint remodeling. Nat Med. 2007 Feb;13(2):156-63.

116. Wang J, Zhou D, He X, Wang Y, Hu W, Jiang L, Dou J. Effect of downregulated beta-catenin on cell proliferative activity, the sensitivity to chemotherapy drug and tumorigenicity of ovarian cancer cells. Cell Mol Biol (Noisy-le-grand). 2011;57 Suppl:OL1606-13.

117. Weng LH, Wang CJ, Ko JY, Sun YC, Wang FS. Control of Dkk-1 ameliorates chondrocyte apoptosis, cartilage destruction, and subchondral bone deterioration in osteoarthritic knees. Arthritis Rheum. 2010 May;62(5):1393-402.

118. Oh H, Chun CH, Chun JS. Dkk-1 expression in chondrocytes inhibits experimental osteoarthritic cartilage destruction in mice. Arthritis Rheum. 2012 Aug;64(8):2568-78.

119. Lewis SL, Khoo PL, De Young RA, Steiner K, Wilcock C, Mukhopadhyay M, Westphal H, Jamieson RV, Robb L, Tam PP. Dkk1 and Wnt3 interact to control head morphogenesis in the mouse. Development. 2008 May;135(10):1791-801.

CHAPTER 2

IN VIVO CYCLIC COMRESSION CAUSES CARTILAGE DEGENERATION AND SUBCHONDRAL BONE CHANGES IN MOUSE TIBIAE

2.1 Introduction

Osteoarthritis (OA) affects nearly 27 million individuals in the United States and is the major cause of disability in the adult population [1]. Both systemic and environmental factors, including ethnicity, nutritional factors, genetic background, sex, obesity, and joint injury contribute to the development of OA [2]. In particular, the onset and development of OA is greatly influenced by alterations in the local mechanical loading environment in the joint that may result from prior joint injuries, occupational activities involving heavy lifting or repeated joint loading, or obesity [2, 3].

Loading environment plays both beneficial and detrimental roles in the properties of articular cartilage and the risk for the eventual development of OA. Dynamic compressive loading of bovine cartilage explants increases proteoglycan uptake and synthesis [4, 5], and regular moderate running routines in hamsters and rats prevent both naturally occurring and injury-related cartilage degeneration [6, 7]. Evidence from animal and clinical studies established mild to moderate exercise as a recommended non-pharmacological intervention that both prevents and alleviates OA symptoms in patients [8-10].

Mechanical loading can also be detrimental to maintaining healthy articular cartilage and preventing the initiation and progression of OA symptoms. A single injurious compression load at a high strain rate or repeated compressive cyclic loading decreases cartilage stiffness and cell viability of chondrocytes and increases aggrecanase expression in bovine cartilage explants [11-

13]. Clinically, lifting heavy objects in certain occupations, increased body mass, and repetitive physical loading are associated with hip and knee OA [3, 14, 15]. The reduction in body weight with an exercise regime effectively reduces pain and increases joint mobility in OA patients [16].

Despite the correlation between the loading environment and the risk for the development of OA in humans, limited studies have investigated the effects of defined mechanical loads and age on the development of OA-like structural alterations in animal models [17]. Animal models that initiate OA through surgical disruption are confounded by the adverse effects of the surgical insult and the post-surgical healing response, as well as the inability to rigorously control the mechanical loading environment within the affected joint [18, 19].

Our studies were undertaken to establish the effects of mechanical loading at defined magnitudes on the structural organization and composition of articular cartilage and subchondral bone. Histological and radiological changes were assessed in mouse knee joints in adult mice subjected to *in vivo* tibial loading at defined magnitudes (4.5N and 9.0N) for durations of 1, 2, and 6 weeks and at 9.0N peak load in young mice. We hypothesized that the alterations in the cartilage and subchondral bone would depend on the magnitude and duration of the load and that the responses to the high peak load would be influenced by the age of the mice.

2.2 Materials and Method

Mechanical Loading Conditions

To test the effects of load duration on the joint changes, we subjected the left tibiae of twenty-one young (10-week-old) C57Bl/6 male mice (Jackson Laboratories, Bar Harbor, ME) to cyclic compressive loading for 1, 2, and 6 weeks at a 9.0N peak load. We also loaded the tibiae of forty-two adult (26-week-old) C57Bl/6 male mice at 4.5N and 9.0N peak loads for 1, 2, and 6

weeks. A load level of 9.0N generates 1200με in the tibial mid-shaft of 10-week-old mice based on *in vivo* strain gauging [20]. *In vivo* tibial loading was applied for 1200 cycles at 4 Hz for 5 days per week at each peak load under general anesthesia (2% Isoflurane, 1.0 L/min, Webster). The applied loading was based on protocols demonstrated previously to have an anabolic effect on the tibial metaphysis in growing and adult mice (Supp Figure 2.1) [20-22]. The left limb was loaded, and the right limb served as the non-loaded control. In preliminary studies in our laboratory, we found that metaphyseal bone mass and architecture of the non-loaded control (right) limbs were not affected by loading of the left limbs. After the specified duration, the mice were euthanized, and the intact knee joints were dissected and fixed in 10% formalin overnight. All experimental procedures were approved by the Institutional Animal Care and Use Committee.

Cartilage and Subchondral Bone Assessment

After tissue fixation overnight, intact joints in PBS were scanned by microcomputed tomography (microCT) with an isotropic voxel resolution of 10 μm (μCT35, Scanco: 55 kVp, 145 μA, 600 ms integration time, no frame averaging) to assess bone morphological changes. A 0.5mm aluminum filter reduced the effects of beam hardening. Knee joints were then decalcified in EDTA for 2 weeks, dehydrated in an ethanol gradient, and embedded in paraffin. Serial coronal sections (6 μm thick) were obtained from posterior to anterior using a rotary microtome (Leica RM2255, Germany). Safranin O/Fast green staining was performed on sections at 90 μm intervals to assess cartilage morphology. Cartilage degeneration was assessed in the tibial plateau using a modified murine cartilage histological scoring system [23].

Bone morphology from microCT was assessed in two regions: the metaphysis (distal to the growth plate) extending 10% of the total bone length, excluding primary spongiosa and cortical

bone; and the epiphysis (proximal to the growth plate) excluding cortical bone. Trabecular bone from both regions was isolated by manually contouring inside the cortical shell. The global threshold was set at 3100 HU to segment mineralized tissue. For each region, cancellous bone volume fraction, trabecular thickness and separation, and tissue mineral density were measured. Also, localized thickness measurements of subchondral cortical bone (Sub. Pl.) and cartilage were performed using Osteomeasure (OsteoMetrics, USA) on representative Safranin O/Fast green stained sections previously used for histological scoring. Six different regions of interest were defined by dividing the tibial plateau into medial and lateral halves, each of which was then further divided into anterior, middle, and posterior regions. A single representative section from each of six regions of each joint from all animals was chosen to measure localized thickness. Five linear projections from the cartilage surface to the boundary between the cartilage and subchondral bone, including calcified cartilage, were used to measure cartilage thickness. The projection was extended into the subchondral bone to measure the subchondral bone thickness [24].

Statistics

In adult mice, the effects of loading, load level, and duration were detected using a 3-factor repeated measure ANOVA with interactions (JMP Pro 9.02, SAS Institute Inc), with loading as the intra-group variable, and load level and duration as inter-group variables. In young mice, the effects of loading and duration were detected using a 2-factor repeated measure ANOVA with interactions with loading as the intra-group variable and duration as inter-group variable. Post-hoc means comparison tests with Bonferroni correction were performed only when interaction

effects were significant. P-values < 0.05 indicated significance. All values are presented as mean ± SD.

2.3 Results

Articular Cartilage Matrix Changes

Mechanical loading induced cartilage matrix changes, including cartilage fibrillation, fragmentation, and erosion in both young and adult mice (Fig. 2.1A). As load duration increased, damage in the cartilage matrix increased, visualized by loss of Safranin O staining and cartilage thinning. The high (9.0N) load level induced more dramatic changes than the low (4.5N) load level in adult mice. After 6 weeks of loading at 9.0N, almost the entire cartilage thickness was lost in the adult mice based on Safranin O staining, while only slight cartilage surface fibrillation was apparent in joints loaded with 4.5N. The high peak load produced marked cartilage thinning in the young mice but the changes were less severe than those observed in the adult mice. We, therefore, did not examine young mice subjected to the low peak load.

The quantitative cartilage scoring confirmed the observations of the histological staining (Fig. 2.1B,C). At both ages the histological score increased with loading: 2.8-fold in young and 1.8-fold in adult mice (loaded and control limbs pooled individually at all time points). Both longer duration of loading and higher load level increased the histological score in adult mice. In young mice, the response to high peak load was delayed and not apparent until the 6-week time point.

Cartilage thickness changes varied with location in the tibial plateau. In young mice, cartilage thinning was apparent at the posterior aspect of the lateral and medial tibial plateau (Fig. 2.2A, Supp Table 2.2). However, cartilage thickness did not change or increased in the loaded joint at the anterior aspect of the lateral plateau. Similar changes in cartilage thickness occurred

in the adult mice with loading (Fig. 2B, Supp Table 2.1) including increased cartilage thinning at the posterior aspect of the lateral tibial plateau, and were promoted by higher load level and longer duration of loading.

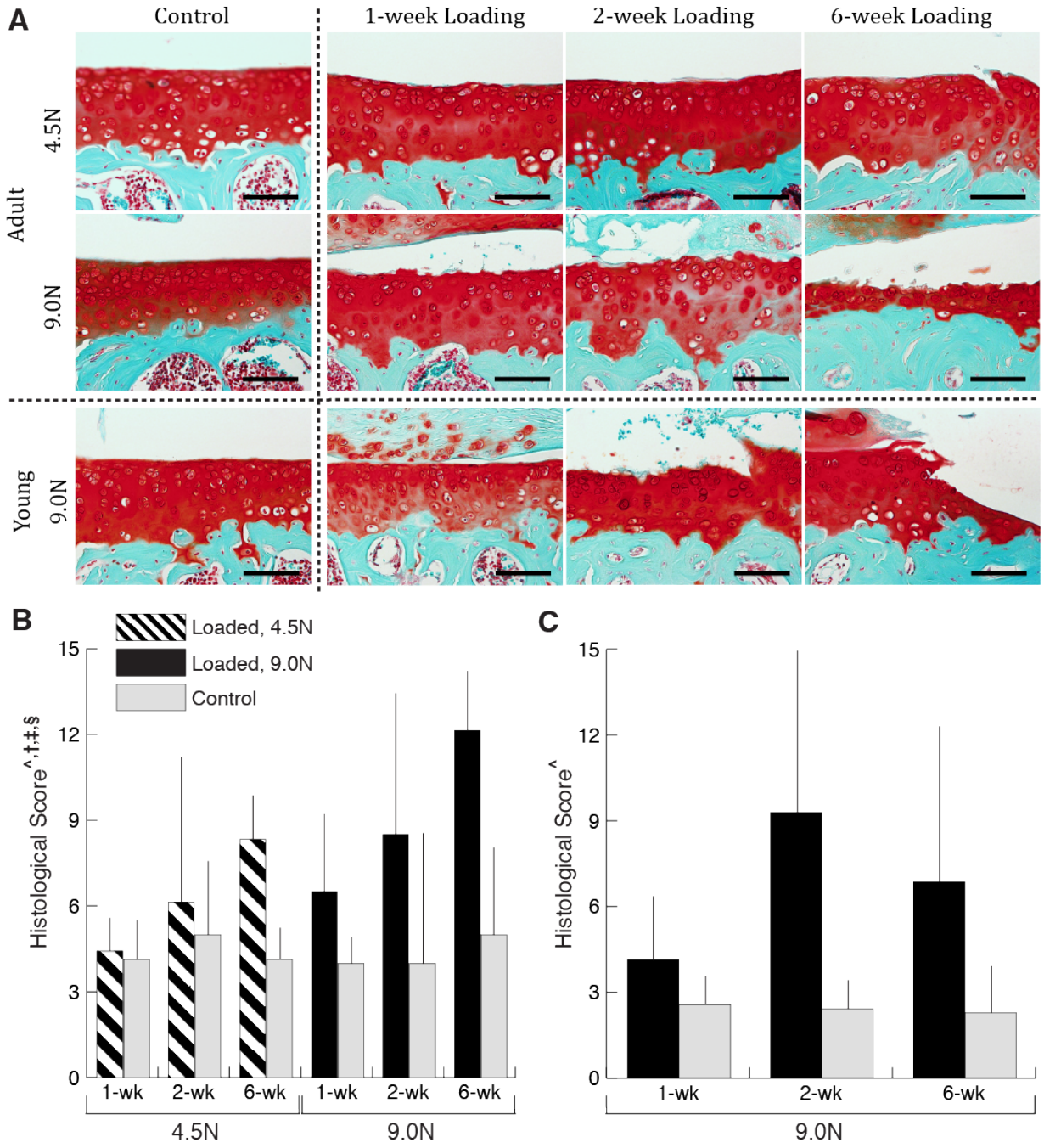

Figure 2.1 Qualitative (A) and quantitative (B, C) measures of cartilage matrix changes. Cartilage damage is evident following mechanical loading in both young and adult mice, and

was exacerbated with longer durations and higher level of loading in adult mice (A, Scale bar = 100 μm). Safranin O/Fast Green staining of the medial side of articular cartilage in young and adult mice loaded for 1-, 2- and 6-weeks and at two load levels (4.5N and 9.0N) for adult mice. Control images represent the non-loaded contralateral limb at 6-week duration at each respective age and load level. Loading increased histological scores in both adult (B) and young (C) mice. Duration of loading increased the histological score in adult mice. Load-induced increases in histological score depended on load level and duration in adult mice. Data presented as mean ± SD.

$^{\wedge}$loading, †duration, ‡loading*duration, §loading*load level effect, $p<0.05$ by repeated measures two-way ANOVA for young mice and repeated measures three-way ANOVA for adult mice.

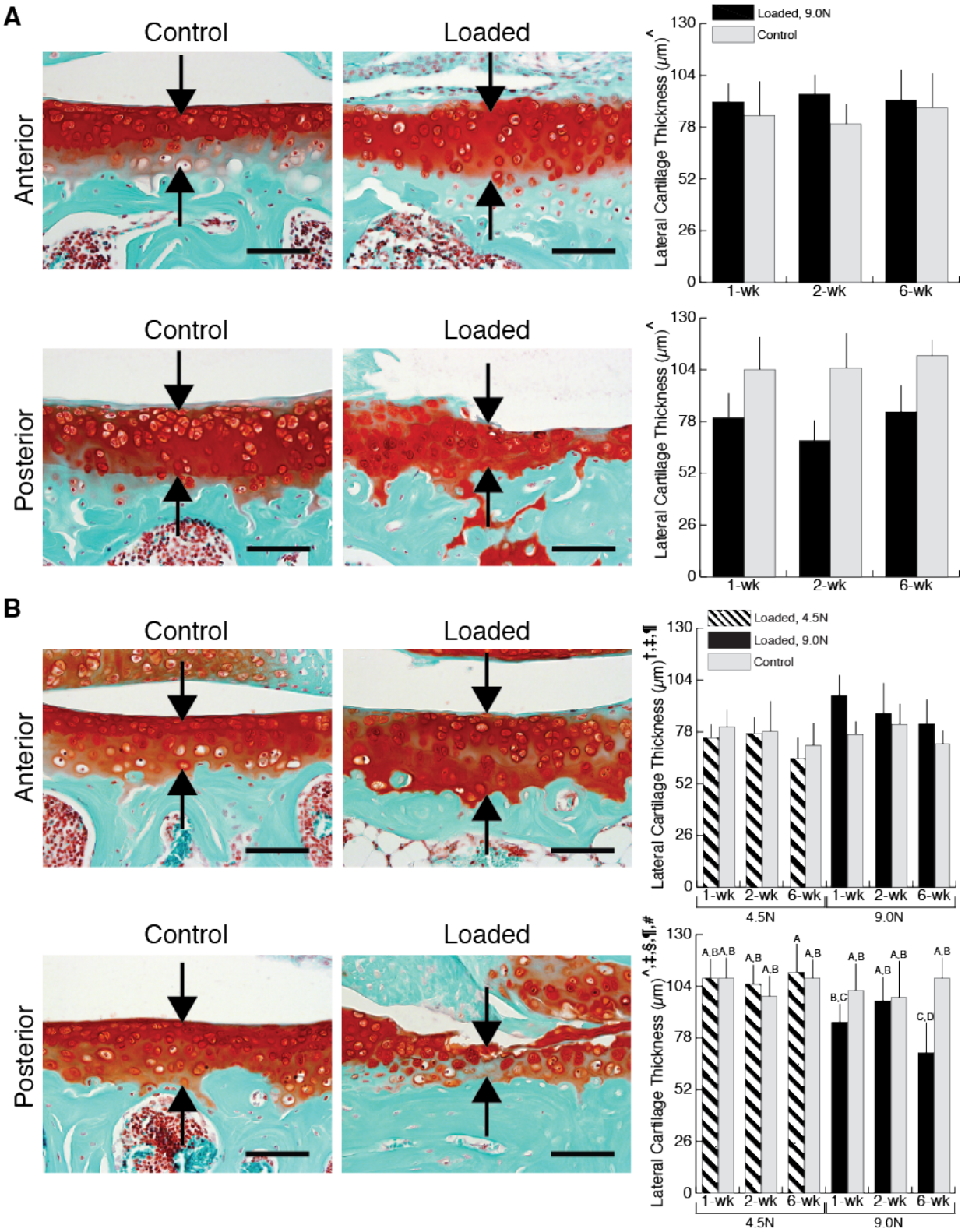

Figure 2.2 Localized cartilage thickness for young (A) and adult (B) mice. Safranin O/Fast Green images (Scale bar = 100 μm) represent control and loaded limbs at 9.0N for 6-week duration at each respective age. Cartilage thinned with loading on the posterior side of the lateral

tibial plateau in young mice. Adult mice also underwent cartilage thinning with loading posteriorly on the lateral plateau. Higher load level and longer duration of loading increased load-induced thinning of laterial-posterior tibial plateau cartilage. Data presented as mean ± SD. ^loading, †duration, ‡load level, §loading*duration, ¶loading*load level, ♯loading*duration*load level effect, $p<0.05$ by repeated measures two-way ANOVA for young mice and repeated measures three-way ANOVA for adult mice. Groups with different letters are significantly different by post-hoc means comparisons with Bonferroni correction.

Epiphyseal and Metaphyseal Bone Adaptation

In addition to cartilage matrix changes, we observed alterations in the epiphyseal cancellous bone in response to in vivo tibial loading. In both adult and young mice, loading at 9N decreased epiphyseal bone mass with a greater decrease observed in the adult mice compared to the young mice (14% versus 4.9%, respectively) (Fig. 2.3). The decreased bone mass was attributable to the increased trabecular separation, which translated to decreased trabecular number in adult mice. In the adult mice, the decreased bone mass was dependent on the load with greater decrease observed in the higher load group (Fig. 2.3D-F).

In contrast to the epiphyseal bone, metaphyseal bone mass increased by 20% with loading in young mice (Fig. 2.4A-C). The increased cancellous bone mass was due to trabecular thickening, which increased by 32%. Also, longer duration of loading further increased the trabecular thickness. No change in metaphyseal bone mass was present in adult mice (Fig. 2.4D-F); loading promoted trabecular thickening, which was counteracted by the increase in trabecular separation that inversely related to lower number of trabeculae.

The adaptive pattern of epiphyseal subchondral cortical bone in response to load differed from the pattern observed in the epiphyseal cancellous bone (Fig. 2.5, Supp Tables 1 and 2). In contrast to the decreased cancellous bone in response to load, both young and adult mice exhibited thickening of the subchondral cortical bone at the posterior-lateral aspect of the tibial plateau. On the anterior side, age-dependent subchondral cortical bone changes occurred. In

young mice at the end of the 6-week loading duration, subchondral cortical bone thinned while in adult mice, the thickness did not change.

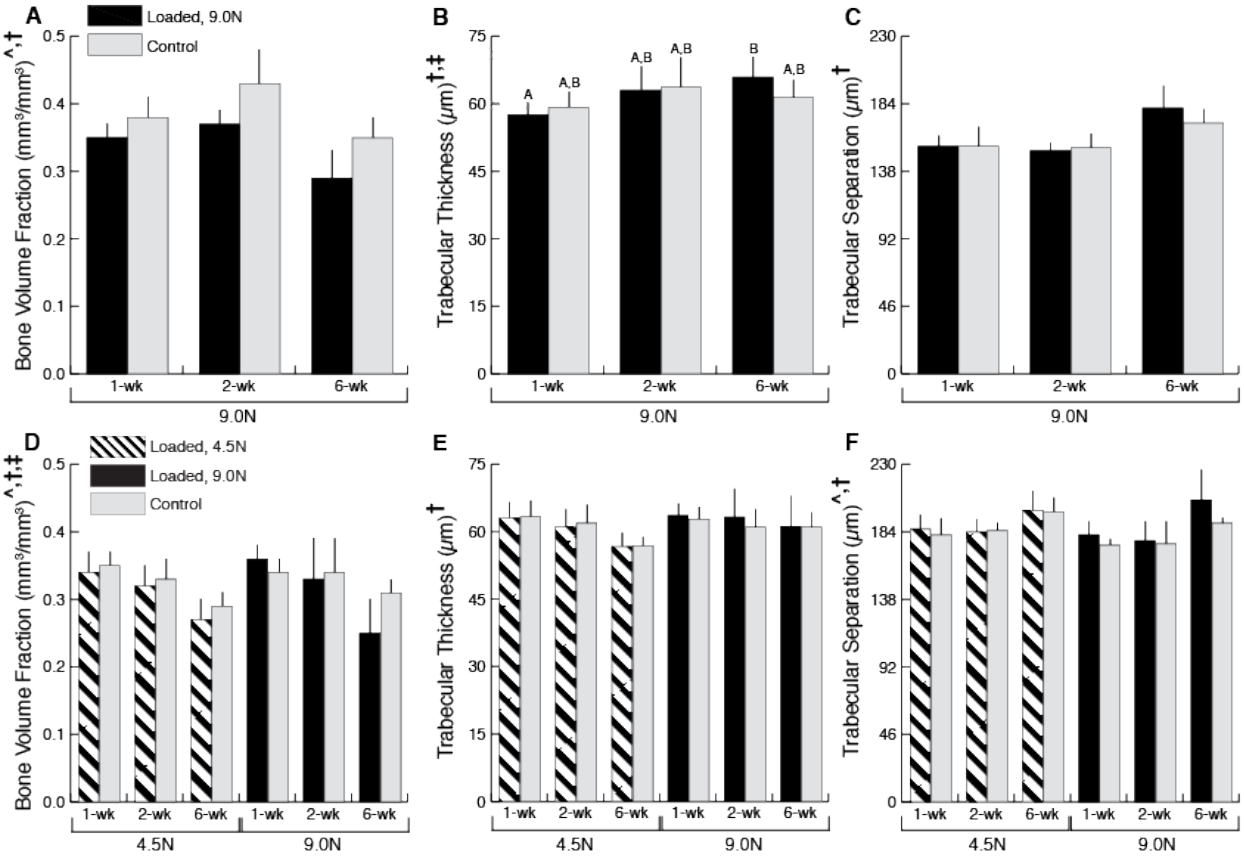

Figure 2.3 Epiphyseal cancellous bone microCT measurements from young (A-C) and adult (D-F) mice. The decreased bone mass was attributable to the increased trabecular separation, which translated to decreased trabecular number, in adult mice. Trabecular thickness was not altered by loading in both adult and young mice. Data presented as mean ± SD.
^loading, †duration, ‡loading*duration effect, $p<0.05$ by repeated measures two-way ANOVA for young mice and repeated measures three-way ANOVA for adult mice. Groups with different letters are significantly different by post-hoc means comparisons with Bonferroni correction.

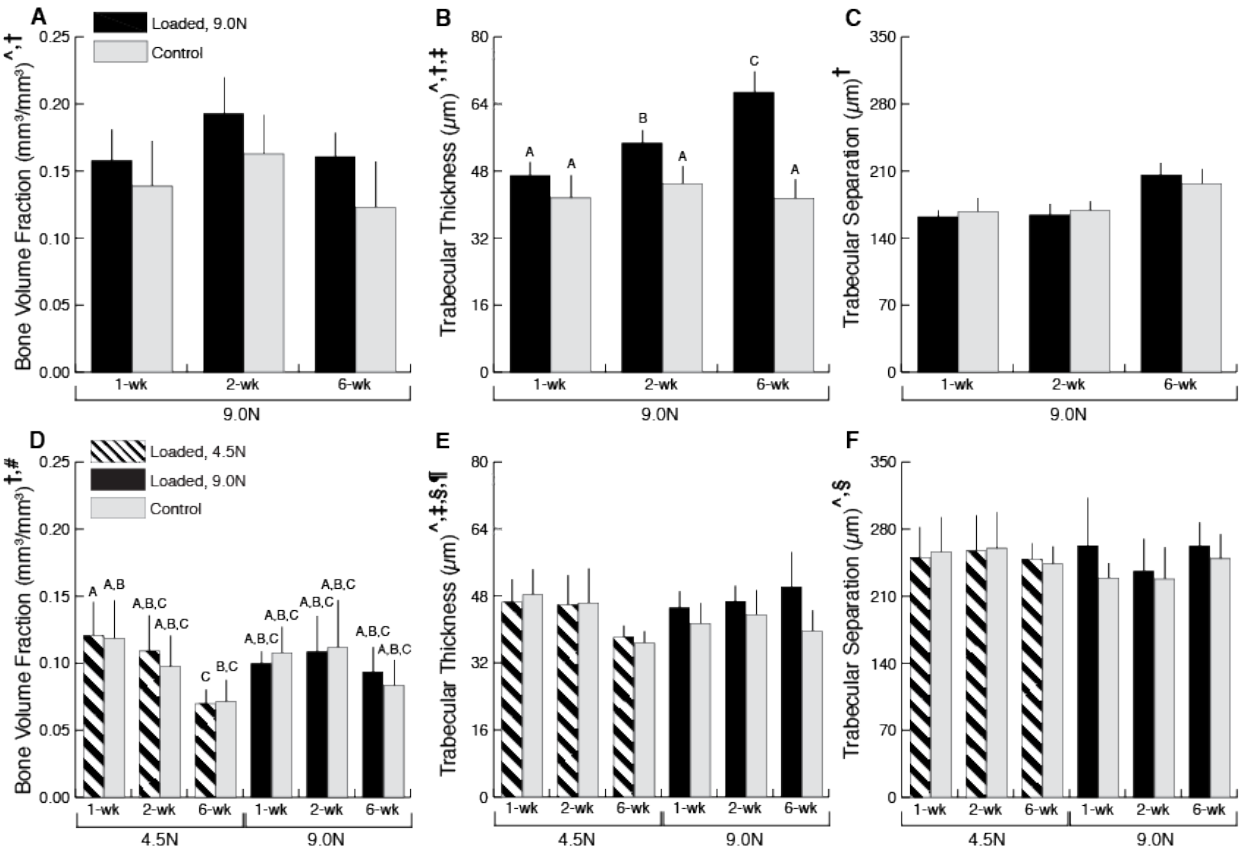

Figure 2.4 Metaphyseal cancellous bone microCT measures for young (A-C) and adult (D-F) mice. Loading increased cancellous mass in young mice through thickening of trabeculae. In adult mice cancellous mass was not altered with loading. Data presented as mean ± SD. ^loading, †duration, ‡loading*duration, §loading*load level, ¶load level*duration, #load*duration*load level effect, $p<0.05$ by repeated measures two-way ANOVA for young mice and repeated measures three-way ANOVA for adult mice. Groups with different letters are significantly different by post-hoc means comparisons with Bonferroni correction.

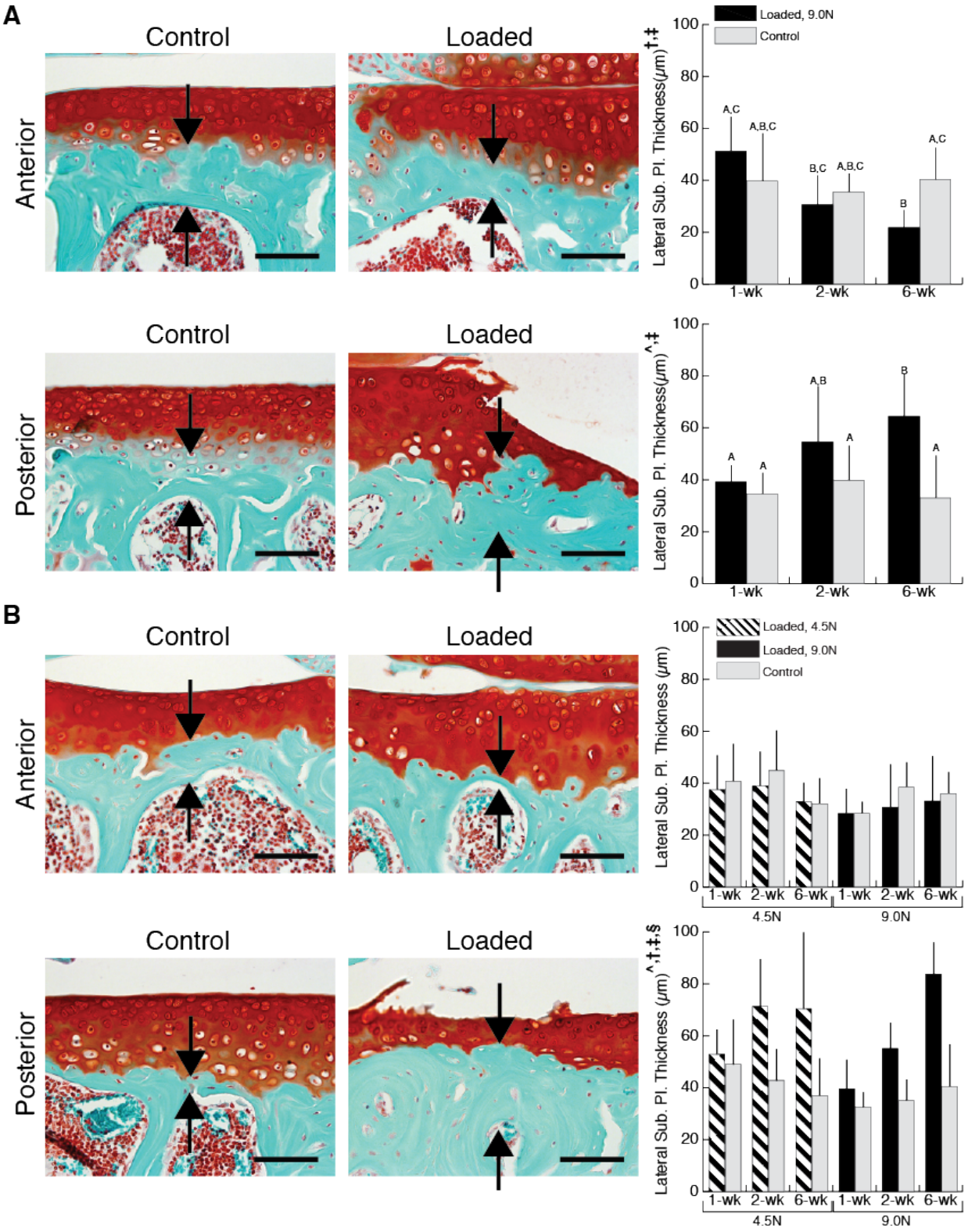

Figure 2.5 Localized subchondral cortical bone thickness in young (A) and adult (B) mice. Safranin O/Fast Green images (Scale bar = 100 μm) represent control and loaded limbs at 9.0N for 6-week duration at each respective age. The subchondral bone thickened with loading at the

posterior aspect of the lateral tibial plateau in young mice. Load level and duration affected load-induced thickening of the subchondral plate on the lateral side. Adult mice also underwent subchondral plate thickening with loading at the posterior aspect of the lateral tibial plateau. Data presented as mean ± SD.
^loading, †duration, ‡loading*duration, §duration*load level effect, $p<0.05$ by repeated measures two-way ANOVA for young mice and repeated measures three-way ANOVA for adult mice. Groups with different letters are significantly different by post-hoc means comparisons with Bonferroni correction.

Osteophyte formation

Mechanical loading also induced periarticular osteophyte formation at the tibial joint margins in the 9.0N-loaded limbs of both young and adult mice (Fig. 2.6). After 1 and 2 weeks of loading, cartilage was present in the marginal periarticular tissue, which then mineralized after 6 weeks of loading. The 4.5N load level did not induce formation of any cartilaginous tissue after 1 or 2 weeks or any mineralized tissue after 6 weeks of loading in adult mice.

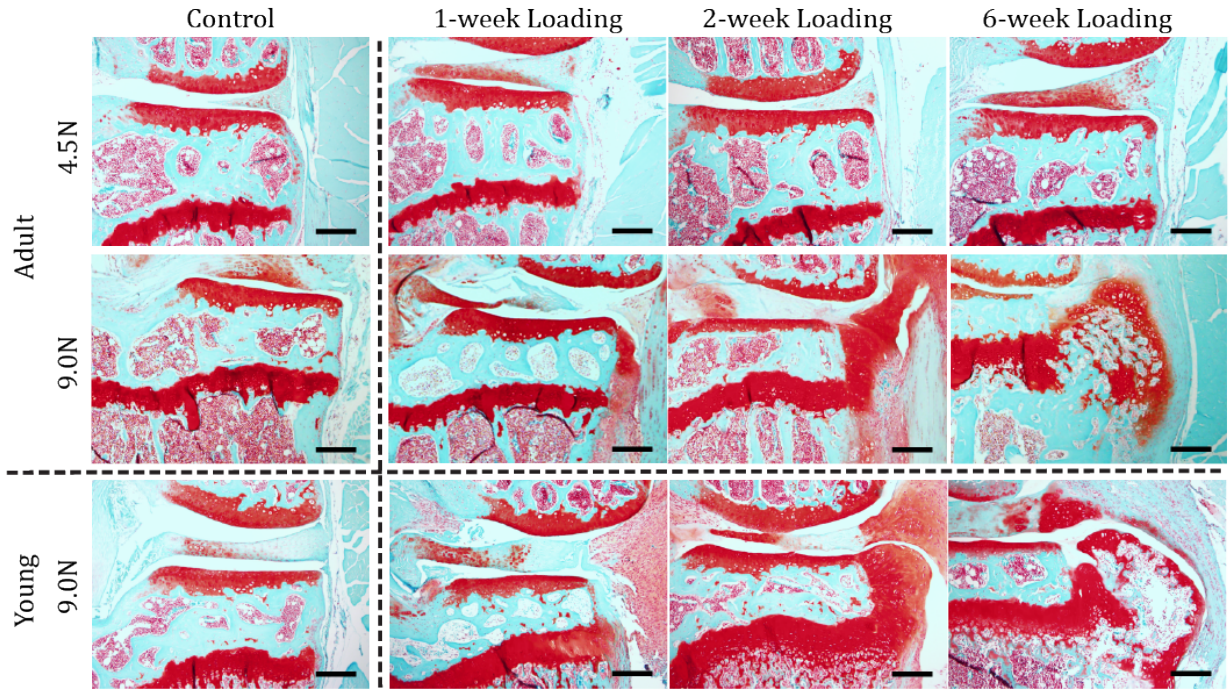

Figure 2.6 Mechanical loading induced osteophyte formation in both young and adult mice at the 9.0N load level. The lower load level did not induce osteophyte formation in adult mice. Safranin O/Fast Green staining of the medial side of the knee joint in young and adult mice loaded for 1-, 2-, and 6-weeks at two different load levels (only for adult mice). Control images

represent non-loaded contralateral limbs at 6-weeks of load duration at each respective age and load level. Scale bar 200 μm.

2.4 Discussion

Noninvasive mechanical loading induced cartilage matrix damage, epiphyseal bone adaptation, and osteophyte formation in both age groups, recapitulating the morphological and anatomic features of OA in both cartilage and bone. Metaphyseal bone adaptation to mechanical loading occurred only in the young mice. In addition to gross morphological changes in cartilage, cartilage thickness decreased and subchondral cortical bone thickness increased in the posterior-lateral aspect of the tibial plateau in response to loading in both age groups, while at the anterior tibial plateau, age-dependent subchondral cortical thickness changes occurred. Cartilage and bone adaptation to loading depended on the load level applied and duration and varied by anatomic location.

Cyclic compressive loading of mouse knee joints induced marked alterations in the cartilage matrix, including fibrillation and thinning as well as altered Safranin O staining that reflected compositional changes in proteoglycan content. Similar cartilage changes were reported previously *in vivo* with tibial loading and long duration treadmill running [17, 25], but subchondral bone changes were not assessed. Compared to treadmill running, tibial loading applies compression to the knee in a flexed loading position and does not replicate the full range of motion experienced during locomotion. In addition to the load-induced cartilage alterations, we demonstrated that the high load magnitude resulted in differential joint tissue responses in young and adult mice, including the extent of cartilage damage, subchondral cortical bone adaptation, and osteophyte formation. In an injurious model of tibial impact loading that noninvasively induced ACL injury in young mice [26], the cartilage and bone adaptive changes

were more severe than in our adult high load group and included considerable ectopic bone formation. In contrast to our data for moderate load levels, the observed benefits of exercise activities in rodent models for short duration [6, 7] suggest that either the in vivo loads engendered with exercise are lower than 4.5N or our model is not replicating the beneficial aspect of exercise loading.

Alterations in the composition and structural integrity of cartilage matrix in response to loading also have been demonstrated *in vitro*. For example, high load levels and long durations of cyclic loading increase chondrocyte death in the superficial zones of bovine cartilage explants [27] and acute impact loading increases proteoglycan release and chondrocyte death [28-30]. We also noted in our study that proteoglycan loss and cartilage thinning (Fig. 2.1) increased with mechanical loading and continued throughout the study period.

Our study did not permit us to define whether the cartilage alterations that we observed depended on the changes in the subchondral bone. However, our findings with limbs loaded for 6 weeks at 9.0N in both young and adult mice demonstrate that the anatomic sites of subchondral cortical bone thickening correspond to the regions of cartilage thinning, suggesting that each tissue responds to the local mechanical environment and to reciprocal changes in the other tissue. Other studies have shown that cartilage degeneration is reduced when subchondral bone turnover and associated increases in cortical thickness are suppressed by alendronate treatment in OA animal models, providing evidence that subchondral bone properties can affect the state of articular cartilage [31, 32]. Clinical observations confirm the anatomic association of cartilage damage and subchondral bone sclerosis and increased bone mineral density in the hip and knee joints of OA patients [33]. Radin and Rose [34] suggested that the increased stiffness in subchondral bone tissue and the associated changes in the shape and contour of the subchondral

plate may adversely affect the capacity of the adjacent articular cartilage to adapt to mechanical loads. Consistent with our findings, recent studies in surgical and spontaneous animal models have shown a close relationship between the process of cartilage damage and subchondral bone histomorphometry [35, 36]. Our results demonstrating that regions of increased cortical subchondral thickness in the posterior aspect of tibial plateau correspond with sites of cartilage thinning provide evidence that both tissues respond to the local loading environment. They cannot, however, establish that the changes in the bone are responsible for the alterations in the cartilage or vice versa.

Thickening of the subchondral cortical bone in the loaded limb also may have contributed to the decreased epiphyseal cancellous bone mass, by stress shielding of the underlying epiphyseal bone. In contrast to our results, other studies showed that epiphyseal cortical bone mass decreases at the onset of early OA and subsequently increases at later stages [37, 38]. These apparently inconsistent observations may reflect differences in the time of tissue sampling after induction of mechanical alterations, but also may be related to additional features of these models, including, for example, surgical insult or chemically induced inflammation [18, 19].

The subchondral cortical bone on the posterior aspect of the tibial plateau that was thickened with loading corresponds to the location where the femoral condyles contact the plateau in the flexed loading position, indicating that loading is likely the primary cause of the subchondral bone changes. Loading in the posterior tibial plateau during flexion of the knee has been documented in studies of human kinematics *in vivo* [39, 40]. Similar to flexion kinematics in human knees, mouse femurs translate to the posterior tibial plateau due to the presence of the posterior cruciate ligament [41]. As a result, flexed knees in our loading model likely experience

cyclic compression at the posterior tibial plateau, the location of subchondral cortical bone thickening.

In addition to subchondral cortical and cancellous bone changes, the loaded joints formed periarticular osteophytes. Clinically, osteophytes are a radiographic and anatomic hallmark of OA. Osteophytes are believed to form in response to local mechanical influences at the joint margins but their role in joint load bearing is unclear. With *in vivo* tibial loading, osteophytes formed at the joint margins only at the high (9N) load level and not in limbs subjected to the moderate (4.5N) load, at least up to 6 weeks. Similar results were reported in models of severe joint instability [42]. However, these results contrast with studies reporting osteophyte formation with reduced levels of loading. For example, immobilization of rabbit knees resulted in cartilage degeneration and osteophyte formation [43, 44]. Further evidence indicating that joint immobilization can adversely affect cartilage homeostasis is provided by the observation that patients with limited mobility due to ankle arthrodesis or spinal cord injury have increased incidence of cartilage-associated OA features [45, 46].

Alterations in articular cartilage and subchondral bone reported in mice were observed in other OA murine models with altered joint loading environments, such as treadmill running, destabilization of medial meniscus (DMM), collagenase injection, or articular fracture [19]. Loss of proteoglycan content and cartilage fibrillation due to mechanical loading in our study is similar to cartilage changes in mice after 18 months of treadmill running or 4 weeks post-DMM surgery [25, 47]. Decreased epiphyseal cancellous mass was observed at early time points in mice injected with collagenase [37]. However, treadmill running, DMM surgery, and collagenase injection showed limited osteophyte formation in mice, whereas our controlled loading protocol consistently induced osteophyte formation. The location and characteristics of osteophytes were

similar to mice injected with TGF-β, suggesting that loading may induce signaling that promotes TGF-β and induces osteophyte formation in our model [48].

The metaphyseal cancellous bone changes that we observed are consistent with findings from previous studies in young male mice, indicating the robustness and reproducibility of our model [20, 49]. Unlike our findings in young mice, metaphyseal bone mass in adult mice did not increase with loading in our study. A previous report demonstrated increased cancellous bone mass in response to mechanical loading in adult female mice of a similar age, but the response to loading was reduced compared to that in young female mice [22]. Thus, in the adult male mice used in our study, the loading responses in the metaphyseal cancellous region may reflect gender differences or the effects of aging that may contribute to reduced mechano-responsiveness.

Further studies are needed to identify both the mechanical and biological mechanisms underlying the load-induced alterations. Additional mechanical characterization involving different loading protocols, stiffness mapping, joint displacements, and contact stress mapping during loading could provide insights into the underlying mechanisms responsible for the observed changes in joint tissues. Also, protein and gene expression patterns in chondrocytes of mechanically loaded joints should be related to tissue level responses to define the biological mechanisms. The robustness and repeatability of our model, which permits the use of controlled, non-invasive mechanical loading protocols, provides a unique experimental system for defining the relationships between mechanical loading and biological responses that influence cartilage, bone, and other joint tissues in animal models of OA. Elucidating mechanical and biomolecular pathways may lead ultimately to the development of non-pharmacological and pharmacological interventions to treat OA in clinical settings.

Acknowledgments

We thank Drs. Cornelia Farnum, Larry Bonassar, Mathias Bostrom, and Chris Hernandez for valuable input. Lyudmila Lukashova, Antonia Hille, Daniel Brooks, and the Cornell CARE staff provided experimental assistance. We thank our funding sources National Institutes of Health Grants R01-AG028664 and P30-AR046121 (MCHM), R01-AG022021 and RC4-AR060546 (MBG), and NSF GRF (FCK).

2.5 REFERENCES

1. Lawrence RC, Felson DT, Helmick CG, Arnold LM, Choi H, Deyo RA, Gabriel S, Hirsch R, Hochberg MC, Hunder GG, Jordan JM, Katz JN, Kremers HM, Wolfe F. Estimates of the prevalence of arthritis and other rheumatic conditions in the United States. Part II. Arthritis Rheum. 2008 Jan;58(1):26-35.
2. Felson DT, Lawrence RC, Dieppe PA, Hirsch R, Helmick CG, Jordan JM, Kington RS, Lane NE, Nevitt MC, Zhang Y, Sowers M, McAlindon T, Spector TD, Poole AR, Yanovski SZ, Ateshian G, Sharma L, Buckwalter JA, Brandt KD, Fries JF. Osteoarthritis: new insights. Part 1: the disease and its risk factors. Ann Intern Med. 2000 Oct 17;133(8):635-46.
3. Kaila-Kangas L, Arokoski J, Impivaara O, Viikari-Juntura E, Leino-Arjas P, Luukkonen R, Heliovaara M. Associations of hip osteoarthritis with history of recurrent exposure to manual handling of loads over 20 kg and work participation: a population-based study of men and women. Occup Environ Med. 2011 Oct;68(10):734-8.
4. Sah RL, Kim YJ, Doong JY, Grodzinsky AJ, Plaas AH, Sandy JD. Biosynthetic response of cartilage explants to dynamic compression. J Orthop Res. 1989;7(5):619-36.
5. Parkkinen JJ, Lammi MJ, Helminen HJ, Tammi M. Local stimulation of proteoglycan synthesis in articular cartilage explants by dynamic compression in vitro. J Orthop Res. 1992 Sep;10(5):610-20.
6. Otterness IG, Eskra JD, Bliven ML, Shay AK, Pelletier JP, Milici AJ. Exercise protects against articular cartilage degeneration in the hamster. Arthritis Rheum. 1998 Nov;41(11):2068-76.

7. Galois L, Etienne S, Grossin L, Watrin-Pinzano A, Cournil-Henrionnet C, Loeuille D, Netter P, Mainard D, Gillet P. Dose-response relationship for exercise on severity of experimental osteoarthritis in rats: a pilot study. Osteoarthritis Cartilage. 2004 Oct;12(10):779-86.

8. Recommendations for the medical management of osteoarthritis of the hip and knee: 2000 update. American College of Rheumatology Subcommittee on Osteoarthritis Guidelines. Arthritis Rheum. 2000 Sep;43(9):1905-15.

9. O'Reilly SC, Muir KR, Doherty M. Effectiveness of home exercise on pain and disability from osteoarthritis of the knee: a randomised controlled trial. Ann Rheum Dis. 1999 Jan;58(1):15-9.

10. Roos EM, Dahlberg L. Positive effects of moderate exercise on glycosaminoglycan content in knee cartilage: a four-month, randomized, controlled trial in patients at risk of osteoarthritis. Arthritis Rheum. 2005 Nov;52(11):3507-14.

11. Kurz B, Jin M, Patwari P, Cheng DM, Lark MW, Grodzinsky AJ. Biosynthetic response and mechanical properties of articular cartilage after injurious compression. J Orthop Res. 2001 Nov;19(6):1140-6.

12. Thibault M, Poole AR, Buschmann MD. Cyclic compression of cartilage/bone explants in vitro leads to physical weakening, mechanical breakdown of collagen and release of matrix fragments. J Orthop Res. 2002 Nov;20(6):1265-73.

13. Lee JH, Fitzgerald JB, Dimicco MA, Grodzinsky AJ. Mechanical injury of cartilage explants causes specific time-dependent changes in chondrocyte gene expression. Arthritis Rheum. 2005 Aug;52(8):2386-95.

14. Felson DT, Anderson JJ, Naimark A, Walker AM, Meenan RF. Obesity and knee osteoarthritis. The Framingham Study. Ann Intern Med. 1988 Jul 1;109(1):18-24.

15. Cameron KL, Hsiao MS, Owens BD, Burks R, Svoboda SJ. Incidence of physician-diagnosed osteoarthritis among active duty United States military service members. Arthritis Rheum. 2011 Oct;63(10):2974-82.

16. Messier SP, Loeser RF, Miller GD, Morgan TM, Rejeski WJ, Sevick MA, Ettinger WH, Jr., Pahor M, Williamson JD. Exercise and dietary weight loss in overweight and obese older adults with knee osteoarthritis: the Arthritis, Diet, and Activity Promotion Trial. Arthritis Rheum. 2004 May;50(5):1501-10.

17. Poulet B, Hamilton RW, Shefelbine S, Pitsillides AA. Characterizing a novel and adjustable noninvasive murine joint loading model. Arthritis Rheum. 2011 Jan;63(1):137-47.

18. Ameye LG, Young MF. Animal models of osteoarthritis: lessons learned while seeking the "Holy Grail". Curr Opin Rheumatol. 2006 Sep;18(5):537-47.

19. Little CB, Zaki S. What constitutes an "animal model of osteoarthritis"--the need for consensus? Osteoarthritis Cartilage. 2012 Apr;20(4):261-7.

20. Lynch ME, Main RP, Xu Q, Walsh DJ, Schaffler MB, Wright TM, van der Meulen MC. Cancellous bone adaptation to tibial compression is not sex dependent in growing mice. J Appl Physiol. 2010 Sep;109(3):685-91.

21. Fritton JC, Myers ER, Wright TM, van der Meulen MC. Loading induces site-specific increases in mineral content assessed by microcomputed tomography of the mouse tibia. Bone. 2005 Jun;36(6):1030-8.

22. Lynch ME, Main RP, Xu Q, Schmicker TL, Schaffler MB, Wright TM, van der Meulen MC. Tibial compression is anabolic in the adult mouse skeleton despite reduced responsiveness with aging. Bone. 2011 Sep;49(3):439-46.

23. Glasson SS, Chambers MG, Van Den Berg WB, Little CB. The OARSI histopathology initiative - recommendations for histological assessments of osteoarthritis in the mouse. Osteoarthritis Cartilage. 2010 Oct;18 Suppl 3:S17-23.

24. Cao L, Youn I, Guilak F, Setton LA. Compressive properties of mouse articular cartilage determined in a novel micro-indentation test method and biphasic finite element model. J Biomech Eng. 2006 Oct;128(5):766-71.

25. Lapvetelainen T, Nevalainen T, Parkkinen JJ, Arokoski J, Kiraly K, Hyttinen M, Halonen P, Helminen HJ. Lifelong moderate running training increases the incidence and severity of osteoarthritis in the knee joint of C57BL mice. Anat Rec. 1995 Jun;242(2):159-65.

26. Christiansen BA, Anderson MJ, Lee CA, Williams JC, Yik JH, Haudenschild DR. Musculoskeletal changes following non-invasive knee injury using a novel mouse model of post-traumatic osteoarthritis. Osteoarthritis Cartilage. 2012 Jul;20(7):773-82.

27. Chen CT, Bhargava M, Lin PM, Torzilli PA. Time, stress, and location dependent chondrocyte death and collagen damage in cyclically loaded articular cartilage. J Orthop Res. 2003 Sep;21(5):888-98.

28. Quinn TM, Allen RG, Schalet BJ, Perumbuli P, Hunziker EB. Matrix and cell injury due to sub-impact loading of adult bovine articular cartilage explants: effects of strain rate and peak stress. J Orthop Res. 2001 Mar;19(2):242-9.

29. Jeffrey JE, Gregory DW, Aspden RM. Matrix damage and chondrocyte viability following a single impact load on articular cartilage. Arch Biochem Biophys. 1995 Sep 10;322(1):87-96.

30. Torzilli PA, Grigiene R, Borrelli J, Jr., Helfet DL. Effect of impact load on articular cartilage: cell metabolism and viability, and matrix water content. J Biomech Eng. 1999 Oct;121(5):433-41.

31. Hayami T, Pickarski M, Wesolowski GA, McLane J, Bone A, Destefano J, Rodan GA, Duong le T. The role of subchondral bone remodeling in osteoarthritis: reduction of cartilage degeneration and prevention of osteophyte formation by alendronate in the rat anterior cruciate ligament transection model. Arthritis Rheum. 2004 Apr;50(4):1193-206.

32. Hayami T, Pickarski M, Zhuo Y, Wesolowski GA, Rodan GA, Duong le T. Characterization of articular cartilage and subchondral bone changes in the rat anterior cruciate ligament transection and meniscectomized models of osteoarthritis. Bone. 2006 Feb;38(2):234-43.

33. Buckland-Wright C. Subchondral bone changes in hand and knee osteoarthritis detected by radiography. Osteoarthritis Cartilage. 2004;12 Suppl A:S10-9.

34. Radin EL, Rose RM. Role of subchondral bone in the initiation and progression of cartilage damage. Clin Orthop Relat Res. 1986 Dec(213):34-40.

35. Botter SM, Glasson SS, Hopkins B, Clockaerts S, Weinans H, van Leeuwen JP, van Osch GJ. ADAMTS5-/- mice have less subchondral bone changes after induction of osteoarthritis through surgical instability: implications for a link between cartilage and subchondral bone changes. Osteoarthritis Cartilage. 2009 May;17(5):636-45.

36. Pastoureau P, Leduc S, Chomel A, De Ceuninck F. Quantitative assessment of articular cartilage and subchondral bone histology in the meniscectomized guinea pig model of osteoarthritis. Osteoarthritis Cartilage. 2003 Jun;11(6):412-23.

37. Botter SM, van Osch GJ, Clockaerts S, Waarsing JH, Weinans H, van Leeuwen JP. Osteoarthritis induction leads to early and temporal subchondral plate porosity in the tibial plateau of mice: an in vivo microfocal computed tomography study. Arthritis Rheum. 2011 Sep;63(9):2690-9.

38. Intema F, Sniekers YH, Weinans H, Vianen ME, Yocum SA, Zuurmond AM, DeGroot J, Lafeber FP, Mastbergen SC. Similarities and discrepancies in subchondral bone structure in two differently induced canine models of osteoarthritis. J Bone Miner Res. 2010 Jul;25(7):1650-7.

39. Li G, DeFrate LE, Park SE, Gill TJ, Rubash HE. In vivo articular cartilage contact kinematics of the knee: an investigation using dual-orthogonal fluoroscopy and magnetic resonance image-based computer models. Am J Sports Med. 2005 Jan;33(1):102-7.

40. Moro-oka TA, Hamai S, Miura H, Shimoto T, Higaki H, Fregly BJ, Iwamoto Y, Banks SA. Dynamic activity dependence of in vivo normal knee kinematics. J Orthop Res. 2008 Apr;26(4):428-34.

41. Dennis DA, Komistek RD, Hoff WA, Gabriel SM. In vivo knee kinematics derived using an inverse perspective technique. Clin Orthop Relat Res. 1996 Oct(331):107-17.

42. Kamekura S, Hoshi K, Shimoaka T, Chung U, Chikuda H, Yamada T, Uchida M, Ogata N, Seichi A, Nakamura K, Kawaguchi H. Osteoarthritis development in novel experimental mouse models induced by knee joint instability. Osteoarthritis Cartilage. 2005 Jul;13(7):632-41.

43. Langenskiold A, Michelsson JE, Videman T. Osteoarthritis of the knee in the rabbit produced by immobilization. Attempts to achieve a reproducible model for studies on pathogenesis and therapy. Acta Orthop Scand. 1979 Feb;50(1):1-14.

44. Smith RL, Thomas KD, Schurman DJ, Carter DR, Wong M, van der Meulen MC. Rabbit knee immobilization: bone remodeling precedes cartilage degradation. J Orthop Res. 1992 Jan;10(1):88-95.

45. Takakura Y, Tanaka Y, Sugimoto K, Akiyama K, Tamai S. Long-term results of arthrodesis for osteoarthritis of the ankle. Clin Orthop Relat Res. 1999 Apr(361):178-85.

46. Vanwanseele B, Eckstein F, Knecht H, Spaepen A, Stussi E. Longitudinal analysis of cartilage atrophy in the knees of patients with spinal cord injury. Arthritis Rheum. 2003 Dec;48(12):3377-81.

47. Glasson SS, Blanchet TJ, Morris EA. The surgical destabilization of the medial meniscus (DMM) model of osteoarthritis in the 129/SvEv mouse. Osteoarthritis Cartilage. 2007 Sep;15(9):1061-9.

48. van Beuningen HM, van der Kraan PM, Arntz OJ, van den Berg WB. Transforming growth factor-beta 1 stimulates articular chondrocyte proteoglycan synthesis and induces osteophyte formation in the murine knee joint. Lab Invest. 1994 Aug;71(2):279-90.

49. Fritton JC, Myers ER, Wright TM, van der Meulen MC. Bone mass is preserved and cancellous architecture altered due to cyclic loading of the mouse tibia after orchidectomy. J Bone Miner Res. 2008 May;23(5):663-71.

Chapter 2 Supplementary Material

Table 2.1. Localized thickness (μm) of articular cartilage and subchondral cortical bone in adult mice. Data presented as mean ± SD. [a]loading, [b]duration, [c]load level, [d]loading*duration, [e]loading*load level, [f]duration*load level, [g]loading*duration*load level effect, $p<0.05$ by repeated measures three-way ANOVA

			4.5N						9.0N					
			1 week		2 weeks		6 weeks		1 week		2 weeks		6 weeks	
			Loaded	Control	Loaded	Control	Loaded	Control	Loaded	Control	Loaded	Control	Loaded	Control
Articular Cartilage	Lateral	Anterior[b,c,e]	75 ± 7	81 ± 8	77 ± 8	78 ± 15	65 ± 10	71 ± 11	96 ± 10	77 ± 6	87 ± 15	82 ± 10	82 ± 12	72 ± 7
		Middle[b]	100 ± 8	91 ± 10	93 ± 9	90 ± 6	94 ± 6	90 ± 5	103 ± 6	94 ± 8	95 ± 7	91 ± 4	88 ± 11	98 ± 12
		Posterior[a,c,d,e,g]	108 ± 10	108 ± 10	105 ± 9	99 ± 10	111 ± 14	108 ± 9	86 ± 9	102 ± 13	96 ± 12	98 ± 18	71 ± 15	108 ± 10
	Medial	Anterior	99 ± 5	100 ± 8	101 ± 10	104 ± 8	101 ± 6	99 ± 9	108 ± 11	104 ± 9	106 ± 5	103 ± 12	97 ± 11	102 ± 6
		Middle[a,d,g]	100 ± 11	105 ± 13	100 ± 9	104 ± 12	104 ± 14	100 ± 10	99 ± 11	109 ± 6	93 ± 12	101 ± 8	89 ± 11	115 ± 11
		Posterior[a,b]	104 ± 10	95 ± 5	86 ± 12	96 ± 16	87 ± 10	92 ± 12	86 ± 19	101 ± 17	83 ± 23	85 ± 8	74 ± 7	96 ± 17
			4.5N						9.0N					
			1 week		2 weeks		6 weeks		1 week		2 weeks		6 weeks	
			Loaded	Control	Loaded	Control	Loaded	Control	Loaded	Control	Loaded	Control	Loaded	Control
Subchondral Cortical Bone	Lateral	Anterior	38 ± 13	41 ± 14	39 ± 13	45 ± 15	33 ± 7	32 ± 10	28 ± 9	28 ± 4	31 ± 16	39 ± 9	34 ± 17	36 ± 8
		Middle[b,d]	47 ± 8	49 ± 15	64 ± 24	61 ± 27	30 ± 7	34 ± 12	49 ± 19	47 ± 14	42 ± 21	39 ± 6	24 ± 16	49 ± 20
		Posterior[a,b,d,f]	53 ± 9	49 ± 17	71 ± 18	43 ± 12	70 ± 29	37 ± 14	40 ± 11	33 ± 6	55 ± 10	35 ± 8	84 ± 13	41 ± 16
	Medial	Anterior[b,c]	87 ± 28	58 ± 19	89 ± 39	81 ± 18	49 ± 10	48 ± 26	61 ± 29	58 ± 25	62 ± 29	47 ± 5	30 ± 30	50 ± 17
		Middle[a,b]	90 ± 39	97 ± 34	80 ± 54	88 ± 36	46 ± 20	39 ± 15	62 ± 27	67 ± 32	71 ± 35	83 ± 45	36 ± 23	68 ± 36
		Posterior	50 ± 14	41 ± 18	49 ± 14	55 ± 31	47 ± 13	42 ± 13	42 ± 22	28 ± 11	47 ± 13	45 ± 7	54 ± 26	57 ± 21

Table 2.2. Localized thickness (μm) of articular cartilage and subchondral cortical bone in young mice. Data presented as mean ± SD. [a]loading, [b]duration, [c]loading*duration, $p<0.05$ by repeated measures two-way ANOVA

			9.0N					
			1 week		2 weeks		6 weeks	
			Loaded	Control	Loaded	Control	Loaded	Control
Articular Cartilage	Lateral	Anterior[a]	91 ± 9	84 ± 17	95 ± 10	80 ± 10	92 ± 15	88 ± 17
		Middle	102 ± 12	101 ± 7	102 ± 4	95 ± 11	99 ± 8	98 ± 7
		Posterior[a]	80 ± 12	104 ± 16	68 ± 10	105 ± 17	83 ± 13	111 ± 7
	Medial	Anterior[a]	99 ± 13	104 ± 8	96 ± 6	103 ± 5	98 ± 11	102 ± 10
		Middle[a]	82 ± 17	102 ± 9	91 ± 16	106 ± 15	82 ± 6	110 ± 9
		Posterior[a]	70 ± 16	89 ± 19	84 ± 17	103 ± 19	76 ± 8	90 ± 16
			9.0N					
			1 week		2 weeks		6 weeks	
			Loaded	Control	Loaded	Control	Loaded	Control
Subchondral Cortical Bone	Lateral	Anterior[b,c]	51 ± 13	40 ± 18	31 ± 11	36 ± 7	22 ± 7	40 ± 12
		Middle[a,c]	52 ± 24	49 ± 7	38 ± 10	45 ± 11	25 ± 11	46 ± 10
		Posterior[a,c]	39 ± 6	35 ± 8	55 ± 21	40 ± 13	64 ± 16	33 ± 16
	Medial	Anterior[a,c]	64 ± 27	61 ± 27	49 ± 28	56 ± 19	20 ± 10	54 ± 25
		Middle	61 ± 14	60 ± 29	53 ± 14	53 ± 12	42 ± 20	67 ± 8
		Posterior[a]	41 ± 7	37 ± 15	52 ± 15	38 ± 11	57 ± 22	38 ± 15

Figure 2.1 (A) Schematic of mouse tibial loading configuration, (B) 4.5N and 9.0N loading wave forms, and (C) rendering of microCT scan of a flexed mouse knee indicating the location of joint contact with loading is in the posterior regions of the tibial plateau.

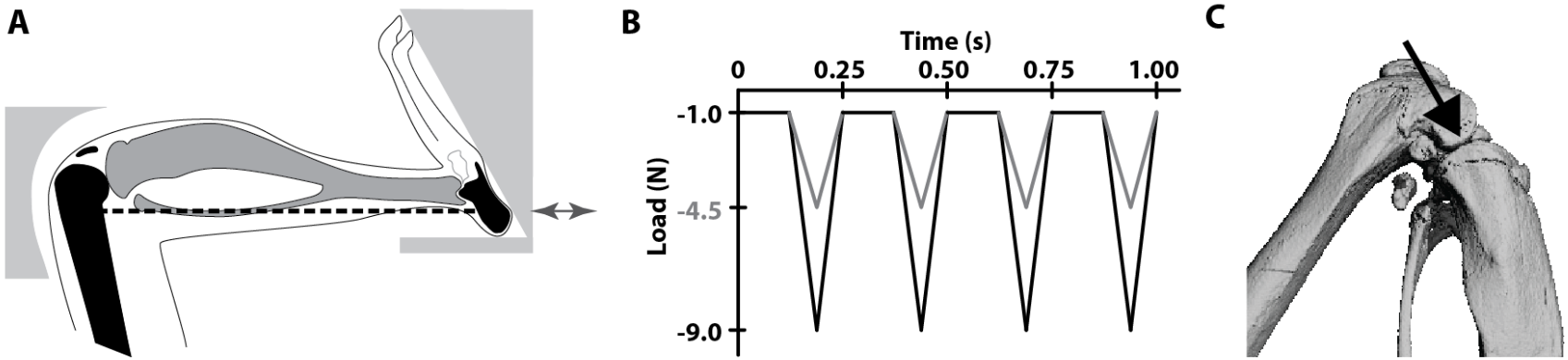

Figure 2.2 Epiphyseal cancellous bone tissue mineral density (mg HA/cm^3) from young (A) and adult (B) mice. Data presented as mean ± SD. ^loading, †duration, ‡load level, §loading*duration, ¶loading*load level, $p<0.05$ by repeated measures two-way ANOVA for young mice and repeated measures three-way ANOVA for adult mice. Groups with different letters are significantly different by post-hoc means comparisons with Bonferroni correction.

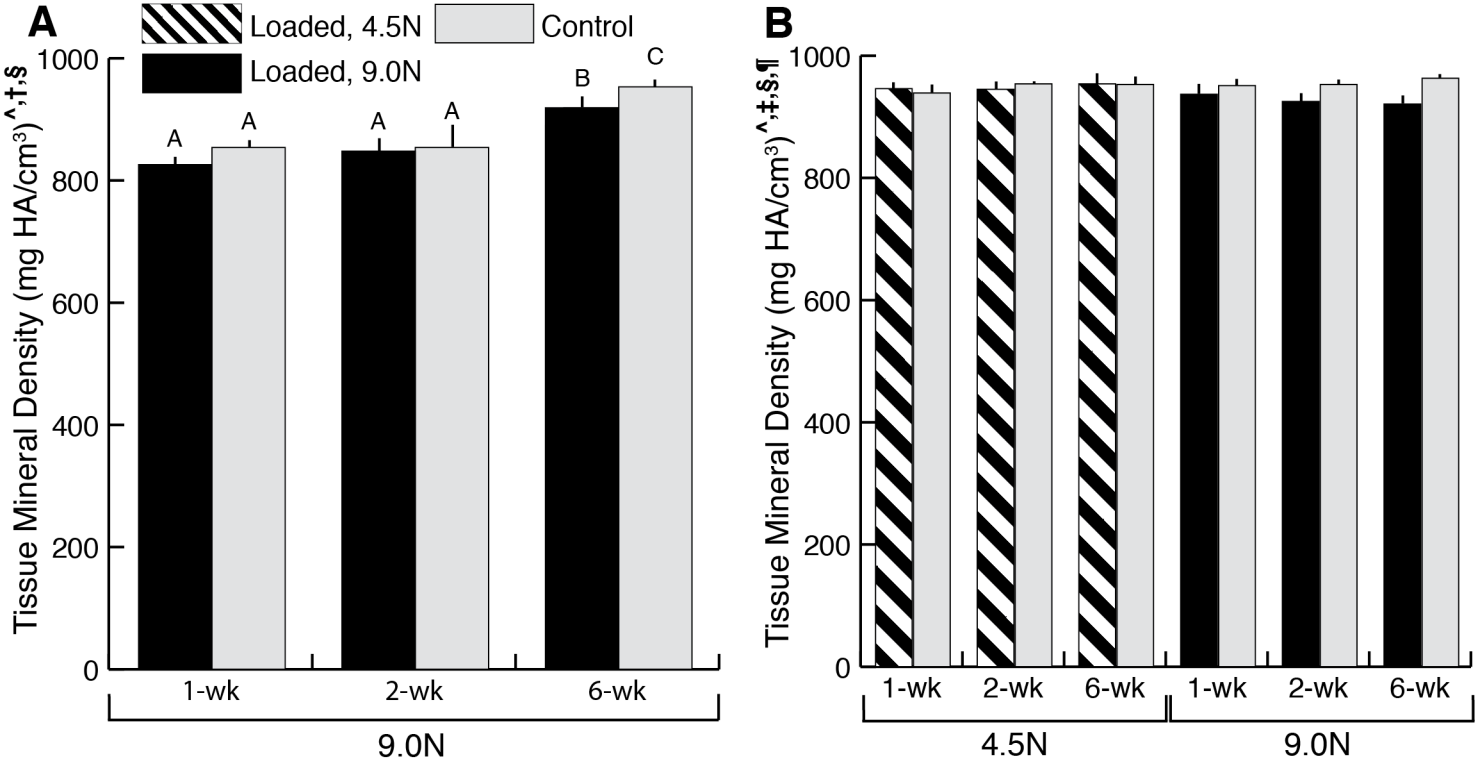

Figure 2.3 Metaphyseal cancellous bone tissue mineral density (mg HA/cm^3) from young (A) and adult (B) mice. Data presented as mean ± SD. ^loading, †duration, ‡loading*duration, $p<0.05$ by repeated measures two-way ANOVA for young mice and repeated measures three-way ANOVA for adult mice. Groups with different letters are significantly different by post-hoc means comparisons with Bonferroni correction.

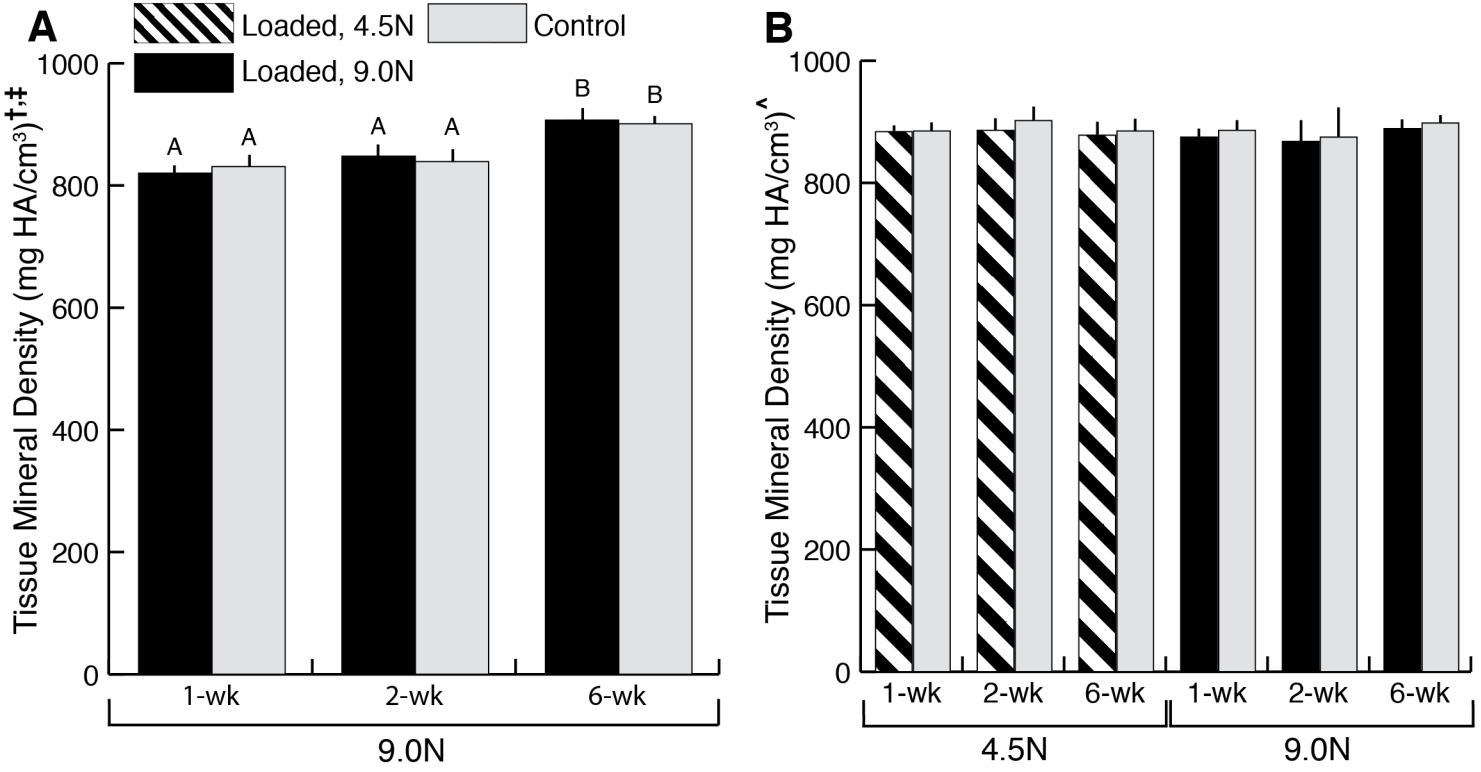

CHAPTER 3

PROGRESSIVE CELL-MEDIATED CHANGES IN ARTICULAR CARTILAGE AND BONE IN MICE ARE INITATED BY A SINGLE SESSION OF CONTROLLED CYCLIC COMPRESSIVE LOADING

3.1 Introduction

The mechanical loading environment plays a crucial role in the development of osteoarthritis (OA). Population cohorts with histories of traumatic joint injuries such as ligament tears have a higher incidence of OA that has been attributed to the resultant alteration in joint mechanics (1). Similarly, excessive physical activity associated with occupational characteristics or athletic activity is associated with an increased incidence of OA (2). Several *in vivo* animal models have demonstrated that creation of an adverse mechanical loading environment is strongly associated with the development of OA. For example, strenuous running in mice and dogs produces articular cartilage degeneration and peri-articular bone changes (3, 4), while less strenuous running prevents the onset of OA (5, 6). In addition, *in vitro* studies showed a single injurious impact loading of cartilage explants decreases cell viability and increases production of catabolic mediators such as MMPs and aggrecanases (7-9), suggesting that a single event of traumatic loading can produce sustained adverse effects on chondrocyte viability and function.

In noninvasive mouse models that uses controlled joint loading protocols, both cyclic and single injurious loading protocols promoted OA pathology in mouse joints similar to humans, such as cartilage loss, subchondral bone alterations, and osteophyte formation (10-13). While a single 12N peak load in the single injurious loading protocol induced traumatic damage at the anterior cruciate ligament, cyclic loading protocols with peak loads at 9N for a total of 1200

cycles/day did not demonstrate any observable traumatic damage at the beginning of loading session.

In a mouse model of controlled mechanical loading of the knee joint, we previously showed that daily cyclic compressive loading produces changes in tibial subchondral bone within 2 weeks and initiates proteoglycan loss in the cartilage over a 6-week period (12). In these studies, it was unclear whether the cartilage and bone changes were related to the adverse effects of repetitive traumatic joint tissue injury or whether the initial joint loading was sufficient to initiate a cell-mediated process that was responsible for the subsequent pathologic alterations. The present studies were undertaken to address this question by assessing the changes in cartilage and peri-articular bone following a single 5-minute session of *in vivo* mechanical loading using the same loading protocol employed in our previous studies. We hypothesized that a single loading session would not create traumatic physical damage in the articular cartilage and subchondral bone immediately after loading, but would initiate cell-mediated processes leading to progressive cartilage and bone OA pathology at later time points.

3.2 Materials and Methods

Mechanical Loading Conditions

We applied a single session of controlled *in vivo* compressive loading to the left tibiae of 26-week-old C57Bl/6 male mice (n = 21, Jackson Laboratories, Bar Harbor, ME) at a peak load level of 9.0N and frequency of 4Hz for 1200 cycles (5 minutes) under general anesthesia (2% Isoflurane, 1.0 L/min, Webster). The applied loading was based on protocols demonstrated previously to create articular cartilage degeneration (12) and to have an anabolic effect on the tibial metaphysis in growing and adult mice (14-16). The left limb was loaded; the right limb

served as the non-loaded control. To assess immediate, cell-mediated changes in response to mechanical loading, analyses were performed at three times (T) after the single loading session: T = 0 (approximately 1 hour after the single loading session), 1- and 2-weeks (n = 7/group) on intact knee joints fixed in 4% PFA overnight (Fig 3.1). All experimental procedures were approved by the Institutional Animal Care and Use Committee.

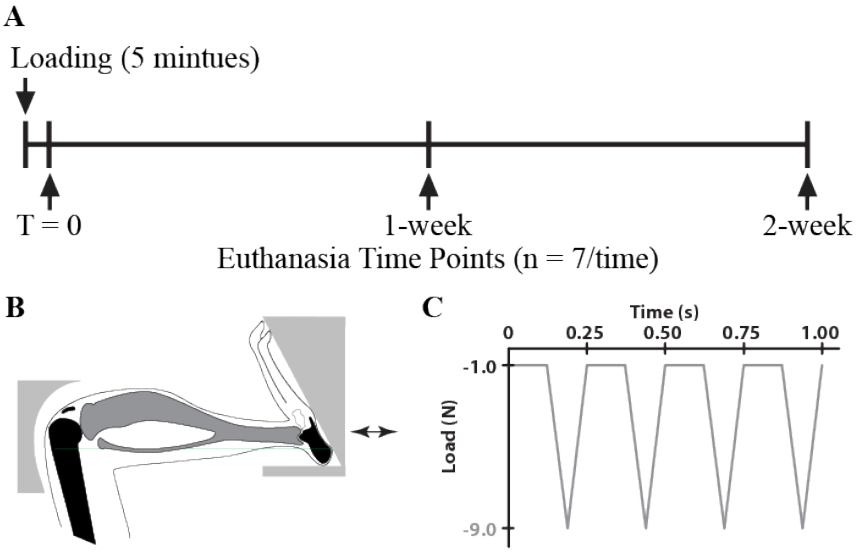

Figure 3.1 (A) Overview of the loading and euthanasia time points, (B) schematic of mouse tibial loading configuration, and (C) *in vivo* loading waveform used in the study for 1200 cycles.

Articular Cartilage and Bone Tissue Assessment

After tissue fixation in 4% PFA overnight, intact joints were scanned by microcomputed tomography (microCT) at 10 μm resolution (μCT35, Scanco, Switzerland) with an X-ray tube potential of 55 kVp in PBS to assess bone morphological changes. Knee joints were then decalcified in formic acid/sodium citrate for one week, dehydrated in an ethanol gradient, and embedded in paraffin. Serial coronal sections of 6 μm thickness were obtained using a rotary microtome (Leica RM2255, Germany). Safranin O/fast Green/hematoxylin staining was performed on sections at 90 μm intervals to assess cartilage morphology. Cartilage degeneration was assessed in the tibial plateau using a modified murine cartilage histological scoring system

(17). The presence of osteophytes was identified by the changes in peri-articular bone and articular morphologies in sections used for histological scoring. The presence of synovial inflammation at the joint margins was examined by hematoxylin and eosin staining.

Localized thickness measurements for articular cartilage and subchondral cortical bone were performed on Safranin O/Fast green-stained slides previously used for histological scoring (Osteomeasure, OsteoMetrics, USA). The tibial plateau was first divided into medial and lateral halves, then further subdivided into anterior, middle, and posterior regions, resulting in six tibial plateau regions for evaluation. A single representative slide from each region was used to measure cartilage and subchondral cortical bone thickness. Five linear projections from the cartilage surface to the boundary between the cartilage and subchondral bone were used to measure cartilage thickness (Ca.Th, μm). The projections were extended into the subchondral bone to measure the subchondral bone thickness (Sub.Pl, μm) (12).

Cancellous bone morphology was assessed in two volumes of interest (VOI) of the microCT scans: the tibial metaphysis and epiphysis. The metaphysis VOI was located distal to the growth plate extending 10% of the total bone length, excluding primary spongiosa and cortical bone. The epiphysis VOI was the cancellous tissue proximal to the growth plate. The global threshold was set at 3900 HU and 3200 HU to segment mineralized tissue from epiphyseal and metaphyseal regions, respectively. Trabecular bone from both VOIs was selected by manually contouring inside the cortical bone. For each region, cancellous bone volume fraction (BV/TV, mm^3/mm^3), trabecular thickness (Tb.Th, μm) and separation (Tb.Sp, μm) were measured.

Cellular Responses

Immunohistochemistry was performed to assess cellular changes in cartilage and subchondral bone following the single session of loading. The effects of loading on chondrocyte phenotype were assessed by examination of cell morphology and expression of the autophagy-associated protein, lapidated microtubule-associated light change (LC3) using the LC3 antibody (Abcam, Cambridge, MA). Osteoclasts associated with localized regions of bone resorption were identified using an antibody to cathepsin K (Abcam, Cambridge, MA). To assess the effects of the loading on synovial pathology, tissue sections were examined for the presence of synovial lining hyperplasia and for the presence of inflammatory cell infiltration. Immunohistochemistry was applied to three sections, one section each from the anterior, middle, and posterior aspects of the tibial plateau. Sections were dewaxed, rehydrated, and incubated with 1% pepsin at 37°C for antigen retrieval for detection of LC3. No antigen retrieval was performed for cathepsin K. Sections were subsequently incubated with 1.5% goat serum for 30 minutes at room temperature and immunostained overnight at 4°C with the respective primary antibody or IgG as a negative control. Secondary antibody incubation and color development were done with avidin/biotin complex (Vector Labs, Burlingame, CA). Chondrocytes that stained positively for LC3 were counted under 40x magnification on both medial and lateral halves of tibial cartilage, normalized to total tibial cartilage area, and averaged for all three sections (Chon.N/CA, #/mm^2). Osteoclasts that positively stained for cathepsin K with at least two nuclei counterstained with hematoxylin were counted within epiphyseal cancellous bone, normalized to the epiphyseal bone cancellous surface area, and averaged over the three sections (OC.N/BS, #/mm).

Statistics

Statistical analyses were performed using repeated measures two-way ANOVA with interactions (JMP Pro 10.0, SAS Institute Inc), with *Loading* as the intra-group variable, and *Time* as an inter-group variable. Post-hoc comparisons of means were performed with Bonferroni correction when interaction effects were significant. P-values of < 0.05 indicated significance.

3.3 Results

Articular Cartilage Matrix Changes

Articular cartilage damage was first evident in the loaded limbs after 1 and 2 weeks (Fig. 3.2A). The histological scores of loaded limbs increased 2.6-fold after 1 week and 4.2-fold after 2 weeks compared to control limbs. The severity of the damage in the loaded limbs was similar at 1 and 2 weeks (Fig. 3.2B), with damage mainly localized to the medial peripheral edge of the articular surface.

Articular cartilage thinning in both lateral and medial compartments occurred only in the posterior aspect of the tibial plateau of loaded joints (Fig. 3.2C). Lateral-posterior articular cartilage was 17% thinner in loaded limbs compared to control limbs. Control limbs did not undergo cartilage degeneration at any time point, as indicated by similar histological score and cartilage thickness.

We next examined the effects of loading on the expression of LC3, a marker of chondrocyte autophagy. Chondrocyte immunostaining for LC3 decreased at 1 and 2 weeks in the loaded limbs following the single loading session compared to $T = 0$ (Fig. 3.2D). Chondrocyte LC3 in the loaded limbs was reduced by 76% at 1-week and 85% at 2-weeks compared to the control limb. The decrease in LC3-positive chondrocytes was similar after 1 and 2 weeks of loading, but no change was observed across all time points in non-loaded control limbs (Fig. 3.2E).

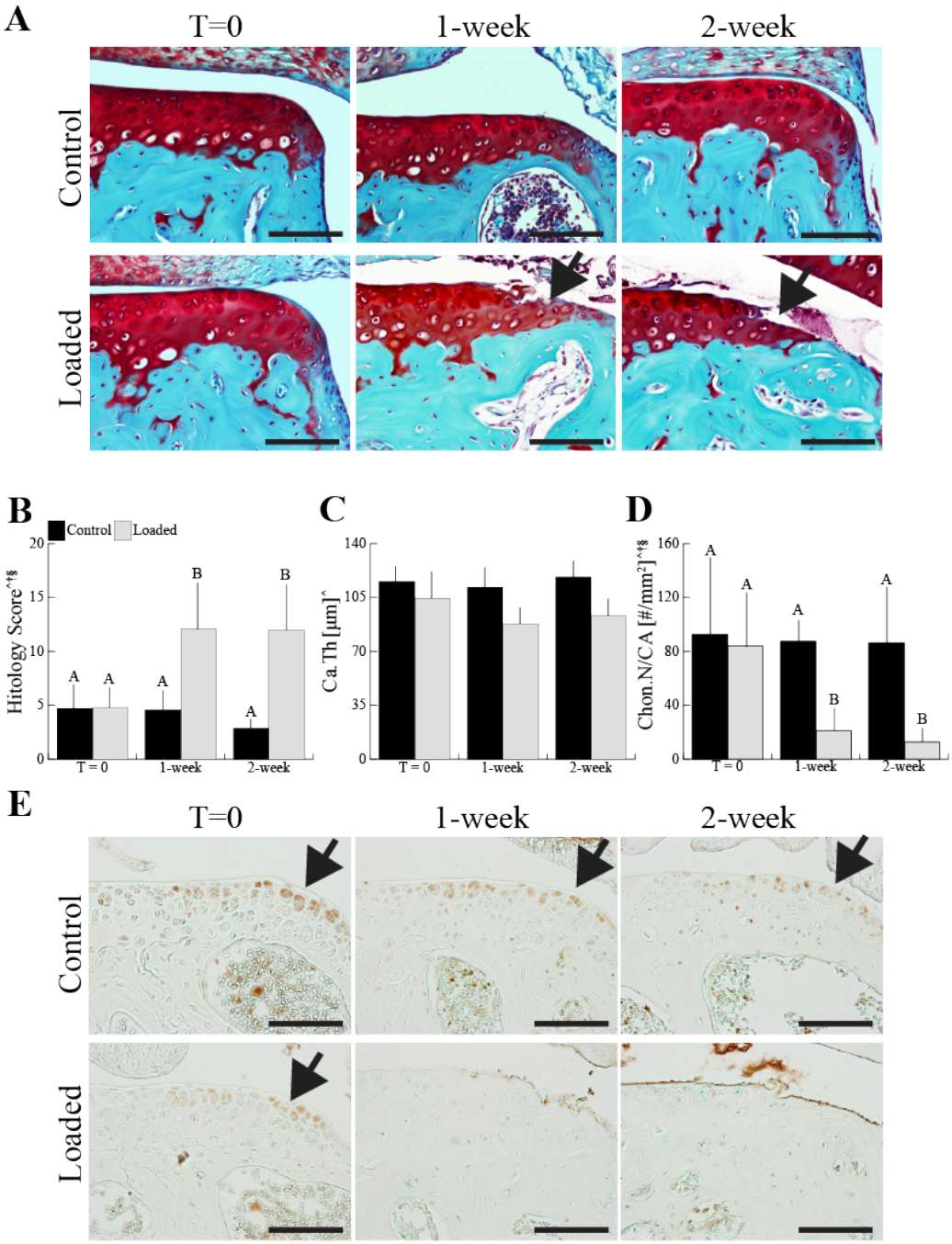

Figure 3.2 Progressive cartilage degeneration occurred following a single loading session in adult mice with no observable immediate physical damage (A, B). Loading also thinned articular cartilage (Ca.Th) at the lateral posterior quadrant (C). Chondrocyte LC3 expression (Chon.N/CA) decreased 1 and 2 weeks after the single loading session but not at time T=0 (D, E). Control images represent a non-loaded contralateral limb at each time point. Scale bar = 100 μm. Data presented as mean ± SD.
^loading, †time, §loading*time, $p<0.05$ by repeated measures two-way ANOVA. Groups with different letters are significantly different by post-hoc comparisons of means with Bonferroni correction.

Epiphyseal and Metaphyseal Bone Adaptation

Epiphyseal bone architecture was altered following a single loading session. No change was observed at any time point in control limbs. In the loaded limbs, epiphyseal cancellous bone mass decreased by 12% after 1 week, but returned to control levels by 2 weeks (Fig. 3.3A). The decreased epiphyseal bone mass at 1 week was attributable to an 8% decrease in trabecular thickness without an increase in trabecular separation (Fig. 3.3A). The decrease was also associated with an increase in surface osteoclast numbers. Metaphyseal bone mass was unchanged in the loaded and control limbs (Fig. 3.3B). Medial posterior subchondral cortical bone thickness decreased by 26% after mechanical loading (Fig. 3.3C). Osteoclast numbers in the epiphysis of loaded limbs increased by 2.4-fold at 1 week and by 1.4-fold at 2 weeks after the single loading session (Fig. 3.3D, E).

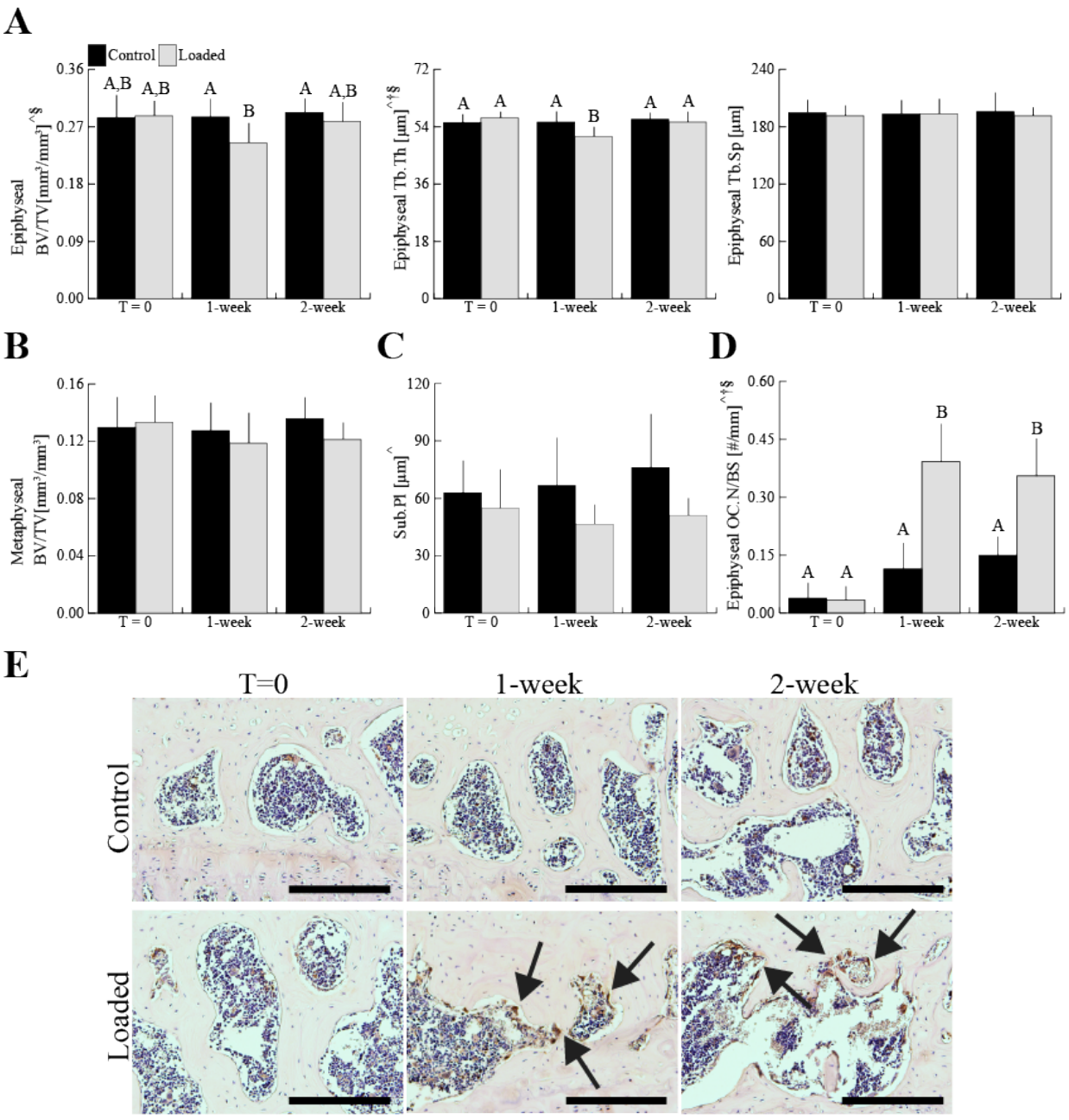

Figure 3.3 In the epiphysis loading decreased epiphyseal cancellous mass (BV/TV) in adult mice at 1-week. This change was due to decreased trabecular thickness (Tb.Th) at 1-week, not to increased trabecular separation (Tb.Sp) (A). Metaphyseal bone mass (BV/TV) did not change with loading (B). Medial posterior subchondral cortical bone thickness (Sub.Pl) decreased with loading (C). Osteoclast number (OC.N/BS) increased in the epiphysis with loading (D, E). Scale bar = 200 µm. Data presented as mean ± SD.
^loading, †time, §loading*time, $p<0.05$ by repeated measures two-way ANOVA. Groups with different letters are significantly different by post-hoc comparisons of means with Bonferroni correction.

Osteophyte Formation

Osteophytes developed at the joint margins following a single loading session in all loaded limbs. Fibrous tissue was evident at the joint margins at 1 week. By 2 weeks, cartilaginous tissue at the joint margins was evident, indicative of early osteophyte formation (Fig 3.4).

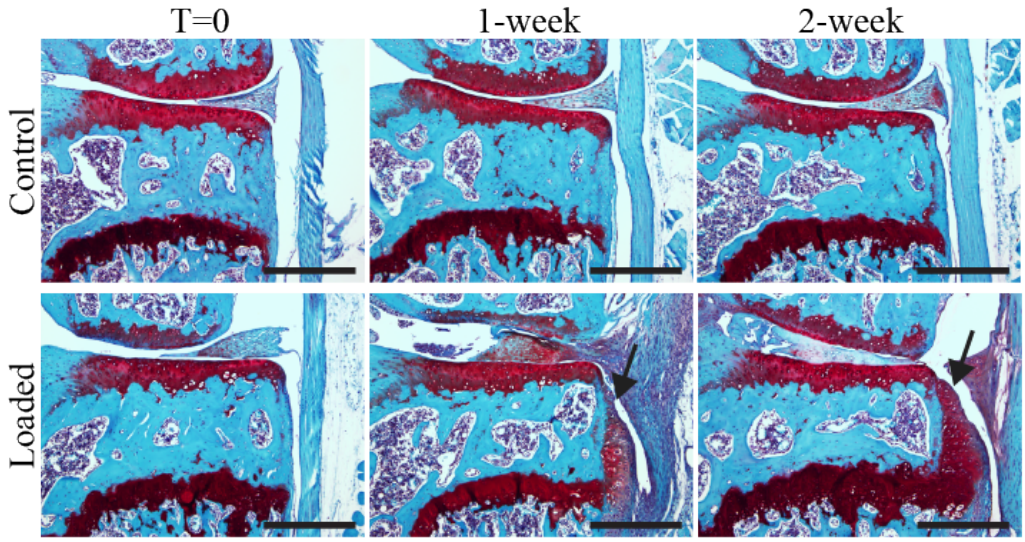

Figure 3.4 A single 5 minute loading session induced osteophyte formation (black arrowheads) 1 and 2 weeks later, but not at time T=0. Scale bar 400 µm.

Synovial Inflammation

Synovial hyperplasia or lymphocyte infiltration was not evident in any of the animals at any time point (Fig 3.5).

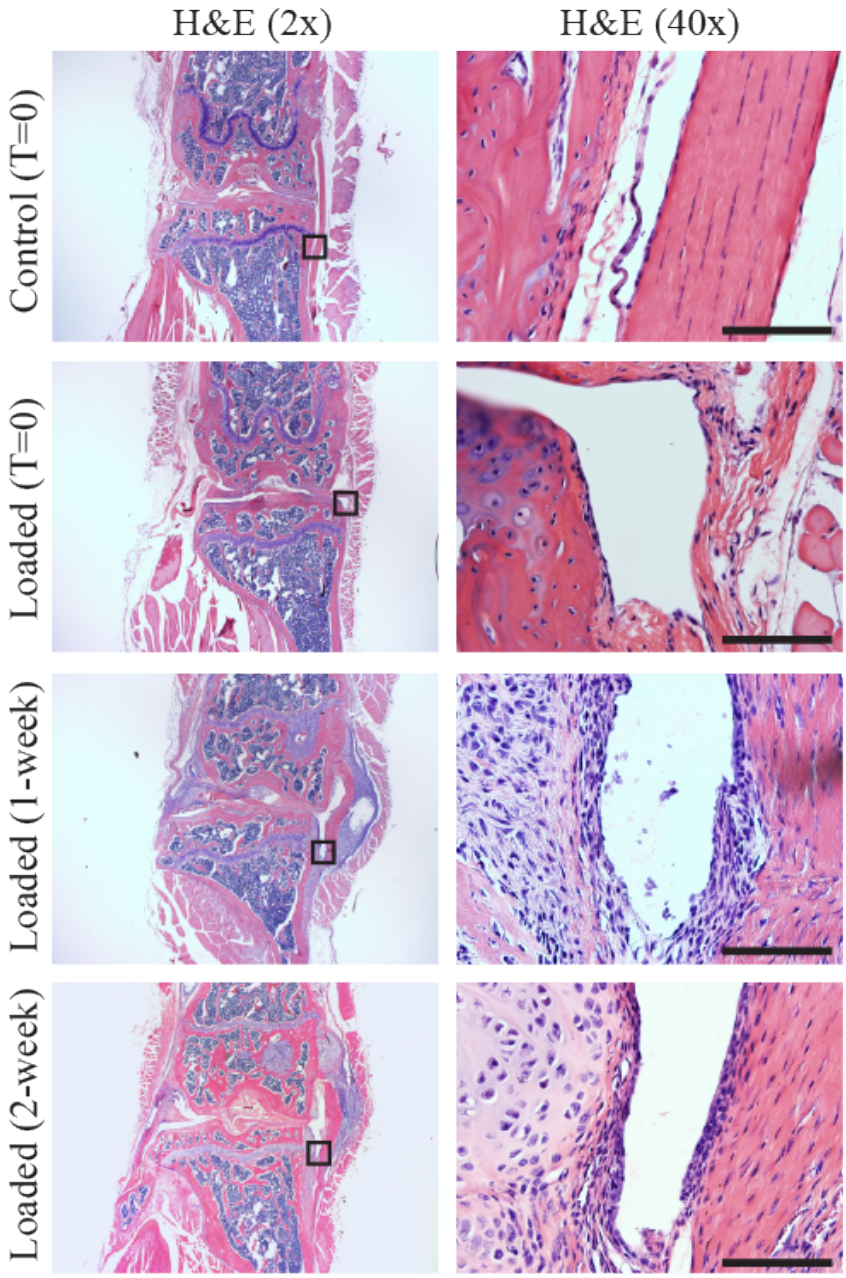

Figure 3.5 A single 5-minute loading session did not induce synovial inflammation indicated by the absence of synovial hyperplasia and lymphocyte infiltration in the synovium at 1 and 2 weeks after the single loading session. Location of the high magnification image indicated by the black boxes. Scale bar 100 μm.

3.4 Discussion

A single loading session did not create immediate physical damage to the articular cartilage or epiphyseal bone of adult mouse knee joints. Increased cartilage damage was detected at 1

week, progressed by 2 weeks after loading, and was accompanied by reduced epiphyseal cancellous mass at 1 week associated with increased osteoclast numbers. The epiphyseal bone changes were no longer detectible by week 2. The brief loading session initiated new fibrous tissue formation at the joint margins that was first detected at 1 week. By week 2, cartilaginous tissue was present at the joint margins, indicative of early osteophyte formation.

Our results demonstrate that a single episode of mechanical loading can initiate a cell-mediated process leading to cartilage degeneration and bone adaptive changes that evolve over a one- to two-week interval. Controlled mechanical loading applied to the mouse knee in other models showed similar changes in the articular cartilage matrix, including loss of proteoglycans and surface fibrillation (10, 11). However, the alterations in the peri-articular bone differed, likely related to differences in the loading protocol parameters used in the other studies. For example, the studies by Poulet et al. included an extended rest period of 10 seconds between loading cycles and noted limited osteophyte development at the joint margins 2 weeks after a single loading session (10), whereas in our study all mice developed osteophytes with a shorter rest insertion period of 0.25 second between loading cycles. Christiansen et al. (11) used higher peak loads (12N) and observed the development of heterotopic ossification and anterior cruciate ligament injury, responses that were not observed in our animals using lower loads.

In our previous study, mice loaded at a peak load of 4.5N demonstrated mild cartilage fibrillation without the formation of osteophytes in the knee despite daily loading for 6 weeks (12). In contrast, mouse knees loaded daily at 9N for 6 weeks exhibited more extensive and severe cartilage degeneration and developed mineralized osteophytes at joint margins (12). Similarly, the surgically induced mouse models of OA, such as destabilized medial meniscus (DMM) and ACL transection, show more advanced degenerative cartilage changes at 8 weeks

post-operatively compared to 4 weeks (18, 19). Our evaluation was limited to two weeks, since our primary objective was to test whether a single loading episode was sufficient to initiate the development of OA cartilage and bone pathology. Further studies are needed to establish whether the pathologic cartilage changes that we observed after 2 weeks will progress at later time points or whether a component of the pathology is reversible. In addition, investigating the contributions of loading rate, peak load, frequency, and total number of cycles to changes in the mouse joint will provide a better understanding of the role of the mechanical environment on the cartilage and bone changes and osteophyte formation.

Similar to reports by others (20), we observed abundant constitutive immunoreactive LC3 in the superficial zone chondrocytes in the control limbs. LC3 is one of several molecules involved in the regulation of cell autophagy. Chondrocyte autophagy has been suggested to play a role in repairing damaged macromolecules and organelles, and through this mechanism, contributes to the preservation of cartilage homeostasis (20-22). This speculation is supported by the observation that restoring autophagy-related activity through pharmacological intervention targeting the mTOR signaling pathway reduced the severity of OA in mice subjected to DMM surgery (23). While chondrocyte autophagy is also suggested to prevent chondrocyte apoptosis, we did not observe increased chondrocyte apoptosis following a single loading session despite the marked reduction in LC3 (data not shown). Our findings do not establish a causal relationship between the decrease in LC3 and de-regulated chondrocyte function, but do provide further evidence that this pathway may be important in maintaining chondrocyte homeostasis under conditions of joint loading or injury.

A single session of loading also produced alterations in the subchondral bone that evolved over the first week. The decreased epiphyseal cancellous mass at 1 week was primarily

attributable to thinning of trabeculae that was not associated with increased trabecular separation. These changes were associated with increased osteoclast number. Kennedy et al. (24) examined the effects of cyclic loading on rat ulnae and observed up-regulation of osteoclastic resorption in regions of microdamage. This effect was accompanied by the appearance of osteocyte apoptosis at these sites and up-regulation of osteoclast-inducing factors in adjacent viable osteocytes. We did not directly examine the subchondral bone for evidence of microdamage or effects on osteocyte viability after the acute loading session. The decrease in the epiphyseal bone at week 1 was no longer detectible at week 2 suggesting that, unlike the cartilage, the bone pathology was reversible. This discrepancy may reflect the differential capacity of cartilage and bone to remodel and repair their extracellular matrices.

Since the single episode of loading did not acutely affect the structure or architecture of the articular cartilage and the subchondral and peri-articular bone, the sequential changes in these tissues must be dependent on the activities of the resident cell types. In addition to effects on articular chondrocytes, epiphyseal osteoclasts, and cells at the joint margin that give rise to osteophytes, the activation of synovial inflammation and possible effects on the meniscus and other joint tissues may contribute to the altered functional properties of the cells in cartilage and bone through the release of soluble mediators that de-regulate the functional activities of these cells (25). We did not detect significant signs of inflammation in the synovial tissue or menisci, but this does not exclude their potential roles in contributing to the de-regulated function of the chondrocytes.

In conclusion, articular cartilage and subchondral bone in mice did not show morphological and compositional alterations immediately after 5 minutes of mechanical loading. Changes were evident in loaded limbs 1 and 2 weeks later, consistent with the induction of cell-mediated

processes in these joint tissues that led to the development of progressive OA pathologic changes. Notably the cartilage pathology progressed over the two-week period, whereas the epiphyseal subchondral changes were transient. We speculate that these may be related in part to the differential capacity of the resident cells to remodel and repair the tissue damage. Future studies are needed to define the threshold for induction of bone and cartilage pathology and to define the specific loading parameters that are involved in the initiation of these pathological changes. Importantly, this model provides a system for assessing the effects of pharmacological interventions such as pro-autophagy or anti-resorptive drugs to gain insights into the pathophysiological mechanisms involved in the bone and cartilage changes and for identifying potential therapeutic interventions to prevent the potential adverse effects of mechanical loading.

Acknowledgments

Lyudmila Lukashova of the HSS microCT core facility and the Cornell CARE staff provided experimental assistance. This work was supported by NIH grants R01-AG028664 (MCHM), and RC4-AR060546 and R01-AG022021 (MBG), NSF GRFP (FCK), and the Clark and Kirby Foundations.

3.5 REFERENCES

1. Felson DT, Lawrence RC, Dieppe PA, Hirsch R, Helmick CG, Jordan JM*, et al.* Osteoarthritis: new insights. Part 1: the disease and its risk factors. Ann Intern Med. 2000 Oct 17;133(8):635-46.
2. Kaila-Kangas L, Arokoski J, Impivaara O, Viikari-Juntura E, Leino-Arjas P, Luukkonen R*, et al.* Associations of hip osteoarthritis with history of recurrent exposure to manual handling of loads over 20 kg and work participation: a population-based study of men and women. Occup Environ Med. 2011 Oct;68(10):734-8.
3. Oettmeier R, Arokoski J, Roth AJ, Helminen HJ, Tammi M, Abendroth K. Quantitative study of articular cartilage and subchondral bone remodeling in the knee joint of dogs after strenuous running training. J Bone Miner Res. 1992 Dec;7 Suppl 2:S419-24.
4. Lapvetelainen T, Nevalainen T, Parkkinen JJ, Arokoski J, Kiraly K, Hyttinen M*, et al.* Lifelong moderate running training increases the incidence and severity of osteoarthritis in the knee joint of C57BL mice. Anat Rec. 1995 Jun;242(2):159-65.
5. Lapvetelainen T, Hyttinen M, Lindblom J, Langsjo TK, Sironen R, Li SW*, et al.* More knee joint osteoarthritis (OA) in mice after inactivation of one allele of type II procollagen gene but less OA after lifelong voluntary wheel running exercise. Osteoarthritis Cartilage. 2001 Feb;9(2):152-60.
6. Otterness IG, Eskra JD, Bliven ML, Shay AK, Pelletier JP, Milici AJ. Exercise protects against articular cartilage degeneration in the hamster. Arthritis Rheum. 1998 Nov;41(11):2068-76.

7. Morel V, Berutto C, Quinn TM. Effects of damage in the articular surface on the cartilage response to injurious compression in vitro. J Biomech. 2006;39(5):924-30.

8. Natoli RM, Athanasiou KA. P188 reduces cell death and IGF-I reduces GAG release following single-impact loading of articular cartilage. J Biomech Eng. 2008 Aug;130(4):041012.

9. Backus JD, Furman BD, Swimmer T, Kent CL, McNulty AL, Defrate LE*, et al.* Cartilage viability and catabolism in the intact porcine knee following transarticular impact loading with and without articular fracture. J Orthop Res. 2011 Apr;29(4):501-10.

10. Poulet B, Hamilton RW, Shefelbine S, Pitsillides AA. Characterizing a novel and adjustable noninvasive murine joint loading model. Arthritis Rheum. 2011 Jan;63(1):137-47.

11. Christiansen BA, Anderson MJ, Lee CA, Williams JC, Yik JH, Haudenschild DR. Musculoskeletal changes following non-invasive knee injury using a novel mouse model of post-traumatic osteoarthritis. Osteoarthritis Cartilage. 2012 Jul;20(7):773-82.

12. Ko FC, Dragomir C, Plumb DA, Goldring SR, Wright TM, Goldring MB*, et al.* In vivo cyclic compression causes cartilage degeneration and subchondral bone changes in mouse tibiae. Arthritis Rheum. 2013 Jun;65(6):1569-78.

13. Poulet B, Westerhof TA, Hamilton RW, Shefelbine SJ, Pitsillides AA. Spontaneous osteoarthritis in Str/ort mice is unlikely due to greater vulnerability to mechanical trauma. Osteoarthritis Cartilage. 2013 May;21(5):756-63.

14. Fritton JC, Myers ER, Wright TM, van der Meulen MC. Loading induces site-specific increases in mineral content assessed by microcomputed tomography of the mouse tibia. Bone. 2005 Jun;36(6):1030-8.

15. Lynch ME, Main RP, Xu Q, Walsh DJ, Schaffler MB, Wright TM*, et al.* Cancellous bone adaptation to tibial compression is not sex dependent in growing mice. J Appl Physiol. 2010 Sep;109(3):685-91.

16. Lynch ME, Main RP, Xu Q, Schmicker TL, Schaffler MB, Wright TM*, et al.* Tibial compression is anabolic in the adult mouse skeleton despite reduced responsiveness with aging. Bone. 2011 Sep;49(3):439-46.

17. Glasson SS, Chambers MG, Van Den Berg WB, Little CB. The OARSI histopathology initiative - recommendations for histological assessments of osteoarthritis in the mouse. Osteoarthritis Cartilage. 2010 Oct;18 Suppl 3:S17-23.

18. Glasson SS, Blanchet TJ, Morris EA. The surgical destabilization of the medial meniscus (DMM) model of osteoarthritis in the 129/SvEv mouse. Osteoarthritis Cartilage. 2007 Sep;15(9):1061-9.

19. Kamekura S, Hoshi K, Shimoaka T, Chung U, Chikuda H, Yamada T*, et al.* Osteoarthritis development in novel experimental mouse models induced by knee joint instability. Osteoarthritis Cartilage. 2005 Jul;13(7):632-41.

20. Carames B, Taniguchi N, Seino D, Blanco FJ, D'Lima D, Lotz M. Mechanical injury suppresses autophagy regulators and pharmacologic activation of autophagy results in chondroprotection. Arthritis Rheum. 2012 Apr;64(4):1182-92.

21. Carames B, Taniguchi N, Otsuki S, Blanco FJ, Lotz M. Autophagy is a protective mechanism in normal cartilage, and its aging-related loss is linked with cell death and osteoarthritis. Arthritis Rheum. 2010 Mar;62(3):791-801.

22. Sasaki H, Takayama K, Matsushita T, Ishida K, Kubo S, Matsumoto T*, et al.* Autophagy modulates osteoarthritis-related gene expression in human chondrocytes. Arthritis Rheum. 2012 Jun;64(6):1920-8.

23. Carames B, Hasegawa A, Taniguchi N, Miyaki S, Blanco FJ, Lotz M. Autophagy activation by rapamycin reduces severity of experimental osteoarthritis. Ann Rheum Dis. 2012 Apr;71(4):575-81.

24. Kennedy OD, Herman BC, Laudier DM, Majeska RJ, Sun HB, Schaffler MB. Activation of resorption in fatigue-loaded bone involves both apoptosis and active pro-osteoclastogenic signaling by distinct osteocyte populations. Bone. 2012 May;50(5):1115-22.

25. Goldring MB, Otero M, Plumb DA, Dragomir C, Favero M, El Hachem K*, et al.* Roles of inflammatory and anabolic cytokines in cartilage metabolism: signals and multiple effectors converge upon MMP-13 regulation in osteoarthritis. Eur Cell Mater. 2011;21:202-20.

CHAPTER 4

ABLATION OF DICKKOPF-1 DOES NOT PROTECT ARTICULAR CARTILAGE FROM DEGENERATION FOLLOWING *IN VIVO* MECHANICAL LOADING

4.1 Introduction

The Wnt pathway plays a critical role in the development and maintenance of musculoskeletal tissues, in particular bone and cartilage. Wnt protagonists are increased during early embryonic development and skeletal maturation, whereas antagonists such as Dickkopf-1 (Dkk1), Wifs, and sclerostin are decreased [1]. Disruption of Wnt signaling pathway can lead to severe developmental defects as well as postnatal skeletal problems such as osteoporosis-pseudoglioma syndrome, sclerosteosis, and osteoarthritis (OA) [2-4].

OA is the leading musculoskeletal problem among the elderly population. Recent findings suggest the bone and cartilage unit at the joint undergo dramatic alterations that are associated with changes in Wnt pathway activity [5]. Elevated levels of Frizzled B and Dkk1 are associated with less severe OA and microarray studies show elevated levels of sclerostin expression in subchondral bone from OA patients [6-8]. As a result, Wnt inhibitors such as sclerostin or Dkk1 have been proposed as pharmaceutical interventions to treat OA [9].

While sclerostin has not been shown to prevent or promote OA from preclinical studies [10], alterations in Dkk1 in mice and humans have suggested as a possible therapeutic target for OA. However, both clinical and preclinical studies show contrasting association of Dkk1 levels in OA development. Clinically elevated serum levels of Dkk1 can be associated with less OA, and preclinical studies showed that mice expressing high levels of Dkk1 led to less severe OA, respectively [6, 11]. In contrast to a potential protective role of Dkk1, expressing high levels of

Dkk1 in mice increased chondrocyte hypertrophy leading to increased levels of aggrecanases and cartilage degeneration, whereas mice receiving Dkk1 antisense showed chondrocyte apoptosis from joint inflammation [12, 13]. While genetic knockout mice have been extensively used to understand OA pathomechanisms, Dkk1 knockout mice are embryonically lethal, further limiting our understanding of Dkk1 in the development and progression of OA.

Complete ablation of Dkk1 results in developmental defects in mice, leading to embryonic lethality. However, deletion of one allele of Wnt3 rescues embryos from the defect in head morphogenesis with Dkk1 knockout alone, creating a novel viable animal model [14]. $Wnt3^{+/-}$;$Dkk1^{-/-}$ mice exhibit high bone mass, while no bone phenotypic differences have been reported between $Wnt3^{+/-}$;$Dkk1^{+/+}$ and $Wnt3^{+/+}$;$Dkk1^{+/+}$ (wild type). No study to date has examined the role of Wnt3, Dkk1, and mechanical loading in articular cartilage and subchondral bone homeostasis. Thus, we investigated the role of Dkk1 in the articular cartilage and subchondral bone response to controlled cyclic tibial loading that induces OA-like joint changes in healthy mouse knee joints [15]. We hypothesized that the absence of Dkk1 would lead to increased articular cartilage degeneration and accelerated OA development.

4.2 Materials and Methods

Mechanical Loading Conditions

We applied two weeks of daily (5 days/week) controlled in vivo compressive loading to the left tibiae of 10-week-old male mice with three genotypic background: WT ($Wnt3^{+/+}$;$Dkk1^{+/+}$), Wnt3 ($Wnt3^{+/-}$;$Dkk1^{+/+}$), and Dkk1 KO ($Wnt3^{+/-}$;$Dkk1^{-/-}$) mice (n = 7-8/group, Table 4.1). Loading protocol consisted of applying a peak load level of 9.0N, frequency at 4Hz for 1200 cycles (5 minutes) under general anesthesia (2% Isoflurane, 1.0 L/min, Webster). The applied

loading was based on protocols demonstrated previously to create articular cartilage degeneration and have an anabolic effect on the tibial metaphysis in growing and adult mice [15-18]. The right limb served as the non-loaded control. After 2 weeks of loading, mice were euthanized, and intact knee joints were fixed in 4% paraformaldehyde overnight. All experimental procedures were approved by the Institutional Animal Care and Use Committee.

Table 4.1 Experimental groups by genotype allele and respective final body mass, tibial lengths, the number of osteophyte occurrences at the end of 2-week loading session.

Experimental Group	**WT**	**Wnt3**	**Dkk1 KO**
Genotype	$Wnt3^{+/+}$;$Dkk1^{+/+}$	$Wnt3^{+/-}$;$Dkk1^{+/+}$	$Wnt3^{+/-}$;$Dkk1^{-/-}$
Body Mass (g)	33.9 ± 4.9	37.9 ± 4.3	31.3 ± 4.9
Tibial Length (mm) Right	17.9 ± 0.58	17.9 ± 0.38	17.2 ± 0.12
Left	18.0 ± 0.40	18.0 ± 0.32	17.3 ± 0.18
Osteophytes (# of occurrences/sample size)	4/8	3/7	7/7

Cartilage and Subchondral Bone Assessment

After tissue fixation overnight, intact joints were scanned by microcomputed tomography (microCT) at 10 μm resolution (μCT35, Scanco, Switzerland) with an X-ray tube potential of 55 kVp in PBS to assess bone morphological changes. Knee joints were then decalcified in formic acid/sodium citrate for one week, dehydrated in an ethanol gradient, and embedded in paraffin. Serial coronal sections of 6 μm thickness were obtained using a rotary microtome (Leica RM2255, Germany). Safranin O/Fast green/Hematoxylin staining was performed on sections at 90 μm intervals to assess cartilage morphology. Cartilage degeneration was assessed in the tibial plateau using a modified murine cartilage histological scoring system [19].

Bone morphology from microCT was assessed in two regions: the metaphysis (distal to the growth plate) extending 10% of the total bone length, excluding primary spongiosa and cortical bone; and the epiphysis (proximal to the growth plate) excluding cortical bone. Only trabecular bone from both regions was selected by manually contouring inside the cortical bone. The global threshold was set at 4100 HU and 3360 HU to segment mineralized tissue in epiphyseal and metaphyseal regions, respectively. For each region, cancellous bone volume fraction (BV/TV), trabecular thickness and separation (Tb.Th, Tb.Sp), and tissue mineral density (TMD) were measured.

Localized cartilage thickness measurements were performed on Safranin O/Fast Green stained slides previously used for histological scoring (Osteomeasure, OsteoMetrics, USA). The tibial plateau was first divided into medial and lateral plateaus, then further divided into anterior, middle, and posterior regions, resulting in six different tibial plateau regions. A single representative slide from each region was used to measure cartilage and subchondral cortical bone thickness. Five linear projections from the cartilage surface to the boundary between cartilage and subchondral bone were used to measure cartilage thickness [15].

Cellular Response Assessment

Immunohistochemistry was performed to assess mechanisms responsible for articular cartilage changes from 2 weeks of mechanical loading. Antibodies for MMP-13 (Chemicon, Temecula, CA), a key metalloproteinase responsible for proteoglycan breakdown in articular cartilage, and unphosphorylated β-catenin (Millipore, Billerica, MA), a cytoplasmic protein important in canonical Wnt signaling, were applied on three sections, one each from the anterior, middle, and posterior aspects of the tibial plateau. Sections were dewaxed, rehydrated, and

incubated in 37°C for antigen retrieval with 2.5% hyaluronidase. Sections were than incubated with serum free protein block (Dako, Carpinteria, CA) for 30 minutes at room temperature and immunostained overnight at 4°C with primary antibodies and IgG as negative controls. Secondary antibody incubation and color development were done by strepdavidin (Dako, Carpinteria, CA). MMP-13 and β-catenin positively stained chondrocytes were counted and normalized by cartilage area under 40x magnification from three sections each from anterior, middle, and posterior aspect of the tibial plateau.

Statistics

Statistical analyses were performed using a 2-factor repeated measure ANOVA with interactions (JMP Pro 10.0, SAS Institute Inc), with *Loading* as the intra-group variable, and *Genotype* as the inter-group variable. Post-hoc means comparison tests were performed with Bonferroni correction when interaction effects were significant. P-values < 0.05 indicated significance. All values are presented as mean ± SD.

4.3 Results

Articular Cartilage Matrix Changes

Mechanical loading increased the severity of articular cartilage degeneration, indicated by an increase in histological scores, in loaded limbs of Dkk1 KO and WT mice compared to control limbs (Fig 4.1A). Loading increased the histological score by 48% in WT mice and 253% in Dkk1 KO mice, respectively (Fig 4.1B). However, in Wnt3 mice, loading did not induce cartilage degeneration, and the left and right scores were similar. The scores of the loaded of the control limbs of WT, Wnt3, and Dkk1 KO mice were not different from each other among all

genotypes. In addition, articular cartilage in Dkk1 KO mice only thinned in the lateral and medial compartments of the posterior aspect of the tibial plateau, whereas remained the same with mechanical loading in WT and Wnt3 cartilage thickness (Fig 4.1C). After 2 weeks of loading, cartilage thinned by 35% in the lateral posterior compartment and 33% in the medial lateral posterior compartment of Dkk1 KO mice.

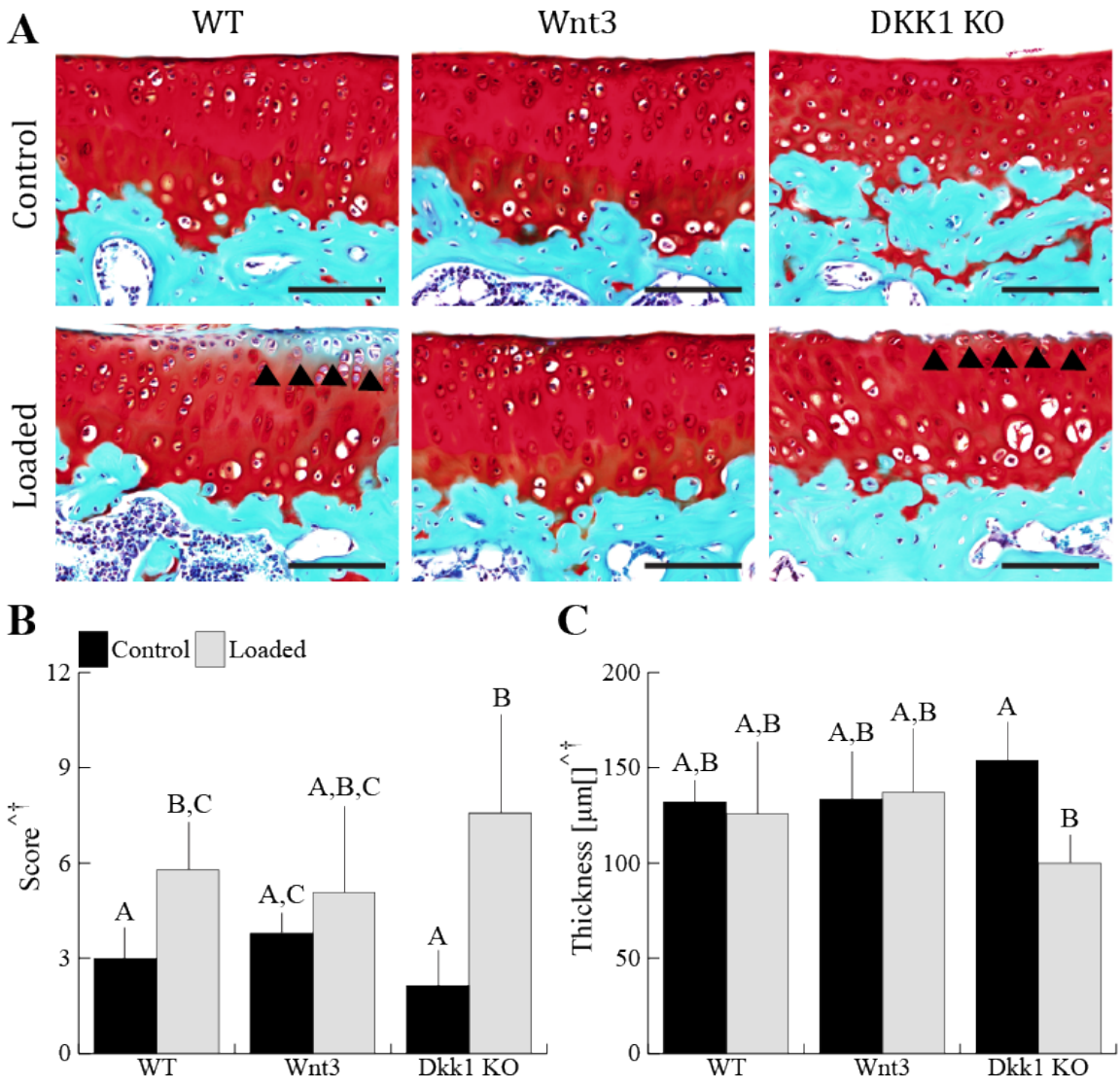

Figure 4.1 Safranin O/Fast Green staining indicated cartilage degeneration occurred following two weeks of loading in WT and Dkk1 KO mice (A, Scale bar = 100 μm). Loading did not promote cartilage degeneration in Wnt3 mice. Control images represent a non-loaded contralateral limb at loaded groups. Histological score also indicated an increase in cartilage degeneration in WT and Dkk1 KO mice, but not in Wnt 3 mice (B). Loading also thinned articular cartilage at the lateral posterior quadrant (C). Data presented as mean ± SD.

^loading, †loading*genotype, $p<0.05$ by repeated measures two-way ANOVA. Groups with different letters are significantly different by post-hoc means comparisons with Bonferroni correction.

Epiphyseal and Metaphyseal Bone Adaptation

Epiphyseal and metaphyseal cancellous architecture changed with mechanical loading and genotype. Mechanical loading decreased epiphyseal cancellous bone mass overall by 5.7% (Fig 4.2A). Also, the decrease in epiphyseal cancellous bone mass from loading was dependent on genotype: 7.1% decrease in WT mice, a 11.6% decrease in Wnt3 mice, and an increase of 1.4% in Dkk1 KO mice. Trabeculae were thicker in Dkk1 KO mice compared to other genotypes, where trabeculae were thicker by 18% and 14% in Dkk1 KO mice compared to WT and Wnt3 mice, respectively (Fig 4.2B). Epiphyseal trabecular separation did not change with loading or genotype (Fig 4.2C). In the metaphyseal region, cancellous bone mass increased with loading by 11% (Fig 4.2D). The increase in cancellous bone mass was attributable to a 17% increase in trabecular thickness (Fig 4.2E). Also, increase trabecular thickness from loading was dependent on genotype, where loading increased thickness by 17% in WT, 8.2% in Wnt3, and 26% in Dkk1 KO mice. Subchondral cortical bone thickness only decreased in both compartments of the middle aspect of the tibial plateau with loading (Fig 4.2F). 2 weeks of loading thinned subchondral cortical bone thickness by 30% in lateral middle compartment and by 19% in medial middle compartment.

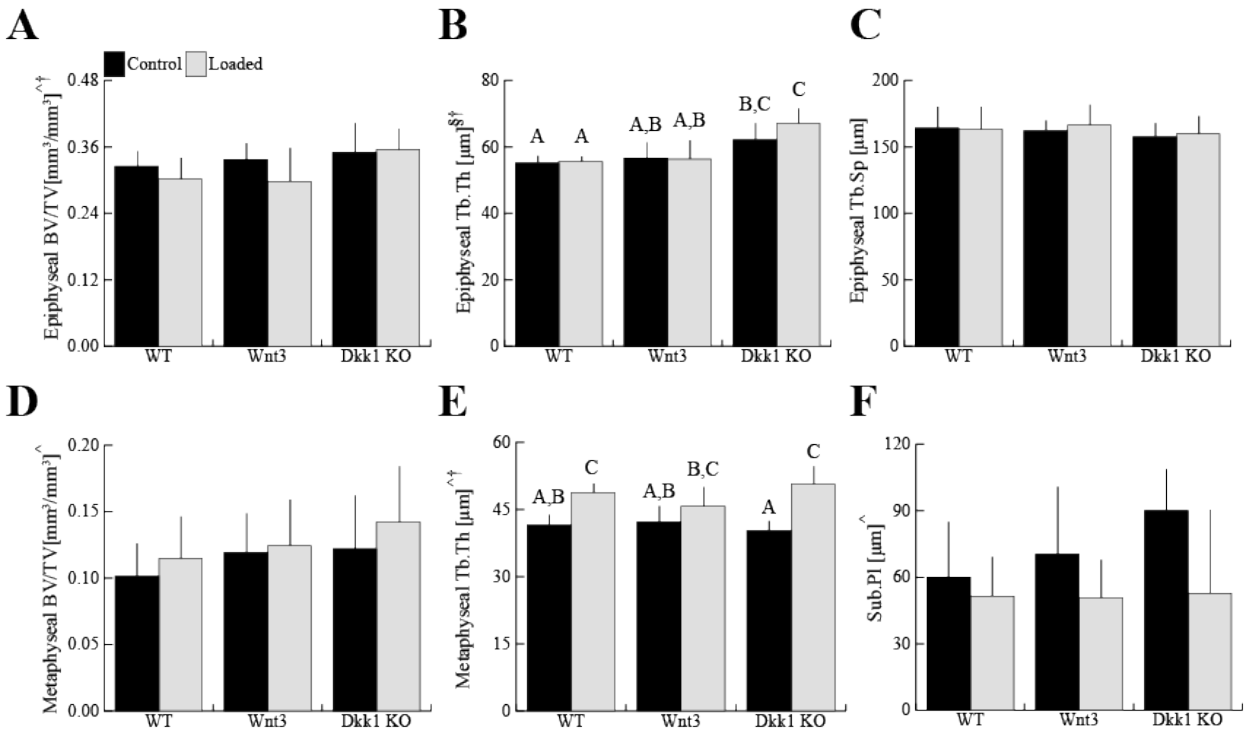

Figure 4.2 Epiphyseal cancellous mass (BV/TV) in 10-week-old mice decreased with loading, which was dependent on the mouse genotype (A). Epiphyseal trabecular thickness (Tb.Th) was significantly higher in Dkk1 KO mice (B). Trabecular separation (Tb.Sp) was not altered by the loading or genotype (C). Metaphyseal bone mass increased with loading (D), which was attributable to increase in metaphyseal trabecular thickness (E). Subchondral cortical plate thickness (Sub.Pl) from the lateral middle compartment thinned with mechanical loading (F). Data presented as mean ± SD.
^loading, §genotype, †loading*genotype, $p<0.05$ by repeated measures two-way ANOVA. Groups with different letters are significantly different by post-hoc means comparisons with Bonferroni correction.

Articular Cartilage Chondrocyte Immunostaining

Mechanical loading altered the number of chondrocytes stained for MMP-13 and β-catenin in WT, Wnt3, and Dkk1 KO mice. The increase in chondrocytes immunostained for MMP-13 due to loading was dependent on genotype; we observed 84% increase in WT, 7.3% increase in Wnt3, and 26% decrease in Dkk1 KO mice (Fig 4.3A). The number of chondrocytes immunostained for β-catenin increased with loading by 85% (Fig 4.3B).

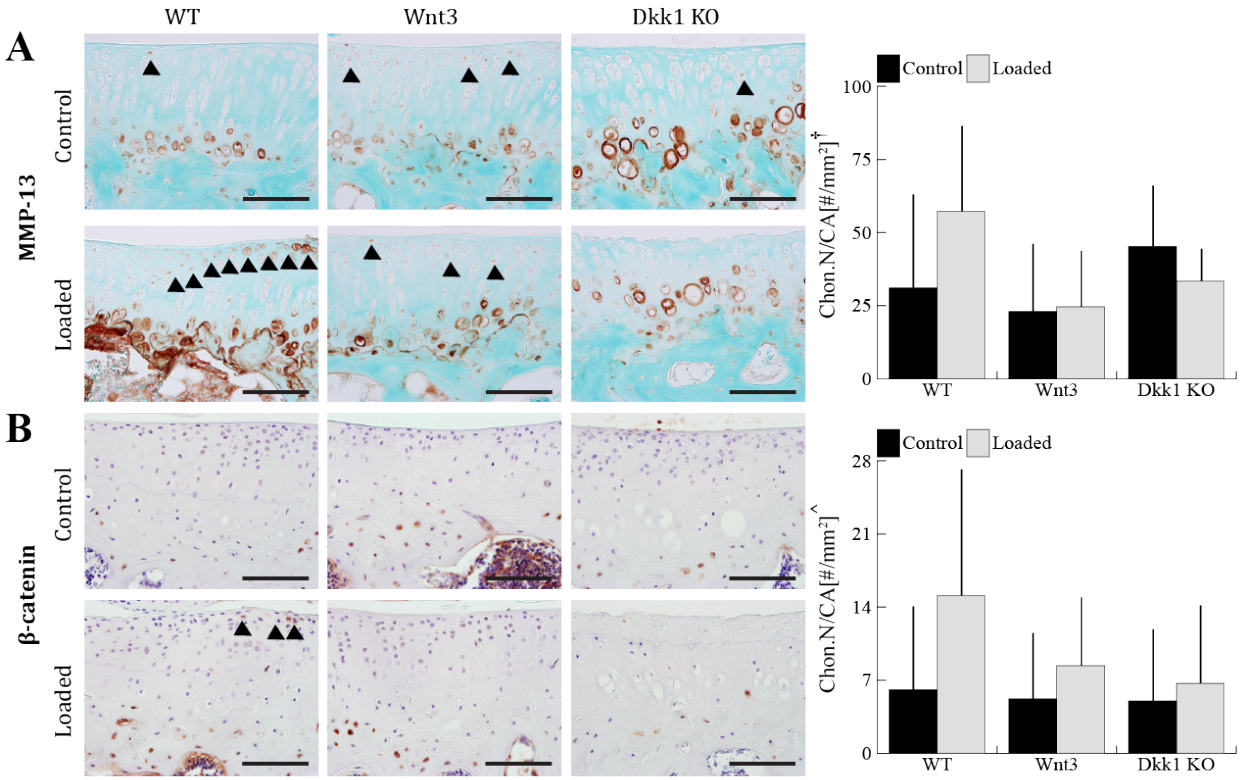

Figure 4.3 Cellular responses: MMP-13 and β-catenin. Increase in the number of chondrocytes immunostained for MMP-13 with loading was dependent on genotype (A). Loading increased the number of chondrocytes immunostained for β-catenin (B). Arrowheads indicate positive antibody staining. Data presented as mean ± SD. Scale bar = 100 μm
^loading, †loading*genotype, $p<0.05$ by repeated measures two-way ANOVA.

Osteophyte Formation

Osteophytes formed in the peri-articular regions of the tibial plateau in response to mechanical loading (Fig 4.4). All (7/7) Dkk1 KO, 4/8 WT, and 3/7 Wnt3 mice formed osteophytes on the loaded limbs. No osteophytes were observed in control limbs from any genotype.

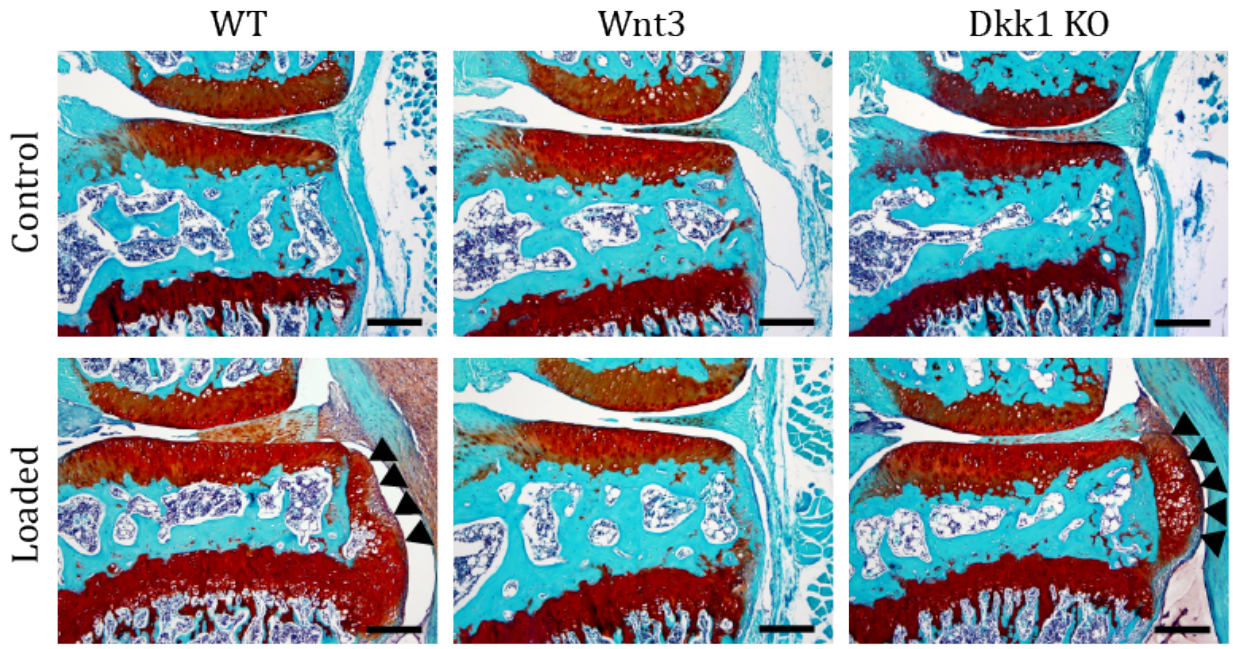

Figure 4.4 Osteophytes (black arrowheads) were present in 4/8 WT, 3/7 Wnt3, and 7/7 Dkk1 KO mice following 2 weeks of mechanical loading. Scale bar 200 µm.

4.4 Discussion

We showed that articular cartilage degeneration accelerated with loading in Dkk1 KO mice compared to Wnt3 mice, but was similar to WT mice. In addition, articular cartilage from Dkk1 KO mice thinned with mechanical loading. These tissue level changes were accompanied by upregulation of MMP-13 and β-catenin expression in chondrocytes of WT mice. Loading decreased epiphyseal cancellous bone mass overall, but increased metaphyseal cancellous bone mass in all mice. All Dkk1 KO mice developed osteophytes in response to loading, whereas approximately half of WT and Wnt3 loaded joints developed osteophytes.

Comparing control limbs only, the haploinsufficiency of Wnt3 and/or ablation of Dkk1 did not lead to cartilage degeneration. Absence or inhibition of an other potent Wnt inhibitor, sclerostin, also did not result in joint degeneration among sclerostin KO mice or rats that underwent destabilization of medial meniscus (DMM) surgery with anti-sclerostin antibody administration [10]. While the canonical Wnt/β-catenin pathway is suggested to play an

important role in the expression of cartilage catabolic factors, other Wnt inhibitors such as Frizzled B and Gremlin 1 can act as a compensatory mechanism to prevent OA in the absence of Dkk1 [20].

Wnt3 mice resisted cartilage degeneration from loading compared to WT mice in our study. The presence of cartilage damage in Dkk1 KO mice with loading, however, indicated that the apparent chondroprotective nature of Wnt3 knockdown was lost by the absence of Dkk1. Our immunohistochemical analysis showed that in the presence of mechanical loading, knockdown of Wnt3 may lead to decreased expression of β-catenin and MMP-13 in articular chondrocytes, leading to a less severe OA phenotype compared to WT or Dkk1 KO animals. No other studies have demonstrated a potential role of Wnt3 in the development of OA or cartilage or bone homeostasis, while Wnt3a showed a potential role in OA [21, 22]. However, Wnt3 may only be active in the presence of mechanical loading, and further investigation of its role in the development of OA could potentially lead to therapeutic intervention.

Limited osteophyte development in WT and Wnt3 mice indicated a potential role of Dkk1 in osteophyte formation in response to mechanical loading. Previously, neutralizing Dkk1 activity by antibody treatment in mouse joints led to inflammatory-mediated osteophyte formation [23]. In our study, mechanical loading may have initiated inflammatory processes that cascaded to osteophyte development in Dkk1 KO mice. In addition to osteophyte formation, ablation of Dkk1 combined with mechanical loading can be detrimental to overall joint homeostasis by increasing subchondral bone stiffness, which will increase the stress in the articular cartilage and expedite the development of OA [24].

Consistent with previous studies, articular cartilage degeneration in WT, Wnt3, and Dkk1 KO mice was accompanied by loss of epiphyseal cancellous mass and thinning of the

subchondral plate [15, 25]. However, in contrast to mice with increased bone mass from sclerostin inhibition via monoclonal antibodies, Dkk1 KO mice did not exhibit higher bone mass compared to their respective littermate or Wnt3 haploinsufficient controls [26, 27]. Mixed background (129xC57Bl/6) of mutant mice with significant developmental disability associated with the loss of Dkk1, Wnt3 knockdown alone may be insufficient to increase the bone mass in Dkk1 KO mice at a similar level seen in SOST KO mice [14, 28].

In conclusion, mechanical loading accelerated articular cartilage damage in Dkk1 KO compared to Wnt3 haploinsufficient mice, returning to WT levels. Wnt3 haploinsufficiency can be chondroprotective against load-induced OA. Additional characterization of the role of Wnt3 and Dkk1 in the development of OA will further enhance our understanding of Wnt pathway and its role in OA. Future studies that perform mechanical loading on mice with chondrocyte specific mutations of Dkk1, combined with pharmaceutical agents that influence another Wnt mediator, for example sclerostin, will help in identifying the signaling mechanism underlying load-induced cartilage degeneration and possibly lead to the development of pharmacological interventions.

Acknowledgments

We thank Lyudmila Lukashova and Stephen Hong for experimental assistance. A Burroughs Welcome Foundation Collaborative Research Grant, NIH grants R01-AG028664, and NSF GRF (FCK) funded this work.

4.5 REFERENCES

1. Guo X, Day TF, Jiang X, Garrett-Beal L, Topol L, Yang Y. Wnt/beta-catenin signaling is sufficient and necessary for synovial joint formation. Genes Dev. 2004 Oct 1;18(19):2404-17.
2. Gong Y, Slee RB, Fukai N, Rawadi G, Roman-Roman S, Reginato AM, Wang H, Cundy T, Glorieux FH, Lev D, Zacharin M, Oexle K, Marcelino J, Suwairi W, Heeger S, Sabatakos G, Apte S, Adkins WN, Allgrove J, Arslan-Kirchner M, Batch JA, Beighton P, Black GC, Boles RG, Boon LM, Borrone C, Brunner HG, Carle GF, Dallapiccola B, De Paepe A, Floege B, Halfhide ML, Hall B, Hennekam RC, Hirose T, Jans A, Juppner H, Kim CA, Keppler-Noreuil K, Kohlschuetter A, LaCombe D, Lambert M, Lemyre E, Letteboer T, Peltonen L, Ramesar RS, Romanengo M, Somer H, Steichen-Gersdorf E, Steinmann B, Sullivan B, Superti-Furga A, Swoboda W, van den Boogaard MJ, Van Hul W, Vikkula M, Votruba M, Zabel B, Garcia T, Baron R, Olsen BR, Warman ML. LDL receptor-related protein 5 (LRP5) affects bone accrual and eye development. Cell. 2001 Nov 16;107(4):513-23.
3. Luyten FP, Tylzanowski P, Lories RJ. Wnt signaling and osteoarthritis. Bone. 2009 Apr;44(4):522-7.
4. Kubota T, Michigami T, Ozono K. Wnt signaling in bone metabolism. J Bone Miner Metab. 2009;27(3):265-71.
5. Lories RJ, Luyten FP. The bone-cartilage unit in osteoarthritis. Nat Rev Rheumatol. 2011 Jan;7(1):43-9.

6. Lane NE, Nevitt MC, Lui LY, de Leon P, Corr M. Wnt signaling antagonists are potential prognostic biomarkers for the progression of radiographic hip osteoarthritis in elderly Caucasian women. Arthritis Rheum. 2007 Oct;56(10):3319-25.

7. Hopwood B, Tsykin A, Findlay DM, Fazzalari NL. Microarray gene expression profiling of osteoarthritic bone suggests altered bone remodelling, WNT and transforming growth factor-beta/bone morphogenic protein signalling. Arthritis Res Ther. 2007;9(5):R100.

8. Power J, Poole KE, van Bezooijen R, Doube M, Caballero-Alias AM, Lowik C, Papapoulos S, Reeve J, Loveridge N. Sclerostin and the regulation of bone formation: Effects in hip osteoarthritis and femoral neck fracture. J Bone Miner Res. 2010 Aug;25(8):1867-76.

9. Lories RJ, Corr M, Lane NE. To Wnt or not to Wnt: the bone and joint health dilemma. Nat Rev Rheumatol. 2013 Mar 5.

10. Roudier M, Li X, Niu QT, Pacheco E, Pretorius JK, Graham K, Yoon BR, Gong J, Warmington K, Ke HZ, Black RA, Hulme J, Babij P. Sclerostin is expressed in articular cartilage but loss or inhibition does not affect cartilage remodeling during aging or following mechanical injury. Arthritis Rheum. 2013 Mar;65(3):721-31.

11. Oh H, Chun CH, Chun JS. Dkk-1 expression in chondrocytes inhibits experimental osteoarthritic cartilage destruction in mice. Arthritis Rheum. 2012 Aug;64(8):2568-78.

12. Weng LH, Wang CJ, Ko JY, Sun YC, Wang FS. Control of Dkk-1 ameliorates chondrocyte apoptosis, cartilage destruction, and subchondral bone deterioration in osteoarthritic knees. Arthritis Rheum. 2010 May;62(5):1393-402.

13. Weng LH, Wang CJ, Ko JY, Sun YC, Su YS, Wang FS. Inflammation induction of Dickkopf-1 mediates chondrocyte apoptosis in osteoarthritic joint. Osteoarthritis Cartilage. 2009 Jul;17(7):933-43.

14. Lewis SL, Khoo PL, De Young RA, Steiner K, Wilcock C, Mukhopadhyay M, Westphal H, Jamieson RV, Robb L, Tam PP. Dkk1 and Wnt3 interact to control head morphogenesis in the mouse. Development. 2008 May;135(10):1791-801.

15. Ko FC, Dragomir C, Plumb DA, Goldring SR, Wright TM, Goldring MB, van der Meulen MC. In vivo cyclic compression causes cartilage degeneration and subchondral bone changes in mouse tibiae. Arthritis Rheum. 2013 Jun;65(6):1569-78.

16. Fritton JC, Myers ER, Wright TM, van der Meulen MC. Loading induces site-specific increases in mineral content assessed by microcomputed tomography of the mouse tibia. Bone. 2005 Jun;36(6):1030-8.

17. Lynch ME, Main RP, Xu Q, Walsh DJ, Schaffler MB, Wright TM, van der Meulen MC. Cancellous bone adaptation to tibial compression is not sex dependent in growing mice. J Appl Physiol. 2010 Sep;109(3):685-91.

18. Lynch ME, Main RP, Xu Q, Schmicker TL, Schaffler MB, Wright TM, van der Meulen MC. Tibial compression is anabolic in the adult mouse skeleton despite reduced responsiveness with aging. Bone. 2011 Sep;49(3):439-46.

19. Glasson SS, Chambers MG, Van Den Berg WB, Little CB. The OARSI histopathology initiative - recommendations for histological assessments of osteoarthritis in the mouse. Osteoarthritis Cartilage. 2010 Oct;18 Suppl 3:S17-23.

20. Leijten J, Bos SD, Landman EB, Georgi N, Jahr H, Meulenbelt I, Post JN, van Blitterswijk CA, Karperien M. GREM1, FRZB and DKK1 mRNA levels correlate with

osteoarthritis and are regulated by osteoarthritis-associated factors. Arthritis Res Ther. 2013;15(5):R126.

21. Yuasa T, Otani T, Koike T, Iwamoto M, Enomoto-Iwamoto M. Wnt/beta-catenin signaling stimulates matrix catabolic genes and activity in articular chondrocytes: its possible role in joint degeneration. Lab Invest. 2008 Mar;88(3):264-74.

22. Thomas RS, Clarke AR, Duance VC, Blain EJ. Effects of Wnt3A and mechanical load on cartilage chondrocyte homeostasis. Arthritis Res Ther. 2011;13(6):R203.

23. Diarra D, Stolina M, Polzer K, Zwerina J, Ominsky MS, Dwyer D, Korb A, Smolen J, Hoffmann M, Scheinecker C, van der Heide D, Landewe R, Lacey D, Richards WG, Schett G. Dickkopf-1 is a master regulator of joint remodeling. Nat Med. 2007 Feb;13(2):156-63.

24. Radin EL, Rose RM. Role of subchondral bone in the initiation and progression of cartilage damage. Clin Orthop Relat Res. 1986 Dec(213):34-40.

25. Botter SM, van Osch GJ, Clockaerts S, Waarsing JH, Weinans H, van Leeuwen JP. Osteoarthritis induction leads to early and temporal subchondral plate porosity in the tibial plateau of mice: an in vivo microfocal computed tomography study. Arthritis Rheum. 2011 Sep;63(9):2690-9.

26. Li X, Ominsky MS, Warmington KS, Morony S, Gong J, Cao J, Gao Y, Shalhoub V, Tipton B, Haldankar R, Chen Q, Winters A, Boone T, Geng Z, Niu QT, Ke HZ, Kostenuik PJ, Simonet WS, Lacey DL, Paszty C. Sclerostin antibody treatment increases bone formation, bone mass, and bone strength in a rat model of postmenopausal osteoporosis. J Bone Miner Res. 2009 Apr;24(4):578-88.

27. Li X, Warmington KS, Niu QT, Asuncion FJ, Barrero M, Grisanti M, Dwyer D, Stouch B, Thway TM, Stolina M, Ominsky MS, Kostenuik PJ, Simonet WS, Paszty C, Ke HZ. Inhibition of sclerostin by monoclonal antibody increases bone formation, bone mass, and bone strength in aged male rats. J Bone Miner Res. 2010 Dec;25(12):2647-56.

28. Li X, Ominsky MS, Niu QT, Sun N, Daugherty B, D'Agostin D, Kurahara C, Gao Y, Cao J, Gong J, Asuncion F, Barrero M, Warmington K, Dwyer D, Stolina M, Morony S, Sarosi I, Kostenuik PJ, Lacey DL, Simonet WS, Ke HZ, Paszty C. Targeted deletion of the sclerostin gene in mice results in increased bone formation and bone strength. J Bone Miner Res. 2008 Jun;23(6):860-9.

CHAPTER 5

SUMMARY AND DISCUSSION

5.1 Summary

The objective of this research was to develop, characterize, and implement a noninvasive mouse model of OA induced by altering the loading environment at the knee joint. Traditional preclinical models of OA involve trauma, which only represents 16% of OA patients [1]. Noninvasive loading models that provide a controlled loading environment and result in robust and reproducible OA pathology similar to that seen in humans will represent the much larger community of OA patients without the history of traumatic joint injuries.

Development of Osteoarthritic Pathology in Mouse Knee Joint Following Cyclic Loading

Traditional preclinical models of OA are generally based on transection of ligaments or meniscus to induce joint instability and trauma [2, 3]. Patients suffering from posttraumatic OA are only a fraction of total OA patient cohorts, and other factors such as genetics, diet, sex, or altered loading contribute significantly in the development of OA [1]. The novel noninvasive loading model developed in this research not only addresses the lack of a nontraumatic OA model in the field, but also provides a well-controlled loading environment that can simulate varying degrees of physical activity. In this study, a peak load level of 9.0N induced articular cartilage matrix damage, epiphyseal bone adaptation, and osteophyte formation, but less severe cartilage degeneration without osteophyte formation and epiphyseal bone adaptation was present at a peak load level of 4.5N, indicating a dose dependency to loading. This dose dependency of joint degeneration has also been observed in other studies examining different distances of

running: 30km of running over 28 days was detrimental whereas 15km over 28 days was beneficial to rats that underwent ACL transection [4]. Mice that underwent in vivo tibial loading also exhibited concurrent changes in subchondral cortical bone thickness and articular cartilage degeneration. While the study did not establish a strong causation between changes in subchondral bone and articular cartilage, future therapeutic interventions will likely need to target both subchondral bone and cartilage to fully restore the joint's original structure.

Single Loading Session Promote Biological Responses Leading to Osteoarthritis Phenotype

Single injurious impact loading sessions have been applied to cartilage explants and rodent joints to produce OA pathology similar in humans [5-8]. Upon application of loading, chondrocytes underwent apoptosis and secreted proteases that degraded collagen and proteoglycans [5]. In addition, preclinical models of injurious loading showed not only cartilage degeneration, but also abnormal heterotopic ossification at locations removed from the tibiofemoral contact area [7, 8]. We applied a single 5-minute session of loading to the knees of mice. The knee joints demonstrated no obvious traumatic tissue damage after the onset of loading but still subsequently developed OA at later time points. While a single loading session promoted development of OA pathology in mouse joints similar to joints from mice that underwent daily cyclic loading for 1 or 2 weeks, the extent of cartilage degeneration was less, and subchondral cortical bone thickening and metaphyseal cancellous bone adaptation were absent in mice with a single loading session. Our multiday loading experiment may represent elite athletes who undergo strenuous training everyday, whereas a single loading session may be more applicable to amateur athletes exposed to short-term excessive exercise that may be detrimental to their joints in the future. However, as the epiphyseal cancellous mass lost at 1-

week was restored to the original level at 2-weeks, the possibility of interventions to restore bone mass and architecture and functionality from OA is promising. In fact, rats that underwent ACL transection were protected from accelerated cartilage degeneration and subchondral bone changes by the administration of alendronate, a potent inhibitor of bone resorption [9]. While clinical studies show limited therapeutic effect of alendronate among OA patients, other inhibitors of bone resorption such as Denosumab or Cathepsin K inhibitor can be alternatively tested [10, 11].

The Role of Dkk1 and Wnt3 in Load-induced Osteoarthritis

Dkk1 is a potent regulator joint remodeling in rheumatoid arthritis (RA), in which administration of Dkk1 antibody to inhibit Wnt signaling reduced the symptoms of RA and also led to development of osteophytes [12]. Whether Dkk1 can also have a potent role in OA is still unknown. This study indicated that the ablation of Dkk1 did not protect the joint from load-induced OA, but in fact accelerated alterations in the joint to resemble human OA. With the activation of the Wnt/β-catenin canonical pathway, which has been strongly suggested to increase cartilage catabolic factors that lead to cartilage degeneration and OA, the lack of chondroprotection in the absence of Dkk1 may have led to accelerated development of OA in Dkk1 knockout mice in response to loading [13, 14]. Also, surprisingly, mice with Wnt3 knockdown were protected from developing OA pathology in response to *in vivo* loading. With no evidence to date for a role of Wnt3 in the development of OA, further characterization is needed to validate the chondroprotective nature of Wnt3 knockdown and understand the underlying mechanism. Ultimately, this study not only provided further understanding of the role of Dkk1 and Wnt3 in the pathogenesis of OA, but also demonstrated that *in vivo* tibial loading

does not always lead to cartilage degeneration, and the joint can be protected from with appropriate mechanical or biological conditions.

Strengths of This Work

The novel, noninvasive mouse tibial loading model developed here provides several advantages over existing traditional OA models. The noninvasive, nontraumatic nature of the applied loading allows investigators to translate mechanistic discoveries of OA to the clinical scenario in which the majority of OA patients have not been exposed to joint injuries. The model avoids potential confounding factors resulting from inflammation due to surgical induction of OA in previously existing models. Also, the model provides a unique platform in which loading applied to the mouse knee joint can be precisely controlled. Depending on the hypothesis, specific loads can be applied to the mouse knee that can potentially be traumatic or beneficial to the joint. In addition, unlike other loading models that apply mechanical loads via varus or valgus loading, mouse tibial loading applies uniaxial loads on the joint that more likely resemble the physiological gait pattern in mice [15, 16]. Lastly, widely available knockout and transgenic mouse models can be utilized in this loading approach to identify specific genes or proteins responsible for joint degeneration in response to mechanical loading, leading to OA. Conversely, specific loading protocols can be investigated to restore transgenic mouse models susceptible to OA pathology.

The systemic approach to investigate alterations in mice joints is another strength of this work. While traditional preclinical OA studies focus on a single tissue, such as articular cartilage or subchondral bone, this work encompasses both tissues as well as synovial membrane and periarticular bone regions. With clinical studies suggesting OA patients suffer from systemic

joint alterations, investigating OA animal models via systemic approaches will further enhance our understanding of how OA develops and progresses.

Limitations of This Work

This loading model has limitations. Currently, the strain or stress that is being transmitted to the articular cartilage and subchondral bone cannot be determined. The peak load level applied to the mouse joint is based on strain measurements on the tibial midshaft where 1200ε is within the functional range of strain magnitude [17]. However, with irregular tibial plateau geometry, unknown compositional properties of joint tissues, and close proximity to where the load is being applied, articular cartilage and subchondral bone will experience dramatically different strain and stress magnitudes. Compared to larger mammals, performing traditional contact stress analysis or pressure measurements on a small mouse joint is a significant challenge. Even if the strain magnitude could be determined, the measured strain will only represent the strain at baseline. Any changes in strain or stress levels due to adaptation over the course of the mechanical loading duration will not be determined until the end of the experiment.

In addition, interpreting and relating findings from mouse articular cartilage and subchondral cortical bone to clinical scenarios need to be performed carefully. While compositional characteristics of the tissues such as the collagen backbone and glycosaminoglycans of cartilage are present in both humans and mice, the chondrocyte density in mouse articular cartilage is approximately 24 times larger than the density from human cartilage [18]. The higher cellularity in mouse cartilage can lead to more rapid response to changes in the external environment compared to human cartilage. Also, structural compositions of meniscus in mice and humans are different, where the mouse meniscus exhibits an ossified central region with bone marrow.

Lastly, the rodent growth plate never completely fuses, as it does in humans, and subchondral cortical bone in mice is much thinner than in humans. As for any preclinical models, investigators should be aware of these differences and interpret the findings accordingly.

Histomorphometric analysis that counted immunostained chondrocytes or osteoclasts in this work needs to be interpreted carefully. With chondrocyte diameter of approximately 7-12μm and osteoclasts 50-100μm, sectional thickness of 6μm used in this work for histomorphometric analysis only captures partial cell volume. Additional selection criteria such as nuclei or pericellular stainings and multiple histology sections from each animal were implemented to identify cell phenotype accurately. With no existing 3-D histomorphometric analysis for immunostained cells, the methods used in this work are the most prevalent ways to capture cell phenotype in the field.

5.2 Future Studies

The findings from this thesis establish a foundation for future work that will investigate pathomechanisms of load-induced OA and appropriate therapeutic interventions. Additional mechanical and biological characterizations of the model and application of the model to mice with conditional inactivation or overexpression of mechanosensitive genes will greatly expand understanding of OA.

Characterization of In Vivo Loading Model

As mentioned in the limitations, due to the size of murine joint, accurate analysis of contact stress and strain is a significant challenge. Finite element analysis (FEA) of the mouse knee joint under the same loading device identified focal stress concentration on the medial side of

tibiofemoral joint [19]. However, the FEA model assumed cartilage and subchondral bone to be homogenous isotropic materials with elastic moduli based on a previous FEA study [20]. Experimental determination of murine articular cartilage stiffness via nanoindentation or atomic force microscopy with appropriate nonlinear heterogeneous FEA study will provide accurate strain and stress distribution at the joint. Articular cartilage stiffness can be measured at different locations on a tibial plateau by atomic force microscopy, which allows measurement of small specimens in a hydrated state [21, 22]. A study can be designed articular cartilage stiffness is obtained from a basal time point up to a 6-week loading duration with multiple time points in between. In addition to determining appropriate experimental mechanical properties of articular cartilage stiffness, controversial issues regarding the order of changes between cartilage and bone during OA development can potentially be answered by measuring subchondral cortical bone stiffness.

Whole joint kinematics can also be investigated during mechanical loading of mouse joints. Lameness and stiffness of joints are one of the key symptoms of OA patients, and determining similar symptoms in mice can be a challenge due to small scale. Investigating joint kinematics in mouse joints can potentially indicate lameness and stiffness of joints seen similar in humans. By comparing movements at tibiofemoral joints prior to and post loading, we can potentially predict joint motions that increase chances of developing OA.

Articular cartilage and subchondral bone composition can determined by spectroscopic analysis, in particular Fourier transform infrared spectroscopy (FT-IR) [23]. Upon induction of OA, the zone of calcified cartilage expands, and this expansion has been shown in our laboratory through histological analysis (data not shown). This morphological change in the zone of calcified cartilage can be further characterized by compositional analysis through FT-IR. During

the expansion of the calcified zone from mechanical loading, FT-IR will measure mineralization in the general vicinity to determine whether the expansion is purely cartilage, or possible interaction exists between subchondral bone and cartilage.

Finally, characterizing biological expressions in both articular cartilage and subchondral bone in response to loading will allow development of future pharmacological interventions. To discover a unique biological factor that contributes to load-induced OA, loaded mouse joints can be analyzed by either microarray or RNAseq to initially select candidate genes that can be developed into a conditional knockout model for further investigation [24, 25].

Conditional Inactivation or Overexpression of Mechanosensitive Gene – SOST

The noninvasive loading model in this thesis demonstrated load level and duration dependent alterations in mouse joints. Mechanosensitive genes from articular cartilage and subchondral bone may be responsible for the dose-dependent changes in the loaded joint. In particular, SOST, the gene encoding sclerostin, may play a crucial role in these changes due to its already established role in mechanosenstivity in bones, sclerostin expression in osteocytes is downregulated following mechanical loading [26, 27]. The role of sclerostin in articular cartilage is still unclear; its overexpression is necessary to protect against cartilage degradation, and its inhibition or ablation did not affect articular cartilage remodeling activity in sclerostin KO mice or rats that underwent DMM surgery [13, 28]. However, no study investigated mechanosenstivity of sclerostin in articular cartilage or its role in load-induced OA. Thus, a study can be designed to address these questions with the following hypothesis: conditional overexpression of SOST in osteocytes protects mouse joints from load-induced OA. Mice expressing high levels of SOST in osteocytes have already been engineered, and the same animal

model can undergo mechanical loading at a peak load that engenders 1200ε in the mid-diaphysis with multiple load durations [26]. With the overexpression of SOST in osteocytes, subchondral cortical bone sclerosis and epiphyseal cancellous bone loss will be absent in response to mechanical loading. This limited alteration in the subchondral bone region will lead to limited alteration in the joint loading environment, maintaining healthy articular cartilage while protecting from load-induced OA. Alternatively, conditional knockout of SOST in mouse osteocytes or chondrocytes can be investigated in conjunction with mechanical loading. With anti-sclerostin antibody (biosozumab) already in clinical trials showing a strong anabolic response among osteoporotic patients, careful investigation of the role of sclerostin in load-induced OA development will not only demonstrate the importance of mechanosensitivity of sclerostin in the joint, but also show biosozumab's therapeutic potential among OA patients [29].

5.3 REFERENCES

1. Felson DT, Zhang Y, Hannan MT, Naimark A, Weissman B, Aliabadi P, Levy D. Risk factors for incident radiographic knee osteoarthritis in the elderly: the Framingham Study. Arthritis Rheum. 1997 Apr;40(4):728-33.
2. Little CB, Zaki S. What constitutes an "animal model of osteoarthritis"--the need for consensus? Osteoarthritis Cartilage. 2012 Apr;20(4):261-7.
3. Ameye LG, Young MF. Animal models of osteoarthritis: lessons learned while seeking the "Holy Grail". Curr Opin Rheumatol. 2006 Sep;18(5):537-47.
4. Galois L, Etienne S, Grossin L, Watrin-Pinzano A, Cournil-Henrionnet C, Loeuille D, Netter P, Mainard D, Gillet P. Dose-response relationship for exercise on severity of experimental osteoarthritis in rats: a pilot study. Osteoarthritis Cartilage. 2004 Oct;12(10):779-86.
5. Backus JD, Furman BD, Swimmer T, Kent CL, McNulty AL, Defrate LE, Guilak F, Olson SA. Cartilage viability and catabolism in the intact porcine knee following transarticular impact loading with and without articular fracture. J Orthop Res. 2011 Apr;29(4):501-10.
6. Lee JH, Fitzgerald JB, Dimicco MA, Grodzinsky AJ. Mechanical injury of cartilage explants causes specific time-dependent changes in chondrocyte gene expression. Arthritis Rheum. 2005 Aug;52(8):2386-95.
7. Christiansen BA, Anderson MJ, Lee CA, Williams JC, Yik JH, Haudenschild DR. Musculoskeletal changes following non-invasive knee injury using a novel mouse model of post-traumatic osteoarthritis. Osteoarthritis Cartilage. 2012 Jul;20(7):773-82.

8. Furman BD, Strand J, Hembree WC, Ward BD, Guilak F, Olson SA. Joint degeneration following closed intraarticular fracture in the mouse knee: a model of posttraumatic arthritis. J Orthop Res. 2007 May;25(5):578-92.

9. Hayami T, Pickarski M, Wesolowski GA, McLane J, Bone A, Destefano J, Rodan GA, Duong le T. The role of subchondral bone remodeling in osteoarthritis: reduction of cartilage degeneration and prevention of osteophyte formation by alendronate in the rat anterior cruciate ligament transection model. Arthritis Rheum. 2004 Apr;50(4):1193-206.

10. Bingham CO, 3rd, Buckland-Wright JC, Garnero P, Cohen SB, Dougados M, Adami S, Clauw DJ, Spector TD, Pelletier JP, Raynauld JP, Strand V, Simon LS, Meyer JM, Cline GA, Beary JF. Risedronate decreases biochemical markers of cartilage degradation but does not decrease symptoms or slow radiographic progression in patients with medial compartment osteoarthritis of the knee: results of the two-year multinational knee osteoarthritis structural arthritis study. Arthritis Rheum. 2006 Nov;54(11):3494-507.

11. Hayami T, Zhuo Y, Wesolowski GA, Pickarski M, Duong le T. Inhibition of cathepsin K reduces cartilage degeneration in the anterior cruciate ligament transection rabbit and murine models of osteoarthritis. Bone. 2012 Jun;50(6):1250-9.

12. Diarra D, Stolina M, Polzer K, Zwerina J, Ominsky MS, Dwyer D, Korb A, Smolen J, Hoffmann M, Scheinecker C, van der Heide D, Landewe R, Lacey D, Richards WG, Schett G. Dickkopf-1 is a master regulator of joint remodeling. Nat Med. 2007 Feb;13(2):156-63.

13. Chan BY, Fuller ES, Russell AK, Smith SM, Smith MM, Jackson MT, Cake MA, Read RA, Bateman JF, Sambrook PN, Little CB. Increased chondrocyte sclerostin may protect

against cartilage degradation in osteoarthritis. Osteoarthritis Cartilage. 2011 Jul;19(7):874-85.

14. Luyten FP, Tylzanowski P, Lories RJ. Wnt signaling and osteoarthritis. Bone. 2009 Apr;44(4):522-7.

15. Roemhildt ML, Beynnon BD, Gardner-Morse M, Badger G, Grant C. Changes induced by chronic in vivo load alteration in the tibiofemoral joint of mature rabbits. J Orthop Res. 2012 Sep;30(9):1413-22.

16. Roemhildt ML, Coughlin KM, Peura GD, Badger GJ, Churchill D, Fleming BC, Beynnon BD. Effects of increased chronic loading on articular cartilage material properties in the lapine tibio-femoral joint. J Biomech. 2010 Aug 26;43(12):2301-8.

17. Main RP, Lynch ME, van der Meulen MC. In vivo tibial stiffness is maintained by whole bone morphology and cross-sectional geometry in growing female mice. J Biomech. 2010 Oct 19;43(14):2689-94.

18. Stockwell RA. The interrelationship of cell density and cartilage thickness in mammalian articular cartilage. J Anat. 1971 Sep;109(Pt 3):411-21.

19. Poulet B, Westerhof TA, Hamilton RW, Shefelbine SJ, Pitsillides AA. Spontaneous osteoarthritis in Str/ort mice is unlikely due to greater vulnerability to mechanical trauma. Osteoarthritis Cartilage. 2013 May;21(5):756-63.

20. Beaupre GS, Stevens SS, Carter DR. Mechanobiology in the development, maintenance, and degeneration of articular cartilage. J Rehabil Res Dev. 2000 Mar-Apr;37(2):145-51.

21. Coles JM, Blum JJ, Jay GD, Darling EM, Guilak F, Zauscher S. In situ friction measurement on murine cartilage by atomic force microscopy. J Biomech. 2008;41(3):541-8.

22. Stolz M, Gottardi R, Raiteri R, Miot S, Martin I, Imer R, Staufer U, Raducanu A, Duggelin M, Baschong W, Daniels AU, Friederich NF, Aszodi A, Aebi U. Early detection of aging cartilage and osteoarthritis in mice and patient samples using atomic force microscopy. Nat Nanotechnol. 2009 Mar;4(3):186-92.

23. Boskey A, Pleshko Camacho N. FT-IR imaging of native and tissue-engineered bone and cartilage. Biomaterials. 2007 May;28(15):2465-78.

24. Poulet B, Ulici V, Stone TC, Pead M, Gburcik V, Constantinou E, Palmer DB, Beier F, Timmons JA, Pitsillides AA. Time-series transcriptional profiling yields new perspectives on susceptibility to murine osteoarthritis. Arthritis Rheum. 2012 Oct;64(10):3256-66.

25. Geyer M, Grassel S, Straub RH, Schett G, Dinser R, Grifka J, Gay S, Neumann E, Muller-Ladner U. Differential transcriptome analysis of intraarticular lesional vs intact cartilage reveals new candidate genes in osteoarthritis pathophysiology. Osteoarthritis Cartilage. 2009 Mar;17(3):328-35.

26. Tu X, Rhee Y, Condon KW, Bivi N, Allen MR, Dwyer D, Stolina M, Turner CH, Robling AG, Plotkin LI, Bellido T. Sost downregulation and local Wnt signaling are required for the osteogenic response to mechanical loading. Bone. 2012 Jan;50(1):209-17.

27. Robling AG, Niziolek PJ, Baldridge LA, Condon KW, Allen MR, Alam I, Mantila SM, Gluhak-Heinrich J, Bellido TM, Harris SE, Turner CH. Mechanical stimulation of bone in vivo reduces osteocyte expression of Sost/sclerostin. J Biol Chem. 2008 Feb 29;283(9):5866-75.

28. Roudier M, Li X, Niu QT, Pacheco E, Pretorius JK, Graham K, Yoon BR, Gong J, Warmington K, Ke HZ, Black RA, Hulme J, Babij P. Sclerostin is expressed in articular cartilage but loss or inhibition does not affect cartilage remodeling during aging or following mechanical injury. Arthritis Rheum. 2013 Mar;65(3):721-31.

29. McColm J, Hu L, Womack T, Tang CC, Chiang AY. Single- and multiple-dose randomized studies of blosozumab, a monoclonal antibody against sclerostin, in healthy postmenopausal women. J Bone Miner Res. 2013 Aug 31.

Appendix A: Chapter 2 Data

Histological Score: Indices of articular cartilage damage measured by Safranin O stain. Each level corresponds to a slide separated at a 90 µm interval. Four boxes in each level correspond to four areas of tibiofemoral articular cartilage.

Knee

Right

Levels (…. wks at Sx)

Duration	Mouse #	Load level (N)	Starting Slide #	1	2	3	4	5	6	7	8	9	10	11	12	13	14	15	16	17	18	Summed score	Highest score
6 wk	A01	9N	26	0.0 0.0	0.0 0.0	0.0 0.0	0.0 3.0	0.0 3.0	0.0 2.0	0.0 0.0	0.0 0.5	0.0												14.5	3.0
				0.0	0.0 0.0	0.5 0.5	0.0 0.0	0.0 0.0	0.0 2.0	0.0 2.0	0.0 0.0	0.0 1.0	0.0	0.0										
6 wk	A02	9N	13	0.0 0.0	0.0 0.0	0.0 0.0	0.0 0.0	0.0 0.0	0.0 2.0	0.0 0.5	0.0													12.0	3.0
				0.0	0.0 0.5	0.0 0.0	0.0 0.0	0.0 0.5	0.0 2.0	0.0 3.0	0.5 0.5	0.5 0.0	0.5	0.5	0.5									
6 wk	A03	9N	19	0.0	0.0	0.0	0.0 0.0	0.5 0.0	0.5 0.5															7.5	1.0
				0.5 0.5	0.5 0.5	0.0 0.5	0.0 0.5	0.0 0.0	0.5 0.5	0.0 0.0	0.0 0.0	0.0 0.5	0.5 1.0											
6 wk	A04	9N	7		0.0	0.0	0.0 0.0	0.0 2.0	0.0 2.0	0.0 2.0	0.0 0.0	1.0	0.0											7.0	2.0
				0.0 0.0	0.0 0.0	0.0 0.0	0.0 0.0	0.0 0.0	0.0 0.0	0.0 0.0	0.0 0.0	0.0 0.0	0.0 0.0	0.0 0.0	0.0									
6 wk	A05	9N	13	0.0	0.0 0.0	0.0 2.0	0.0 2.0	0.0 1.0	0.0 1.0	0.5 1.0														13.0	2.0
				0.0 0.0	0.0 0.5	0.0 1.0	0.0 0.0	0.0 0.0	0.0 1.0	0.0 1.0	0.0 1.0	0.0 0.0	1.0											
6 wk	A06	9N	7		0.0	0.0 0.0	0.0 2.0	0.0 2.0	0.0 2.0	0.0 0.0	0.5 0.5	0.5 0.5												10.0	2.0
				0.0 0.0	0.0 0.0	0.0 0.0	0.0 1.0	0.0 0.0	0.0 0.0	0.0 1.0	0.0 0.0	0.0 0.0	0.0 0.0	0.0 0.0	0.0									
6 wk	A07	9N	13		0.0	0.0	0.0 0.0	0.0 1.0	0.0 2.0	0.5 0.5	0.5 0.5	0.5												11.0	2.0
				0.0 1.0	0.0 0.5	0.0 1.0	0.0 0.5	0.0 0.5	0.0 0.5	0.0 0.5	0.0 1.0	0.0 0.0	0.0 0.0	0.0	0.0									
6 wk	B08	4.5N	13			0.0 0.0	0.0 0.0	0.0 0.0	0.0 0.5	0.0 0.5	0.0 0.5	0.5 1.0	0.5 0.5											9.5	1.0
				0.0 0.5	0.0 0.5	0.0 0.5	0.0 0.5	0.0 0.5	0.0 0.5	0.0 0.5	0.0 0.5	0.0 0.0	0.0 0.5	0.0 0.5	0.0	0.5								
6 wk	B09	4.5N	19			0.0 0.0	0.0 0.0	0.0 0.0	0.0 1.0	0.0 0.0	0.0 0.5	0.0			0.5									5.0	1.0
				0.0	0.5	0.0 0.5	0.0 0.5	0.0 0.5	0.0 0.5	0.0 0.0	0.0 0.0	0.0 0.0	0.0 0.5	0.0	0.0	0.0	0.0							
6 wk	B10	4.5N	13	0.0	0.0	0.0	0.0 0.0	0.0 1.0	0.0 1.0	0.5 3.0	0.0													8.0	3.0
				0.0 0.0	0.0 0.5	0.0 0.5	0.0 0.5	0.0 0.0	0.0 0.5	0.0 0.5	0.0 0.0	0.0 0.0	0.0 0.0	0.0	0.0									
6 wk	B11	4.5N	19				0.0 0.0	0.0 0.0	0.0 1.0	0.0 2.0	0.0 0.5	0.0 0.5	0.5	0.5										9.0	2.0
				0.0 0.0	0.0 0.5	0.0 0.5	0.0 0.5	0.0 0.5	0.0 0.5	0.0 0.5	0.0 0.0	0.0 0.5	0.0 0.0	0.0 0.5	0.0	0.0								
6 wk	B12	4.5N	19			0.0	0.0	0.0	0.0 0.0	1.0	0.0	0.5	0.5											5.5	1.0
				0.0 0.0	0.0 0.5	0.0 1.0	0.0 0.0	0.0 0.0	0.0 0.0	0.0 0.5	0.0 1.0	0.0 0.0	0.0 0.0	0.0	0.5									
6 wk	B13	4.5N	13	0.0	0.0	0.0 0.0	0.0 0.0	0.0 3.0	0.0 0.5	0.5 0.5	0.5	0.5												10.5	3.0
				0.5 0.0	0.0 0.5	0.0 0.5	0.0 0.5	0.0 0.5	0.0 0.5	0.0 1.0	0.0 0.5	0.0 0.5	0.0	0.0	0.0									
6 wk	B14	4.5N	19			0.0	0.0	0.0	0.0	0.0	0.0 0.5	0.0 0.5	0.5 0.5	0.5	0.5	1.0								8.5	1.0
				0.5	0.5	0.0 0.5	0.0 0.5	0.0 0.5	0.0 0.5	0.0 0.5	0.0 0.5	0.0	0.0	0.0	0.0	0.0								
2 wk	C15	9N	19	0.0	0.0	0.0	0.0	0.0	0.0 0.0	0.5 0.0	0.5 0.0	0.5 0.0	0.0 0.5	0.0										3.0	0.5
				0.0	0.0	0.0 0.0	0.0 0.0	0.0 0.0	0.0 0.0	0.0 0.0	0.0 0.0	0.0 0.5	0.0 0.0	0.0 0.0	0.5 0.0									
2 wk	C16	9N	25					0.0 0.0	2.0 2.0	0.0 0.0	0.0 0.0	0.5	0.0	0.5	0.5									7.0	2.0
				0.0	0.0 0.0	0.0 1.0	0.0 0.0	0.0 0.0	0.0 0.0	0.0 0.5	0.0 0.0	0.0 0.0	0.0 0.0	0.0	0.0	0.0		0.0						
2 wk	C17	9N	25			0.0	0.0 0.0	0.0 0.0	0.0 0.0	0.0 0.0	0.0 0.0	0.0 0.5	0.5 0.5	0.5										4.0	0.5
				0.0 0.0	0.0 0.0	0.0 0.0	0.0 0.5	0.0 0.0	0.0 0.0	0.0 0.5	0.0 0.0	0.0 0.0	0.0 0.0	0.0	0.5									
2 wk	C18	9N	25	0.0	0.0	0.0	0.0	0.0	0.0	1.0 0.0	0.5 0.0	0.0 0.0	0.5 0.5	0.5 0.5										6.0	1.0
				0.0 0.0	0.0 0.0	0.0 0.0	0.0 0.5	0.0 0.0	0.0 0.0	0.0 0.5	0.0 0.5	0.0 0.0	0.0 0.0	0.0 0.5	0.0									
2 wk	C19	9N	19		0.0	0.0	0.0	0.5 1.0	0.5 1.0	0.5 0.0	0.5	0.5	0.5	0.5										18.5	1.0
				0.0 1.0	0.5 1.0	0.0 1.0	0.0 0.0	0.5 1.0	0.5 1.0	1.0 1.0	0.5 1.0	0.0 1.0	0.0 0.0	0.5 0.0	1.0									
2 wk	C20	9N	13	0.0	0.0	0.0	0.0	0.0	0.0	0.5 0.0	0.0 0.0	0.0 0.0	0.0 0.5	0.5 0.5										5.0	1.0
				0.0	0.0 0.0	0.0 0.0	0.0 1.0	0.0 0.0	0.0 0.0	0.0 0.5	0.0 0.5	0.0 1.0	0.0 0.0	0.0 0.0	0.0 0.0									
2 wk	D21	4.5N	13	0.0	0.0	0.0	0.0	0.0	0.0	0.0 0.0	0.0 0.0	0.5 0.5	0.5 0.5	0.5 0.0	0.5									5.0	1.0
				0.0	0.0 0.0	0.0 0.0	0.0 0.5	0.0 0.0	0.0 0.0	0.0 0.0	0.0 0.0	0.0 0.5	0.0 0.5	0.0 0.0	0.5									
2 wk	D22	4.5N	26				0.0	2.0	0.0 1.0	0.0 2.0	0.0 0.5	0.0 0.5	0.0	0.0	0.5	0.5								14.5	2.0
				0.0	0.0	0.0 0.0	0.0 0.0	0.0 2.0	0.0 0.0	0.0 1.0	0.0 1.0	1.0 0.0	1.0 0.0	1.0	0.0	0.0	0.0	0.5						
2 wk	D23	4.5N	25			0.0 0.0	0.0 0.0	0.0 0.0	0.0 0.0	0.0 0.0	0.0 0.0	0.0 0.0	0.0	0.5										9.0	2.0
				0.0	2.0	1.0	1.0 0.0	0.0 0.0	0.0 1.0	0.0 0.5	0.0 1.0	1.0 0.0	0.5 0.0	0.0	0.0	0.5	0.0							
2 wk	D24	4.5N	7	0.0	0.0	0.0	0.0	0.0	0.0 1.0	0.5 0.0	0.5 0.0	0.5 0.0	0.5 0.5	0.5										7.0	1.0
				0.0	0.0	0.0 1.0	0.0 0.5	0.0 0.5	0.0 0.5	0.0 0.0	0.0 0.0	0.0 0.0	0.0 0.0	0.0 0.0	0.5 0.0		0.5							
2 wk	D25	4.5N	13	0.0	0.0	0.0	0.0	0.5 0.0	0.5 2.0	0.5 2.0	0.5													10.0	2.0
				0.0 0.0	0.0 0.5	0.0 0.5	0.0 0.0	0.0 0.5	0.5 0.0	1.0 0.0	0.0 0.0	0.0 0.5	0.0 0.0	0.0 0.0	0.0									
2 wk	D26	4.5N	1		0.0	0.0	0.0 2.0	0.0 0.5	0.0 0.5	0.0 0.5	0.5 0.5	0.5												8.5	2.0
				0.0	0.0	0.0 1.0	0.0 0.5	0.0 0.5	0.0 0.5	0.0 0.0	0.0 0.0	0.0 0.5	0.0 0.0	0.0	0.0									
2 wk	D27	4.5N	19				0.0	0.0 0.0	0.0 0.0	0.0 0.0	0.5 0.0	0.0 0.5	0.0 1.0	0.5	0.5	1.0									

	1 wk	E28	9N	25			0.0		0.0		0.0	0.0	0.0	0.0	0.0	0.0	0.5	0.5	0.5	0.5	0.5/	0.5	0.5																			
						0.0	0.0	0.5	0.0	0.0	0.0	0.0	0.0	0.5	0.0	0.5	0.0	0.0	0.0	0.5	0.0	0.0	0.0	0.5	0.0		0.5		0.0												6.0	0.5
	1 wk	E29	9N	25	0.0		0.0		0.0		0.0		0.0	0.0	0.0	0.0	0.0	2.0	0.5	0.0	0.5	0.5	0.5	0.5		0.5																
					0.5	0.0	0.0	0.0	0.0	0.0	0.0	0.0	0.0	0.0	0.0	0.5	0.0	0.0	0.0	1.0	0.0	1.0	0.0	1.0	0.0	0.0	0.0		0.0												9.0	2.0
	1 wk	E30	9N	13						0.0	0.0	0.0	0.0	0.0	0.0	0.0	0.0	0.0	0.0	0.5	0.5	0.0	1.0		0.5																	
						0.0	0.0	0.0	0.0	0.5	0.0	0.5	0.5	0.5	0.0	0.0	0.0	0.0	0.5	0.5	0.5	0.0	0.0	0.0	0.5	0.5															7.0	1.0
	1 wk	E31	9N	13							0.0		0.0	0.0	0.0	0.0	0.0	0.0	0.0	0.5	0.0	0.5	0.0		0.5																	
					0.5	0.5	0.5	0.5	0.0	0.5	0.0	0.5	0.0	0.5	0.0	0.5	0.0	0.0	0.0	0.0	0.0	0.0	0.0	0.0	0.0																5.5	0.5
	1 wk	E32	9N	13					0.0	0.0	0.0	0.0	0.0	2.0	0.0	0.0	0.0	0.0	0.5	0.0	0.0	0.0	0.5	0.5	0.5																	
						0.5	0.0	0.5	0.0	0.5	0.0	0.5	0.0	0.5	0.0	0.5	0.0	0.5	0.5	0.5	0.0	0.0	0.0	0.0	0.0		0.5														9.0	2.0
	1 wk	E33	9N	19				0.0		0.0	0.0	0.0	0.0	2.0	0.0	0.0	0.5	0.5	0.0		0.5		0.5		0.5																	
						0.0		0.0	0.0	0.5	0.0	0.5	0.0	0.5	0.0	0.5	0.0	0.5	0.0	0.0	0.0	0.0	0.0		0.0		0.0		0.5												7.5	2.0
	1 wk	F34	4.5N	19							0.0		0.0	0.0	0.0	1.0	0.0	1.0	0.0	0.5	0.5	0.5	0.5	0.5	0.0	0.5	0.5	0.5														
						0.0	0.0	0.0	0.0	0.0	0.0	0.5	0.0	0.5	0.0	1.0	0.0	1.0	0.0	1.0	0.0	0.5	0.5	0.0	0.0	0.0	0.0	0.0	0.0		0.5										11.5	1.0
	1 wk	F35	4.5N	19			0.0		0.0		0.0		0.5	0.0	0.5	0.0	0.5	0.0	0.5	0.0	0.5																					
					0.5	0.0	0.5	0.0	0.0	1.0	0.0	0.5	0.0	0.5	0.0	0.5	0.0	0.5	0.0	0.0	0.0	0.0	0.0	0.5	0.5																7.5	1.0
	1 wk	F36	4.5N	1			0.0		0.0		0.0	0.0	0.0	0.0	0.0	1.0	0.0	0.0	0.0	0.0	0.5	0.5		0.5																		
					0.0		0.0	0.0	0.0	0.5	0.0	0.5	0.0	0.5	0.0	0.0	0.0	0.0	0.0	0.0	0.0	0.0	0.0	0.0	0.5	0.0	0.0	0.0	0.5	0.5											5.5	1.0
	1 wk	F37	4.5N	1					0.0		0.0		0.0		0.0	0.0	0.5	0.0	0.0	0.0	0.5	0.5	0.5																			
					0.0		0.0		0.0	0.5	0.0	0.5	0.0	0.5	0.0	0.5	0.0	0.0	0.0	0.0	0.0	0.5	0.5	0.0	0.5	0.0		0.5													6.0	0.5
	1 wk	F38	4.5N	13					0.0		0.0	0.0	0.0	0.0	0.0	0.0	0.0	0.0	0.5	0.5																						
					0.0	0.0	0.0	0.5	0.0	0.5	0.0	0.0	0.0	0.0	0.0	0.5	0.0	0.5	0.0	0.5	0.0	0.5	0.0	0.0	0.5	0.0															4.5	0.5
	1 wk	F39	4.5N	1	0.0		0.0		0.0		0.0		0.0		0.5	0.0	0.0	1.0	0.5	0.0		0.5																				
					0.0		0.0		0.0	0.5	0.0	1.0	0.0	0.5	0.5	0.0	0.0	0.5	0.0	0.0	0.0	0.0	0.0	0.5	0.0	0.0	0.5	0.0		0.5											7.0	1.0
	1 wk	F40	4.5N	19					0.5	0.5	0.0	0.0	0.0	0.0	0.0	0.0	0.5	0.5	0.0																							
						0.0	0.0	0.5	0.0	0.5	0.0	0.0	0.0	0.0	0.0	0.0	0.5	0.0	0.0	0.0	0.0	0.0	0.5	0.0	0.0																4.0	0.5
																																									8.75	**1.63**
																																									0.77	**0.17**

Left	**Duration**	**Mouse #**	**Load level (N)**	**Starting Slide #**	**1**		**2**		**3**		**4**		**5**		**6**		**7**		**8**		**9**		**10**		**11**		**12**		**13**		**14**		**15**		**16**		**17**		**18**		**Summed score**	**Highest score**
	6 wk	A01	9N	43	1.0		3.0		3.0		2.0		0.5	3.0	2.0	3.0	3.0	4.0	2.0	1.0	0.5	3.0	0.5	3.0	0.5	3.0		0.5														
																			3.0		0.5	4.0	0.0	3.0	0.0	0.5	0.0	0.0	0.0	0.0	0.5	0.0									50.0	4.0
	6 wk	A02	9N	50	0.5		2.0		0.5	1.0	1.0	0.5	2.0	2.0	2.0	2.0	2.0	2.0	0.5	0.5	0.5	0.5	0.5	0.5	0.5	0.5		0.5		0.5		0.5										
																			0.5	0.5	0.5	0.5	0.0	0.5	0.5	0.5	0.0	0.0	0.0	0.5	0.5	0.5	0.5	0.5	0.5	0.5	0.5	1.0		0.5	32.0	2.0
	6 wk	A03	9N	20	3.0		0.0		0.0	0.0	0.0	0.0	0.0	0.0	2.0	0.0	0.0	0.0	2.0	0.5	0.0	0.0	0.5	0.5	0.5	0.0		0.5		0.5		0.5										
											3.0		2.0	0.0	2.0	0.0	2.0	0.0	2.0	0.5	0.0	0.0	0.0	0.0	0.5	0.0	0.5	0.0	0.5	0.5	0.0	0.5	0.0	0.0	0.0	0.0		0.0			24.5	3.0
	6 wk	A04	9N	49	4.0		2.0	0.0	0.0	0.0	0.0	0.0	0.0	0.0	0.0	0.0	0.0	0.0	0.0	0.5	0.5	0.5	0.5	0.5		0.5																
													4.0	0.0	0.0	0.0	2.0	0.0	0.0	0.0	0.5	0.0	0.0	0.0	0.0	0.0			0.5	0.5	0.0	1.0	0.0	1.0							18.5	4.0
	6 wk	A05	9N	55	1.0	2.0	3.0	5.0	2.0	4.0	0.5	3.0	3.0	3.0	4.0	3.0	2.0	0.5	0.5	0.5	1.0	0.0		0.0		0.5		0.5														
												3.0	3.0	3.0	3.0	0.5	1.0	0.0	0.5	0.0	0.0	0.0	0.0	0.0	0.0	0.0	0.0	0.0	0.0	0.0	0.0	0.0									53.0	5.0
	6 wk	A06	9N	50	4.0	3.0	3.0	3.0	1.0	3.0	2.0	3.0	2.0	2.0	3.0	0.0	3.0	1.0	2.0	0.5	0.5	0.0		0.5		0.5																
													2.0	0.0	2.0	0.0	2.0	0.0	2.0	0.0	2.0	0.0	0.0	1.0	0.0	1.0	0.5	0.5	0.0	0.5											50.5	4.0
	6 wk	A07	9N	43		1.0	0.0	0.0	3.0	1.0	0.0	0.5	1.0	0.5	1.0	0.5	1.0	1.0	0.5	0.5	2.0	0.5		0.5		0.5																
														0.5		0.5		0.5	3.0	0.0	3.0	0.0	2.0	0.5	0.0	0.5	0.5	0.0	0.0	0.0	0.5	0.5									27.0	3.0
	6 wk	B08	4.5N	13					0.0		0.0	0.0	0.0	0.0	0.0	0.0	0.5	0.0	0.5	0.0		1.0		0.5		0.5		0.5														
					0.0	0.0	0.0	0.0	0.5	0.0	0.5	0.0	1.0	0.0	0.5	0.0	1.0	0.0	2.0	0.0	1.0	0.0	0.0	0.5	0.5	0.0		0.0		0.5											11.5	2.0
	6 wk	B09	4.5N	25					0.0	0.0	0.0	0.0	0.0	0.0	0.0	0.0	0.0	0.0	0.5	0.0	0.5	0.0	0.5	0.0	0.5	1.0																
					0.0		0.0	0.0	0.5	0.0	1.0	0.0	1.0	0.0	0.5	0.0	0.5	0.0	0.5	0.5	0.5	0.5	0.0	0.0		0.0		0.5		0.5											9.5	1.0
	6 wk	B10	4.5N	31	0.5		0.0		1.0		2.0	0.0	3.0	4.0	2.0	4.0	2.0	4.0	0.5	4.0		3.0		2.0		1.0		1.0		0.5												
											2.0		3.0		1.0		1.0	3.0	1.0	3.0	1.0	3.0	0.5	3.0	0.0	2.0	0.0	0.0	0.5	0.0		0.0									58.5	4.0
	6 wk	B11	4.5N	13					0.0	0.0	0.0	0.0	0.5	0.0	0.0	0.5		0.5		1.0		1.0		0.5		1.0																
					2.0		1.0	0.0	0.5	0.0	1.0	0.0	0.5	0.0	0.5	0.0	0.0	1.0	1.0	0.5	0.0	0.5		0.0		0.0		0.0		0.5											14.0	2.0
	6 wk	B12	4.5N	19		0.0	0.0	0.0	0.0	0.0	0.0	0.5	0.5	0.0	0.5	0.5		0.5																								
					0.0	0.5	0.5	0.0	0.5	0.0	0.5	0.0	0.5	0.5	1.0	0.0	1.0	0.0	1.0	0.5	0.0	0.0		0.0																	9.0	1.0
	6 wk	[illegible]	4.5N	[illegible]	0.0		0.0		0.0		0.0	0.0	2.0	0.0	0.0	0.0	0.5	0.5		0.0		0.5		0.5		0.5															[illegible]	[illegible]

6 wk		4.5N						0.0	0.0	0.0	0.0	2.0	0.0	2.0	0.5	0.0	0.5	0.5	0.5		0.5																				
	B14		13	0.0	0.5	0.5	0.5	0.5	0.0	0.5	0.0	1.0	0.0	0.5	0.5	0.5	0.0	0.5	1.0	0.0	0.5	0.0	0.0		0.5															14.0	2.0
2 wk		9N		0.0		0.0	2.0	0.0	1.0	0.0	1.0	0.0	1.0	0.0	1.0	0.0	0.0	0.0	0.0	0.5	2.0		0.0		0.5		0.5														
	C15		49									1.0	1.0	0.0	2.0	0.0	0.0	0.0	0.0	0.5	0.0	0.0	0.0	0.5	0.0	0.0	0.0	0.0	0.0	0.0	0.5	0.0	0.5		0.0					15.5	2.0
2 wk		9N						0.0		0.0		0.0	0.0	0.0	0.0	0.0	0.0		0.0		0.0		0.0		0.0		0.0		1.0		0.5										
	C16		43	0.0		0.0		1.0	0.5	1.0	0.0	0.0	0.0	0.0	0.0	0.5	0.0	0.5	0.0	0.0	0.0	0.0	0.0	0.0	0.0		0.0		0.0		0.5									5.5	1.0
2 wk		9N		0.0		2.0		0.0		0.0		0.0	0.0	0.0	0.0	0.0	0.0	0.5	0.0	0.5	0.0	0.5	0.0		0.0		0.0		0.0		0.0		0.0								
	C17		48									2.0		0.0		0.0	0.5	0.0	0.5	0.0	0.0	0.0	0.0	0.0	0.0	0.5	0.0	0.5	0.0	0.0	0.0	0.0	0.0		0.5		0.5		0.0	8.5	2.0
2 wk		9N		1.0		3.0	2.0	2.0	2.0	2.0	2.0	0.0	2.0	0.0	2.0	0.5	0.5		2.0		0.5		0.5		0.5														
	C18		67									0.5		0.0	0.5	0.5	0.5	0.5	0.0	0.5	0.0	1.0	0.0	0.5	0.0	0.5	0.0	0.5	0.5	1.0	0.5		0.0							30.0	3.0
2 wk		9N				0.0		0.0		0.0		0.5	0.0	0.0	0.0	0.0	0.0	0.5	0.0	0.5	0.0	0.5	0.0	0.5	0.0		0.0		0.5		0.5		1.0								
	C19		31	0.0		1.0		0.5	0.5	0.0	0.5	1.0	0.0	0.5	0.0	0.5	0.5	0.5	0.0	1.0	0.0	0.0	1.0	0.0	1.0	0.0	1.0		0.5		0.0		0.0		0.5					15.0	1.0
2 wk		9N		1.0		0.0		0.5		1.0		0.5		0.5	0.5	0.5	1.0	0.5	0.0	3.0	3.0		3.0		4.0		3.0		3.0		3.0		2.0		1.0						
	C20		55															0.0		0.0	3.0	1.0	3.0	1.0	3.0	0.5	2.0	1.0	1.0	1.0	0.0	0.5	0.0	0.0	0.0					48.0	4.0
2 wk		4.5N							0.0		0.0	0.0	0.0	0.0	0.0	0.0	0.0	3.0	0.5	0.5	0.5	0.5	0.5	0.0	0.0	0.5	0.5														
	D21		31	0.0		0.0	0.0	0.0	0.0	1.0	0.0	1.0	0.0	0.5	0.5	0.5	0.0	1.0	0.0	0.0	0.0	0.0	0.5	0.0	0.0	0.0	0.0		0.0		0.0									11.5	3.0
2 wk		4.5N								0.0		0.0		1.0	0.0	0.5	0.0	0.5	0.0	0.5	0.0	0.5	0.0		0.5		0.5		0.5												
	D22		25	0.0		1.0		0.0		1.0	0.0	0.0	0.0	0.0	0.0	0.5	0.0	2.0	0.0	2.0	0.0	0.5	0.0		1.0		1.0		0.5		0.0		0.5		0.0					14.5	2.0
2 wk		4.5N						0.0		0.5		0.0	0.0	0.5	0.5	0.5	0.0		0.0		0.0		0.5																		
	D23		25	0.0		1.0	0.0	0.0	0.5	0.5	0.5	0.5	0.0	0.5	0.5	0.0	0.5	1.0	1.0	0.0	0.0		0.0		0.5		0.0		0.0											9.5	1.0
2 wk		4.5N								0.0		0.0		0.0	0.0	1.0	0.0	0.0	0.0	0.5	0.0	0.5	0.0		0.0		0.5		0.5		0.5										
	D24		25	0.0		0.0		0.0		0.0	0.0	0.0	0.0	0.5	0.0	0.5	0.0	0.5	0.0	0.0	0.0	0.0	0.0		0.0		0.0		0.5		0.0		0.5		0.5					6.5	1.0
2 wk		4.5N							0.0		0.0	1.0	0.0	0.0	0.0	1.0	0.0	1.0	0.0	0.5	0.5		0.5		0.5														
	D25		19	0.5		1.0	0.0	0.5	0.0	0.0	0.5	0.0	0.0	0.0	0.0	2.0	1.0	3.0	0.0	3.0	0.0	3.0	0.0	0.0	0.0	0.0	0.0		0.0											19.5	3.0
2 wk		4.5N						0.0		1.0		1.0	0.0	0.0	0.0	2.0	0.0	0.0	0.0	0.5	0.0	0.0	0.0	0.0	0.0	0.5	0.0		1.0		1.0										
	D26		37	0.0		0.0		0.0	0.0	0.0	0.0	0.0	0.0	0.0	0.0	0.0	0.0	0.0	0.0	0.0	0.0	0.0	0.0	0.0	0.0	0.5	0.0		0.0		0.0		0.5							8.0	2.0
2 wk		4.5N							0.0	0.0	0.0	0.0	0.0	0.0	0.0	0.0	0.0	0.5	0.5	0.5	0.0	0.5	0.5		1.0														
	D27		25	0.0		0.0		0.0	0.5	0.5	0.0	0.0	0.0	0.0	0.0	0.5	0.0	0.0	0.0	0.0	0.0	0.0	0.0		0.0		0.0		0.5											5.5	1.0
1 wk		9N		0.0		0.5		0.0	1.0	0.0	2.0	0.5	0.0	0.5	2.0		0.0		0.5		0.5		0.5		0.5		1.0												
	E28		31							0.0	0.5	0.0	0.5	0.5	0.0	0.5	0.0	0.5	0.0	0.5	0.0	0.5	0.0	0.5	0.0	0.0	0.5	0.0	0.5		0.0		0.0		0.0					14.5	2.0
1 wk		9N		0.5		0.0		0.0	0.0	0.0	0.0	0.0	0.0	0.0	0.0	0.5	0.0	0.5	1.0	0.5	0.5		0.5		0.5		0.5												
	E29		19					0.0		0.0	0.5	1.0	0.0	0.5	0.0	0.5	0.0	0.5	0.0	0.5	0.0	0.5	0.0	0.5	0.0	0.5	0.0	0.0	0.5	0.0	0.5		0.5							11.5	1.0
1 wk		9N		1.0		3.0		3.0		0.5	0.0	0.5	2.0	0.5	2.0	0.5	2.0		0.0		0.5		0.5		0.0														
	E30		43					3.0		0.5		0.5	0.0	0.5	0.5	0.5	0.0	0.5	0.0	0.5	0.0	0.5	1.0	0.5	0.5	0.0	0.5		0.5											26.0	3.0
1 wk		9N		0.0		0.0		2.0		0.0		3.0		3.0		3.0		2.0		0.5	0.0		0.0		0.0		0.0		0.0		0.0		0.5						
	E31		25							0.0		0.0		0.0		0.0	0.0	0.5	0.0	0.0	0.0	0.5	0.0	0.5	0.0	0.5	0.0	0.0	0.0	0.0	0.0		0.0		0.5		0.0		0.5	17.0	3.0
1 wk		9N		0.5		0.0		0.5		0.0		1.0	0.0	2.0	0.0	0.5	1.0	0.5	0.0		0.0		0.0		0.5		0.5		0.5		0.5								
	E32		25							2.0		0.0		1.0		0.5		0.5	0.5	0.5	0.0	0.5	0.0	0.5	0.0	0.5	0.0	0.0	0.0	0.0	0.5		0.5		0.5		0.5		0.5	17.0	2.0
1 wk		9N			0.0		0.0	0.0	0.0	0.0	0.0	0.0	1.0	0.0	2.0	0.0	1.0	0.5	0.5	0.5	0.5		0.5																
	E33		13				0.0		0.0	0.0	0.0	0.5	0.0	0.5	0.0	0.5	0.0	0.5	0.0	0.5	0.0	0.5	0.5	0.5	0.0	0.0	0.0	0.0	0.5											11.0	2.0
1 wk		4.5N								0.0		0.0		0.0		0.0	0.0	0.5	0.0		0.0		0.5		0.5		0.5		1.0		0.5										
	F34		13	0.5		0.0		0.5		0.5		0.0		0.5	0.0	0.5	0.0	0.5	0.0	0.5	0.0	0.0	0.0		0.0		0.0		0.0		0.0		0.5		0.5					8.0	1.0
1 wk		4.5N								0.0		0.0	0.0	0.0	0.0	0.0	0.0	0.5	0.0		0.5		0.5		0.5		0.5												
	F35		25	0.5		0.0		0.5		0.5	0.0	0.5	0.5	0.5	0.0	0.5	0.0	0.5	0.0	0.5	0.5	0.0	0.0		0.0		0.0		0.0		0.5		0.5							8.5	0.5
1 wk		4.5N						0.0		0.0		0.0	0.0	0.0	0.0	0.5	0.0	0.0	0.0	0.5	0.0	0.5	0.5		0.5		0.5												
	F36		19	0.0		0.0		0.5	0.0	0.0	0.0	0.0	0.0	0.5	0.0	0.5	0.0	0.5	0.5	0.5	0.0	0.0	0.0	0.0	0.0		0.0		0.5		0.5									7.0	0.5
1 wk		4.5N							0.0	0.0	0.0	0.0	0.5	0.0	0.0	0.0	0.0		0.5		0.5		0.5																
	F37		13	0.0		0.5	0.0	0.0	0.0	0.5	0.0	0.5	0.0	0.5	0.0	0.0	0.0	0.5	0.0	0.0	0.5	0.5	0.5		0.0		0.0		0.0		0.5									6.5	0.5
1 wk		4.5N						0.0		0.0		1.0	0.0	1.0	0.0	0.0	0.0	0.0	0.0	0.0	0.0	0.0	0.0		0.0		0.0												
	F38		19	0.0		0.0	0.0	0.0	0.0	0.0	0.0	0.0	0.0	0.0	0.0	0.0	0.0	0.0	0.5	0.0	1.0	0.0	0.5	0.5	0.0		0.0		0.0		0.0									4.5	1.0
1 wk		4.5N						0.0		0.0		0.0		0.0	0.0	0.0	0.0	0.0	0.0		0.5		0.5		0.0		0.5												
	F39		13	0.0		0.0		0.5		0.0	0.0	0.0	0.0	0.5	0.0	0.0	0.0	0.5	0.0	1.0	0.0		0.0		0.0		0.0		0.0		0.5									4.5	1.0
1 wk		4.5N						0.0		0.0	0.0	0.0	0.0	0.0	0.0	0.5	0.0		0.0		0.0		0.0		0.5														
	F40		25	0.0		0.0	0.0	0.0	0.0	0.0	0.0	0.0	0.5	0.0	0.0	0.5	2.0	1.0	0.0	0.0	0.5	0.0	0.0	0.0	0.0		0.0		0.5											6.0	2.0
																																								22.98	**2.50**
																																								3.42	**0.25**

Metaphyseal Cancellous Bone MicroCT Data: Indices of cancellous bone architecture distal to the growth plate in mice loaded at multiple load levels and durations

Animal	Leg	Load Level	Duration	BV/TV	Tb.Th [mm]	Tb.Sp [mm]	TMD [mg/HA ccm]
A1	L	9N	6 wk	0.1037	0.0647	0.2997	880.9115
A1	R	9N	6 wk	0.0904	0.0481	0.2597	885.3866
A2	L	9N	6 wk	0.0807	0.0517	0.2726	891.3745
A2	R	9N	6 wk	0.0705	0.0372	0.276	884.5043
A3	L	9N	6 wk	0.1172	0.0471	0.25	898.3708
A3	R	9N	6 wk	0.0957	0.0413	0.2405	891.2484
A4	L	9N	6 wk	0.1127	0.0442	0.224	869.4401
A4	R	9N	6 wk	0.1142	0.0432	0.2329	916.3973
A5	L	9N	6 wk	0.0779	0.0412	0.2537	909.6531
A5	R	9N	6 wk	0.087	0.0353	0.2106	904.4216
A6	L	9N	6 wk	0.07	0.0461	0.2587	877.634
A6	R	9N	6 wk	0.0621	0.0352	0.2448	897.5514
A7	L	9N	6 wk	0.0934	0.0564	0.2792	895.4084
A7	R	9N	6 wk	0.065	0.0375	0.2812	908.1404
B10	L	4.5N	6 wk	0.0758	0.0409	0.2516	884.3782
B10	R	4.5N	6 wk	0.1052	0.0435	0.2272	931.5244
B11	L	4.5N	6 wk	0.0833	0.0361	0.234	903.2241
B11	R	4.5N	6 wk	0.0741	0.0354	0.237	878.7054
B12	L	4.5N	6 wk	0.0579	0.041	0.2718	886.269
B12	R	4.5N	6 wk	0.0491	0.0356	0.277	889.1055
B13	L	4.5N	6 wk	0.0585	0.0362	0.2553	861.6874
B13	R	4.5N	6 wk	0.0583	0.0342	0.2486	877.0037
B14	L	4.5N	6 wk	0.0697	0.0356	0.2579	880.5964
B14	R	4.5N	6 wk	0.0757	0.036	0.2369	900.892
B8	L	4.5N	6 wk	0.0737	0.0408	0.231	888.7903
B8	R	4.5N	6 wk	0.0796	0.0379	0.226	910.1573
B9	L	4.5N	6 wk	0.0769	0.0399	0.2427	845.2367

B9	R	4.5N	6 wk	0.0929	0.0417	0.2375	855.5735
C15	L	9N	2 wk	0.1258	0.0489	0.1992	812.3981
C15	R	9N	2 wk	0.1246	0.0456	0.2071	783.2154
C16	L	9N	2 wk	0.0955	0.0516	0.2255	885.1345
C16	R	9N	2 wk	0.0705	0.0363	0.2412	866.2886
C17	L	9N	2 wk	0.0835	0.0455	0.231	880.8485
C17	R	9N	2 wk	0.0855	0.038	0.2138	903.4762
C18	L	9N	2 wk	0.0922	0.0415	0.2625	860.4899
C18	R	9N	2 wk	0.1072	0.0426	0.2233	878.7686
C19	L	9N	2 wk	0.154	0.0486	0.2115	914.1913
C19	R	9N	2 wk	0.1704	0.0483	0.1976	912.9937
C20	L	9N	2 wk	0.0998	0.0443	0.288	856.0148
C20	R	9N	2 wk	0.1127	0.0509	0.2858	903.2241
D21	L	4.5N	2 wk	0.0985	0.0379	0.2155	855.8257
D21	R	4.5N	2 wk	0.0905	0.0425	0.2215	908.0774
D22	L	4.5N	2 wk	0.129	0.0543	0.2913	909.6531
D22	R	4.5N	2 wk	0.1179	0.0557	0.2974	911.1659
D23	L	4.5N	2 wk	0.1398	0.0526	0.2558	906.5647
D23	R	4.5N	2 wk	0.1184	0.0541	0.2448	931.1462
D24	L	4.5N	2 wk	0.0745	0.0406	0.2325	882.4243
D24	R	4.5N	2 wk	0.0634	0.0356	0.2277	874.6716
D25	L	4.5N	2 wk	0.0952	0.0488	0.3203	890.24
D25	R	4.5N	2 wk	0.0958	0.0462	0.3184	904.5477
D26	L	4.5N	2 wk	0.1388	0.0491	0.2495	887.1515
D26	R	4.5N	2 wk	0.1214	0.0526	0.2707	914.3804
D27	L	4.5N	2 wk	0.0885	0.0381	0.2371	872.3395
D27	R	4.5N	2 wk	0.0766	0.0379	0.2402	871.8352
E28	L	9N	1 wk	0.1027	0.0442	0.2331	898.3077
E28	R	9N	1 wk	0.1271	0.0431	0.2121	890.7441
E29	L	9N	1 wk	0.1084	0.0513	0.3509	874.2935
E29	R	9N	1 wk	0.1214	0.0496	0.2572	913.9392
E30	L	9N	1 wk	0.1031	0.0486	0.2811	867.7383

E30	R	9N	1 wk	0.1242	0.0426	0.2323	890.0509
E31	L	9N	1 wk	0.1077	0.0426	0.2242	863.9565
E31	R	9N	1 wk	0.0958	0.0388	0.2295	865.2802
E32	L	9N	1 wk	0.088	0.043	0.2634	882.4243
E32	R	9N	1 wk	0.0982	0.0382	0.2246	878.7054
E33	L	9N	1 wk	0.0888	0.0413	0.2253	864.5238
E33	R	9N	1 wk	0.0815	0.0366	0.2207	879.651
F34	L	4.5N	1 wk	0.1438	0.0507	0.2463	890.366
F34	R	4.5N	1 wk	0.1103	0.0532	0.2735	881.5419
F35	L	4.5N	1 wk	0.1324	0.0519	0.2198	889.5466
F35	R	4.5N	1 wk	0.1305	0.0508	0.2214	887.6558
F36	L	4.5N	1 wk	0.1433	0.0474	0.2112	891.4375
F36	R	4.5N	1 wk	0.1513	0.0517	0.2163	888.223
F37	L	4.5N	1 wk	0.1099	0.0439	0.2459	871.2679
F37	R	4.5N	1 wk	0.1102	0.0456	0.2394	867.6753
F38	L	4.5N	1 wk	0.0803	0.037	0.249	890.8702
F38	R	4.5N	1 wk	0.068	0.0362	0.262	874.2935
F39	L	4.5N	1 wk	0.0987	0.0445	0.2976	870.4486
F39	R	4.5N	1 wk	0.118	0.0514	0.3169	907.8253
F40	L	4.5N	1 wk	0.1358	0.0507	0.2851	881.983
F40	R	4.5N	1 wk	0.143	0.0493	0.2672	888.5381

Epiphyseal Bone MicroCT Data: Indices of cancellous bone architecture proximal to the growth plate in mice loaded at multiple load levels and durations

Animal	Leg	Load Level	Duration	BV/TV	Tb.Th [mm]	DT-Tb.Sp [mm]	TMD [mg HA/ccm]
A1	L	9N	6 wk	0.3186	0.0697	0.1796	933.4784
A1	R	9N	6 wk	0.3317	0.0631	0.1897	949.8661
A2	L	9N	6 wk	0.2192	0.0611	0.2254	907.8253
A2	R	9N	6 wk	0.3417	0.0655	0.1868	963.2915
A3	L	9N	6 wk	0.2598	0.0558	0.1914	917.7839

A3	R	9N	6 wk	0.324	0.0642	0.1895	962.472
A4	L	9N	6 wk	0.2289	0.0525	0.2049	903.9805
A4	R	9N	6 wk	0.3052	0.0594	0.1928	967.5145
A5	L	9N	6 wk	0.1958	0.0562	0.2207	916.3973
A5	R	9N	6 wk	0.2992	0.0586	0.1858	966.8212
A6	L	9N	6 wk	0.3079	0.0657	0.1921	940.9159
A6	R	9N	6 wk	0.2766	0.0569	0.1968	969.3423
A7	L	9N	6 wk	0.2172	0.0676	0.231	927.3015
A7	R	9N	6 wk	0.2924	0.0594	0.1891	963.0393
B10	L	4.5N	6 wk	0.2938	0.0581	0.1914	916.7755
B10	R	4.5N	6 wk	0.3376	0.0622	0.1785	977.4731
B11	L	4.5N	6 wk	0.2741	0.0564	0.201	965.4344
B11	R	4.5N	6 wk	0.2767	0.0574	0.2009	960.7703
B12	L	4.5N	6 wk	0.2646	0.0584	0.2202	962.9763
B12	R	4.5N	6 wk	0.2689	0.0568	0.2074	956.5472
B13	L	4.5N	6 wk	0.2272	0.0509	0.1972	932.722
B13	R	4.5N	6 wk	0.2769	0.0544	0.1988	947.66
B14	L	4.5N	6 wk	0.2838	0.0578	0.1845	955.4758
B14	R	4.5N	6 wk	0.2905	0.0553	0.1827	958.4382
B8	L	4.5N	6 wk	0.3052	0.0578	0.1874	973.061
B8	R	4.5N	6 wk	0.3167	0.0576	0.1915	964.489
B9	L	4.5N	6 wk	0.282	0.0586	0.2012	936.1256
B9	R	4.5N	6 wk	0.3015	0.0598	0.2053	932.9111
C15	L	9N	2 wk	0.2673	0.0572	0.1867	930.8312
C15	R	9N	2 wk	0.2992	0.0571	0.1896	943.059
C16	L	9N	2 wk	0.3311	0.0637	0.1684	919.4857
C16	R	9N	2 wk	0.3032	0.0591	0.1771	956.7363
C17	L	9N	2 wk	0.3177	0.0626	0.1851	924.5282
C17	R	9N	2 wk	0.3164	0.058	0.1817	962.9763
C18	L	9N	2 wk	0.2677	0.0557	0.1934	908.7708

C18	R	9N	2 wk	0.3417	0.0621	0.1787	949.3619
C19	L	9N	2 wk	0.4051	0.0685	0.1591	946.5255
C19	R	9N	2 wk	0.4317	0.0677	0.1467	953.837
C20	L	9N	2 wk	0.3897	0.0716	0.174	919.5488
C20	R	9N	2 wk	0.3336	0.062	0.1851	951.0006
D21	L	4.5N	2 wk	0.3154	0.0584	0.1791	933.1002
D21	R	4.5N	2 wk	0.3046	0.0586	0.1804	958.4382
D22	L	4.5N	2 wk	0.3321	0.0637	0.1962	944.3195
D22	R	4.5N	2 wk	0.3705	0.0674	0.1825	956.4843
D23	L	4.5N	2 wk	0.3547	0.0623	0.1803	941.6093
D23	R	4.5N	2 wk	0.3616	0.0627	0.1909	952.2612
D24	L	4.5N	2 wk	0.2846	0.0558	0.1849	938.1426
D24	R	4.5N	2 wk	0.3124	0.0582	0.1827	951.1267
D25	L	4.5N	2 wk	0.3567	0.0661	0.1702	963.6066
D25	R	4.5N	2 wk	0.344	0.0627	0.1802	952.8916
D26	L	4.5N	2 wk	0.3226	0.0638	0.1894	933.5414
D26	R	4.5N	2 wk	0.3341	0.0663	0.193	955.2236
D27	L	4.5N	2 wk	0.2911	0.0584	0.1896	958.4382
D27	R	4.5N	2 wk	0.2987	0.0575	0.1853	949.614
E28	L	9N	1 wk	0.3719	0.0647	0.1794	966.506
E28	R	9N	1 wk	0.3692	0.0633	0.1727	965.7496
E29	L	9N	1 wk	0.3571	0.0641	0.1971	932.9111
E29	R	9N	1 wk	0.3581	0.0644	0.1762	947.8491
E30	L	9N	1 wk	0.3773	0.0659	0.182	928.436
E30	R	9N	1 wk	0.3589	0.0649	0.1794	938.4578
E31	L	9N	1 wk	0.3681	0.0645	0.1807	941.105
E31	R	9N	1 wk	0.3194	0.0602	0.1814	943.7522
E32	L	9N	1 wk	0.3459	0.0635	0.1694	938.4578
E32	R	9N	1 wk	0.3435	0.0649	0.1711	956.8624
E33	L	9N	1 wk	0.3186	0.0586	0.1829	919.1707

E33	R	9N	1 wk	0.3289	0.0589	0.174	952.7655
F34	L	4.5N	1 wk	0.3468	0.0667	0.1927	953.0176
F34	R	4.5N	1 wk	0.3538	0.0667	0.2011	931.7766
F35	L	4.5N	1 wk	0.3691	0.066	0.1819	946.0214
F35	R	4.5N	1 wk	0.3554	0.0645	0.1699	945.6435
F36	L	4.5N	1 wk	0.3687	0.067	0.185	952.2612
F36	R	4.5N	1 wk	0.381	0.0675	0.1791	962.5981
F37	L	4.5N	1 wk	0.3289	0.0598	0.1739	940.4747
F37	R	4.5N	1 wk	0.3324	0.0603	0.1822	925.4736
F38	L	4.5N	1 wk	0.2936	0.0595	0.1959	962.5352
F38	R	4.5N	1 wk	0.3062	0.0593	0.1868	933.5414
F39	L	4.5N	1 wk	0.3409	0.0618	0.174	933.6045
F39	R	4.5N	1 wk	0.3356	0.0594	0.17	930.8942
F40	L	4.5N	1 wk	0.3195	0.0608	0.1961	936.819
F40	R	4.5N	1 wk	0.3521	0.0654	0.1845	945.8953

Localized Articular Cartilage and Subchondral Cortical Bone Thickness: Six slides representing each quadrant were stained with Safranin O and analyzed for articular cartilage and subchondral cortical bone thickness using Osteomeasure.

					Cartilage-Lateral			Cartilage-Medial			Sub Bone-Lateral			Sub Bone Medial		
Duration	**Mouse**	**Limb**	**Applied Load**	**Starting Slide**	**Post**	**Trans**	**Ant**	**Post**	**Trans**	**Ant**	**Post**	**Trans**	**Ant**	**Post**	**Trans**	**Ant**
6 wk	A01	Left	9 N	43	87.1	90.7	93.1	64.0	71.2	112.6	78.0	50.1	69.0	49.7	34.5	91.8
6 wk	A02	Left	9 N	50	84.0	83.0	72.4	77.6	79.8	94.2	89.4	19.0	36.7	75.8	34.4	9.7
6 wk	A03	Left	9 N	20	87.5	107.1	79.9	84.9	100.0	88.7	97.1	34.2	16.8	96.7	87.3	20.5
6 wk	A04	Left	9 N	49	60.1	75.0	64.2	72.8	89.7	86.6	90.5	5.2	28.9	38.6	22.9	13.6
6 wk	A05	Left	9 N	55	50.6	91.9	98.8	71.9	100.2	106.8	59.7	11.6	25.5	15.9	18.4	7.6
6 wk	A06	Left	9 N	50	64.7	89.2	84.7	69.4	88.2	85.6	80.5	14.5	20.4	42.4	29.1	18.0
6 wk	A07	Left	9 N	43	59.6	75.6	79.9	74.8	92.8	102.9	91.3	30.4	34.8	56.8	27.7	45.2
6 wk	B08	Left	4.5 N	13	114.9	96.9	68.9	82.1	90.4	104.3	51.5	26.5	38.4	53.7	38.2	48.4
6 wk	B09	Left	4.5 N	25	116.4	105.0	74.1	80.5	127.1	106.8	48.1	36.2	32.8	42.7	78.0	65.2

6 wk	B10	Left	4.5 N	31	79.2	90.8	97.2	67.3	72.0	95.5	51.1	21.6	19.9	94.2	117.0	93.4
6 wk	B11	Left	4.5 N	13	106.2	91.5	75.6	75.0	102.8	93.2	84.8	29.7	26.1	42.8	33.7	49.4
6 wk	B12	Left	4.5 N	19	119.4	90.1	64.2	95.8	107.1	93.6	40.1	37.4	41.6	36.3	38.8	47.7
6 wk	B13	Left	4.5 N	19	85.5	89.2	48.8	100.0	88.4	99.4	81.1	19.8	34.8	69.3	23.9	34.5
6 wk	B14	Left	4.5 N	13	123.4	91.5	57.0	88.5	108.5	106.1	117.0	32.9	23.6	35.2	61.2	47.2
2 wk	C15	Left	9 N	49	79.6	93.3	96.3	76.4	92.8	104.5	63.1	25.1	50.6	50.8	47.2	43.7
2 wk	C16	Left	9 N	43	108.1	107.7	63.7	79.0	85.1	100.9	54.3	44.6	13.8	25.3	29.3	45.1
2 wk	C17	Left	9 N	48	89.7	90.1	78.7	83.2	83.2	101.5	48.0	23.2	23.7	50.8	51.8	46.1
2 wk	C18	Left	9 N	67	89.6	90.3	99.3	63.2	114.0	115.7	50.2	24.4	21.2	40.2	77.3	52.3
2 wk	C19	Left	9 N	31	109.5	93.0	81.3	126.5	97.6	106.4	71.3	71.6	23.1	59.8	122.4	119.7
2 wk	C20	Left	9 N	55	101.7	95.8	103.7	68.2	83.6	106.7	44.1	62.5	52.3	56.6	96.1	64.5
2 wk	D21	Left	4.5 N	31	96.4	88.3	69.8	68.2	106.5	115.8	67.6	51.4	40.1	50.2	45.0	27.7
2 wk	D22	Left	4.5 N	25	96.0	90.9	82.1	98.4	97.5	112.3	67.3	63.9	44.2	43.6	78.6	131.5
2 wk	D23	Left	4.5 N	25	107.6	106.2	92.6	85.7	97.2	99.4	71.6	99.4	61.0	67.2	71.8	132.0
2 wk	D24	Left	4.5 N	25	97.4	103.2	74.7	93.1	89.9	87.9	52.2	36.3	24.5	23.9	22.3	48.5
2 wk	D25	Left	4.5 N	19	121.6	85.4	74.6	95.6	104.5	98.8	91.4	86.2	45.6	48.7	167.8	101.2
2 wk	D26	Left	4.5 N	37	111.0	82.1	71.8	86.3	90.5	96.1	97.8	71.7	32.9	63.1	137.5	94.2
2 wk	D27	Left	4.5 N	25	107.3	94.4	75.2	72.7	115.5	94.5	51.5	37.6	24.1	47.1	34.2	88.0
1 wk	E28	Left	9 N	31	93.4	99.6	87.5	69.5	107.9	115.9	31.5	61.2	32.8	25.6	72.2	62.3
1 wk	E29	Left	9 N	19	81.2	109.0	98.4	109.1	112.1	107.8	58.4	66.0	20.3	66.2	76.2	98.1
1 wk	E30	Left	9 N	43	90.8	107.8	82.3	81.4	85.8	106.1	36.2	68.1	35.5	70.3	101.0	88.9
1 wk	E31	Left	9 N	25	82.3	99.2	104.4	108.9	86.6	87.0	32.5	32.6	38.8	46.0	33.3	22.2
1 wk	E32	Left	9 N	25	71.4	104.8	94.8	67.2	95.5	114.5	48.3	43.1	27.7	23.9	57.7	43.6
1 wk	E33	Left	9 N	13	95.5	94.8	109.9	81.5	106.6	113.8	30.6	23.7	14.7	22.0	30.9	49.2
1 wk	F34	Left	4.5 N	13	95.6	103.7	83.6	102.3	101.9	100.2	52.1	46.1	50.6	50.2	145.4	60.7
1 wk	F35	Left	4.5 N	25	102.1	103.9	82.8	110.6	83.8	103.3	57.9	49.9	30.0	40.2	52.9	135.9
1 wk	F36	Left	4.5 N	19	124.1	91.5	69.2	117.0	99.0	96.3	54.2	59.1	30.7	43.4	77.4	79.4
1 wk	F37	Left	4.5 N	13	110.2	92.3	74.4	106.4	96.4	91.0	38.9	49.7	33.5	55.5	74.1	112.1
1 wk	F38	Left	4.5 N	19	113.2	111.8	66.0	104.3	119.7	95.7	43.4	32.6	26.1	32.8	42.7	61.3
1 wk	F39	Left	4.5 N	13	110.2	107.5	75.0	104.8	97.4	98.0	56.7	50.6	31.4	53.4	131.2	85.3
1 wk	F40	Left	4.5 N	25	100.2	92.2	74.2	84.5	98.8	105.2	67.3	42.5	60.3	77.3	106.9	71.1
6 wk	A01	Right	9 N	26	114.8	93.9	61.3	90.2	102.8	99.7	66.8	68.7	38.7	68.1	105.1	73.1
6 wk	A02	Right	9 N	13	116.7	100.4	81.4	129.8	125.3	96.0	56.8	77.4	35.8	75.8	108.9	66.3
6 wk	A03	Right	9 N	19	91.3	79.5	70.6	107.6	132.5	94.5	32.5	64.9	35.4	47.2	95.2	53.1
6 wk	A04	Right	9 N	7	105.6	99.8	77.2	85.2	107.7	103.3	44.9	30.7	32.5	66.4	60.1	26.2

6 wk	A05	Right	9 N	13	105.4	118.2	66.8	93.3	109.0	101.9	25.3	29.9	52.4	82.3	53.1	49.9
6 wk	A06	Right	9 N	7	121.9	91.4	74.2	87.4	112.3	107.3	24.6	37.9	29.4	28.3	24.4	34.8
6 wk	A07	Right	9 N	13	101.4	100.2	70.8	80.6	112.4	109.8	32.3	34.4	28.6	31.8	28.1	44.2
6 wk	B08	Right	4.5 N	13	98.7	92.7	71.6	76.7	95.8	104.9	22.3	28.9	30.0	34.8	38.1	36.9
6 wk	B09	Right	4.5 N	19	116.5	87.5	70.1	108.0	113.6	111.5	56.6	56.5	28.3	65.1	56.0	95.6
6 wk	B10	Right	4.5 N	13	102.8	108.4	79.8	85.9	106.1	102.6	35.8	39.7	43.8	44.0	122.8	81.7
6 wk	B11	Right	4.5 N	19	100.9	87.9	53.6	88.9	104.8	88.7	34.4	38.9	30.4	30.9	57.6	35.3
6 wk	B12	Right	4.5 N	19	110.4	89.4	87.5	89.0	97.1	87.9	31.7	24.6	25.4	45.9	25.5	53.1
6 wk	B13	Right	4.5 N	13	100.1	99.3	67.6	84.1	103.0	97.2	50.2	23.0	27.2	43.5	33.4	21.3
6 wk	B14	Right	4.5 N	19	119.8	84.5	76.3	102.6	85.6	103.1	26.8	31.9	51.0	29.9	23.7	44.2
2 wk	C15	Right	9 N	19	70.7	89.8	80.7	78.1	92.5	114.8	26.2	27.8	48.5	46.1	40.1	48.8
2 wk	C16	Right	9 N	25	93.5	96.0	79.8	99.2	100.1	103.0	27.8	36.2	25.3	44.6	39.9	47.1
2 wk	C17	Right	9 N	25	102.1	90.0	66.3	79.3	93.6	85.3	39.4	41.5	33.8	47.3	47.7	56.1
2 wk	C18	Right	9 N	25	89.0	87.8	78.6	86.4	105.2	115.3	48.2	41.4	38.3	32.3	115.1	46.0
2 wk	C19	Right	9 N	19	123.9	95.2	90.3	88.1	114.4	93.0	35.3	43.9	35.7	52.6	125.0	44.6
2 wk	C20	Right	9 N	13	110.5	87.7	95.1	77.4	100.8	107.1	33.9	43.5	49.6	43.9	131.6	42.0
2 wk	D21	Right	4.5 N	13	81.8	87.4	90.1	76.7	86.7	96.5	30.9	34.4	50.2	39.7	50.8	72.6
2 wk	D22	Right	4.5 N	26	103.9	96.1	81.6	127.1	101.1	107.4	54.3	78.8	42.7	46.2	88.4	111.3
2 wk	D23	Right	4.5 N	25	98.2	91.4	59.5	89.7	113.7	113.1	52.7	70.3	42.6	37.8	114.3	82.6
2 wk	D24	Right	4.5 N	7	92.6	80.9	88.1	96.2	96.8	94.7	39.4	43.3	70.0	43.3	59.2	54.7
2 wk	D25	Right	4.5 N	13	112.5	99.0	84.8	93.6	111.8	114.7	25.9	60.3	31.2	55.1	133.3	88.7
2 wk	D26	Right	4.5 N	1	96.2	89.9	89.0	102.4	119.0	107.7	57.8	109.3	54.3	123.2	122.2	71.2
2 wk	D27	Right	4.5 N	19	106.6	83.8	53.4	82.8	96.1	96.3	38.7	33.7	23.1	38.1	48.5	82.4
1 wk	E28	Right	9 N	25	103.1	92.2	73.2	105.3	112.8	95.4	33.0	43.6	21.6	26.3	40.0	98.1
1 wk	E29	Right	9 N	25	98.7	93.6	72.9	90.1	117.8	93.5	31.1	69.0	30.7	22.2	90.6	51.6
1 wk	E30	Right	9 N	13	120.4	93.1	86.5	82.8	103.8	104.2	37.5	56.4	32.2	49.8	118.2	53.7
1 wk	E31	Right	9 N	13	84.9	85.6	80.4	90.6	104.3	100.3	40.2	30.4	28.9	25.6	54.6	60.2
1 wk	E32	Right	9 N	13	93.8	91.5	68.8	105.3	104.0	112.1	28.6	39.7	25.2	25.6	65.3	64.0
1 wk	E33	Right	9 N	19	113.6	109.4	78.1	129.3	112.4	117.3	25.0	41.4	31.7	19.9	33.6	18.9
1 wk	F34	Right	4.5 N	19	106.5	70.6	66.9	91.9	101.0	94.4	34.0	46.3	28.1	43.8	121.9	50.2
1 wk	F35	Right	4.5 N	19	111.4	93.4	74.4	94.8	122.0	96.2	44.0	67.5	40.7	43.1	96.1	100.0
1 wk	F36	Right	4.5 N	1	112.0	92.3	81.5	88.4	118.9	99.1	60.4	59.6	44.5	26.9	102.5	56.7
1 wk	F37	Right	4.5 N	1	117.0	99.7	86.7	98.1	87.2	117.5	71.3	45.2	46.2	28.7	69.1	51.5

1 wk	F38	Right	4.5 N	13	86.2	93.5	77.6	94.8	110.1	97.3	28.3	19.4	28.8	28.6	44.4	41.7
1 wk	F39	Right	4.5 N	1	106.0	97.8	91.4	102.7	100.6	98.4	38.0	48.3	66.9	34.0	149.6	57.6
1 wk	F40	Right	4.5 N	19	113.9	86.4	85.3	96.2	91.7	97.5	66.9	57.4	30.0	78.7	95.9	49.9

Appendix B: Chapter 3 Data

Histological Score: Indices of articular cartilage damage measured by Safranin O stain. Each level corresponds to a slide separated at a 90 µm interval. Four boxes in each level correspond to four areas of tibiofemoral articular cartilage.

Knee

Right

Recovery	Mouse #	Starting Slide #	Levels 1	2	3	4	5	6	7	8	9	10	11	12	13	14	15	16	17	18	19	20	Summed score	Highest score
2 wk	A01	7	0.0 0.0	0.0 0.0	0.0 0.0	0.0 2.0	0.0 0.0	0.0 0.0	0.0 0.0	0.0 0.0	0.0 0.0	0.0 0.5	0.0 0.0	0.0 0.5	0.0 0.0	0.0 0.0	0.0	0.0							3.0	2.0
2 wk	A02	19	0.0 0.0	0.0 0.0	1.0 0.0	0.5 0.0	0.0 0.0	0.0 1.0	0.0 0.5	0.0 0.5	0.0 0.0	0.0 0.0	0.0 0.0	0.0	0.0	0.0									8.0	2.0
2 wk	A03	13	0.0 0.0	0.0 2.0	0.0 0.0	0.0 0.0	0.0 0.0	0.0 0.5	0.0 0.5	0.0 0.0	0.0 0.0	0.0 0.0	0.0 0.0	0.0 0.0	0.0 0.0	0.0 0.0	0.0 0.0	0.0 0.0	0.0						3.0	2.0
2 wk	A04	13	0.0 0.0	0.0 0.0	0.0 0.0	0.0 0.0	2.0 0.0	0.0 0.0	0.0 0.0	0.0 0.0	0.0 1.0	0.0 1.0	0.0 0.0	0.0 0.0	0.0 0.0	0.0 0.0	0.0								4.0	2.0
2 wk	A05	7	0.0 0.0	0.0 0.0	0.0 0.0	0.0 0.0	0.0 0.0	0.0 0.5	0.0 0.0	0.0 0.0	0.0 0.0	0.5 0.0	0.5 0.0	0.0 0.0	0.0										2.0	0.5
2 wk	A06	7	0.0 0.0	0.0 0.0	0.0 0.0	0.0 0.0	0.0 0.0	0.0 0.0	0.0 0.0	0.0 0.0	0.0 2.0	0.0 0.0	0.0 0.0	0.5 0.5	0.0	0.5									5.0	2.0
2 wk	A07	1	0.0 0.0	0.0 0.0	0.5 0.0	0.0 0.0	0.0 0.0	0.0 1.0	0.0 0.5	0.0 0.5	0.0 0.5	0.0 0.5	0.0 0.0	0.0	0.5										6.5	1.0
1 wk	B08	7	0.0 0.0	0.0 0.0	1.0 0.5	0.0 0.5	0.0 0.5	0.0 0.5	0.0 0.5	0.0 0.0	0.0 0.5	0.0 0.5	0.0 0.0	0.0	0.0	0.5	0.5								7.5	1.0
1 wk	B09	1	0.0 0.0	0.0 0.0	0.5 0.0	0.5 0.0	0.5 0.0	0.0 0.5	0.0 0.5	0.0 0.5	0.0 0.0	0.0 0.0	0.0 0.0	0.0	0.0	0.0	0.0	0.5							8.0	2.0
1 wk	B10	1	0.0 0.0	3.0 0.0	0.0 0.0	0.0 0.0	0.0 0.0	0.0 0.0	0.0 0.5	0.0 0.5	0.0 0.5	0.0 2.0	0.0 0.0	0.0	0.0	0.0	1.0								8.5	3.0
1 wk	B11	1	0.0 0.0	0.5 0.0	0.5 0.0	0.5 0.0	0.0 0.0	0.0 0.5	0.0 0.5	0.0 2.0	0.0 0.0	0.0 0.0	0.0 0.5	0.0	0.5	0.0	0.0								6.0	2.0
1 wk	B12	1	0.0 0.0	2.0 0.0	0.5 0.0	0.5 0.0	0.0 0.0	0.0 0.0	0.0 0.0	0.5 0.5	0.0 0.0	0.0 0.0	0.5 0.0	0.0	0.0										5.5	2.0
1 wk	B13	1	0.0 0.0	0.0 0.0	0.5 0.0	0.5 0.0	0.0 0.0	0.0 0.5	0.0 0.5	0.0 1.0	0.0 1.0	0.0 0.0	0.0 0.5	0.0	0.5	0.0									7.0	1.0
1 wk	B14	1	0.0 0.0	0.0 0.0	0.5 0.0	0.0 0.0	0.0 0.0	0.0 0.0	0.0 0.5	0.0 0.0	0.0 0.0	0.0 0.0	0.0 0.5	0.0	0.5	1.0									4.0	1.0
0 day	C15	1	0.5 0.0	0.0 0.0	0.0 0.0	0.0 0.0	0.0 0.0	0.0 0.0	0.0 0.0	0.0 0.0	0.0 0.0	0.0 0.0	0.0 0.0	0.0	0.0	0.5	0.0								1.5	0.5
0 day	C16	1	0.5 0.0	0.0 0.5	0.0 0.5	0.0 0.5	2.0 0.0	0.0 0.5	0.0 0.5	0.0 0.5	0.0 0.0	0.0 0.0	0.0 0.0	0.0	0.5										7.0	2.0
0 day	C17	1	0.0 0.0	0.0 0.0	0.0 0.0	0.0 0.0	2.0 0.0	2.0 0.0	0.0 0.5	0.0 0.0	0.0 0.0	0.0 2.0	0.5 0.0	0.0	0.0	0.0	0.0	0.5	0.0						8.0	2.0
0 day	C18	1	0.0 0.0	0.0 0.0	0.0 0.0	0.0 2.0	0.0 2.0	0.0 2.0	0.0 0.5	0.0 0.0	0.0 0.0	0.0 0.0	0.0 0.0	0.0	0.0	0.0	0.0	0.5	0.0						6.0	2.0
0 day	C19	1	0.0 0.0	2.0 0.0	0.0 0.0	0.0 0.0	0.0 1.0	0.0 0.5	0.0 0.5	0.0 1.0	0.0 0.0	0.0 0.0	0.0 0.0	0.0	0.0	0.0									5.0	2.0
0 day	C20	1	0.0 0.0	0.0 0.0	0.0 0.0	0.0 0.0	0.0 0.0	0.0 0.5	2.0 0.5	0.0 0.5	0.0 0.5	0.0 0.5	0.0 2.0	0.0 0.0	0.0 0.0	0.0 0.0	0.0 0.0	0.0 0.0	1.0 0.0	0.0					7.0	2.0
0 day	C21	7	0.0 0.0	0.0 2.0	0.0 1.0	1.0 0.0	0.0 1.0	0.0 1.0	0.0 0.5	0.0 0.0	0.0 0.0	0.0 2.0	0.0 0.0	0.0 0.0	0.0 0.0	0.0									13.5	2.0
																						Mean		6.00	1.71
																						SEM		0.59	0.14

Left

Duration	Mouse #	Starting Slide #	1	2	3	4	5	6	7	8	9	10	11	12	13	14	15	16	17	18	19	20	Summed score	Highest score
2 wk	A01	1	0.0	0.0	0.0	0.0	0.0 0.0	0.0 3.0	0.0 3.0	0.0 3.0	0.5 3.0	3.0	3.0	4.0	3.0	0.0									37.0	4.0
					2.0	0.0	0.0	0.0	0.5 0.0	0.0	0.0 3.0	0.0 0.0	0.5 3.0	0.5 2.0	0.0 0.0	0.0 0.0	0.0	0.0	0.0	0.0	0.0					
2 wk	A02	7	0.5	0.0	0.0 2.0	0.0 2.0	0.0 2.0	2.0 2.0	2.0 2.0	0.0 2.0	0.0 2.0	0.0 2.0	3.0												33.0	3.0
								0.0	0.0 2.0	0.5 2.0	0.0 2.0	0.0 0.0	0.0 0.0	0.0 0.0	0.5 0.0	0.5 0.0	2.0 0.0	0.0 0.0	0.0 0.0	0.0	0.0	0.0			
2 wk	A03	19	0.0	0.0	0.0 0.0	0.0 2.0	0.0 2.0	0.0 3.0	0.0 3.0	1.0 3.0	0.0 3.0	0.0 2.0	2.0	2.0											33.0	3.0
						2.0	1.0	0.0	0.0 2.0	0.0 2.0	0.0 1.0	0.0 0.0	0.0 0.0	2.0 0.0	0.0 0.0	0.0										
2 wk	A04	1	0.0	0.0	0.0	0.0 1.0	0.0 2.0	2.0 2.0	0.0 3.0	0.0	3.0 3.0	0.0 3.0	3.0	3.0	3.0	3.0	3.0								36.5	3.0
								3.0	0.0	0.0 2.0	0.0 0.0	0.0 0.0	0.0 0.0	0.0 0.0	0.5 0.0	0.0 0.0	0.0 0.0	0.0 0.0	0.0 0.0	0.0	0.0				
2 wk	A05	1	0.0 0.0	0.0 0.0	1.0 1.0	2.0 1.0	0.0 1.0	2.0 2.0	3.0 3.0	3.0 4.0	3.0 5.0	5.0	0.0												51.0	5.0
							1.0	2.0 2.0	1.0 3.0	0.5 3.0	0.0 2.0	0.0 0.0	0.0 0.0	0.0 0.0	0.0 0.0	0.0 0.0	0.5 0.0	0.0 0.0	0.0 0.0	0.0					

2 wk			3.0		0.5	2.0	1.0	3.0	2.0	3.0	3.0	4.0	2.0	4.0	2.0	3.0	0.5	3.0	0.5	2.0	0.5	2.0		0.0		0.0		0.5																
	A07	1							2.0		2.0	3.0	0.5	2.0	1.0	2.0	1.0	1.0	0.5	2.0	0.5	0.0	0.0	0.0	0.5	0.0	0.0	0.0	0.0	0.0	0.0	0.5		0.0									60.0	4.
1 wk			0.0		0.5		2.0		0.5		0.0		0.5	1.0	0.5	2.0		2.0		2.0		2.0		2.0		2.0		0.5																
	B08	13					1.0		0.5		0.5		0.5	0.5	0.5	2.0	0.5	2.0	0.5	1.0	0.5	1.0	2.0	0.0	0.0	0.0		0.5		0.5		0.5		0.5		0.0							32.5	2.
1 wk			0.5		0.5		0.5		2.0	0.0	0.5	1.0	0.5	1.0	0.5	1.0		2.0		1.0		2.0		0.0		0.5																		
	B09	1			2.0		2.0		1.0	0.0	1.0	2.0	0.5	2.0	0.5	1.0	0.5	0.0	0.5	0.0	0.0	0.0	0.0	0.0	0.0	0.0		0.5		0.5		0.0		0.0									27.5	2.
1 wk			0.0		0.0		0.0		2.0	2.0	0.0	2.0	0.0	2.0	0.5	2.0	0.5	2.0	0.5	2.0		0.0		0.0		0.5																		
	B10	1			2.0		2.0		0.0		1.0	2.0	0.0	2.0	0.5	3.0	0.5	2.0	0.0	1.0	0.5	0.0	0.5	0.0	0.0	0.0	0.0	0.0		0.0		0.0		0.0		0.0							33.0	3.
1 wk			3.0		0.0	2.0	0.0	2.0	2.0	2.0	0.0	2.0	2.0	2.0	0.5	0.0	0.5	2.0	0.5	2.0	0.0	0.0		0.0		0.5																		
	B11	1	2.0		0.0	2.0	0.0	3.0	0.0	0.0	1.0	0.0	0.5	0.0	0.5	0.0	0.5	0.0	0.5	0.0	0.5	0.0	0.0	0.0	0.0	0.0	0.0	0.0		0.0		0.0											33.5	3.
1 wk			2.0		2.0	2.0	2.0	0.0	0.0	1.0	2.0	0.0	0.0	0.0	0.5	0.0	0.5	0.0		0.0		0.5																						
	B12	1		0.0	2.0	2.0	0.5	0.0	0.0	0.0	0.0	0.0	0.0	0.0	0.5	0.0	0.5	0.0	0.5	0.0	0.5	0.0	0.5	0.0	0.0	0.0	0.0	0.0															19.5	2.
1 wk			2.0		2.0		0.0		0.0	2.0	2.0	3.0	0.0	2.0	0.0	2.0	0.5	0.0	0.5	0.0	0.5	0.0		0.0		0.0		1.0		0.5														
	B13	1			2.0		1.0		0.5	2.0	0.0	3.0	0.0	3.0	0.0	2.0	0.0	0.0	0.0	0.0	0.5	0.0	0.5	0.0	2.0	0.0	0.5	0.0		0.0		0.0		0.0		0.0							35.0	3.
1 wk			0.0		0.0		0.0	0.0	0.0	2.0	0.0	0.0	0.0	0.0	0.5	0.0		0.0		0.0		0.0		0.0																				
	B14	1					1.0		0.0		0.5	2.0	0.5	0.0	0.5	1.0	0.5	0.0	0.5	0.0	0.5	0.0	0.5	0.0	0.5	0.0	0.0	0.0		0.0		0.0		0.0		0.0							10.5	2.
0 day						2.0	0.0	0.0	0.0	0.0	2.0	0.0	0.0	0.0	0.0	0.0	2.0	0.0	0.0	0.0		0.0																						
	C15	1		0.0	2.0	0.0	0.0	0.0	0.0	0.0	2.0	0.0	0.0	0.0	0.0	0.0	0.0	0.0	0.5	0.0	0.5	0.0	0.5	0.0	0.0	0.0	0.0	0.0	0.0	0.0		0.0											11.5	2.
0 day				2.0		2.0		2.0	0.0	0.0	0.0	0.0	0.0	0.0	0.0	0.0		0.0		0.0		1.0																						
	C16	7	2.0	0.0	0.0	0.0	0.0	0.0	2.0	0.0	0.0	0.0	0.5	0.0	0.0	0.0	0.5	0.0	0.0	0.0	0.0	0.0	0.0	0.0		0.0		0.0		0.0													12.0	2.
0 day			0.0		0.0		0.0		0.0		0.0	0.0	0.0	0.0	0.0	0.0		0.0		0.0		0.0		0.5																				
	C17	1					0.0	0.0	0.0	0.0	0.5	0.0	0.0	0.0	0.5	0.5	0.0	0.0	0.5	0.0	0.0	0.0	0.0	0.0	0.5	0.5	0.5	0.0		0.0		0.0		0.0									4.0	0.
0 day			3.0		0.0		0.0		0.0		0.0		0.5		0.5					0.0		2.0		0.0		0.0		0.0		0.0		0.5												
	C18	1	0.0		0.0		0.0		0.0		0.0		0.0		2.0		2.0	0.0	0.0	0.0	0.0	0.0		0.0		0.0		0.0		0.0		0.0		0.0		0.0		0.0		0.0			10.5	3.
0 day				0.0		0.0	2.0	0.0	3.0	0.0	3.0	0.0	0.0	0.0	0.0	0.0	0.0	0.0	0.0	0.5																								
	C19	1				0.0	2.0	0.0	0.0	0.0	0.0	0.0	1.0	0.0	0.0	0.0	0.0	0.0	0.0	0.0	0.5	0.0	0.5	0.0	0.0	0.0	0.0	0.0	0.0	0.0													12.5	3.
0 day									0.0	1.0	0.0	1.0	0.0	1.0	0.0	0.5	1.0	0.5	0.0	0.0	0.0	0.0	0.5	0.5																				
	C20	1	0.0	0.0	0.0	2.0	1.0	1.0	0.0	0.0	0.0	1.0	0.0	1.0	0.0	0.5	0.0	0.0	0.0	0.0	0.0	2.0	0.0	0.0	0.0	0.0	0.0		0.0														14.5	2.
0 day				0.0		0.0	1.0	0.0	1.0	0.0	0.0	0.0	0.0	0.0	0.5	0.5	0.5	0.5																										
	C21	1		0.0	1.0	0.0	1.0	0.0	0.0	0.0	0.0	0.0	0.0	0.0	0.0	0.0	0.5	0.0	0.5	0.0	0.0	0.0	0.0	0.0	0.0	0.0		0.0															7.0	1.
																																									Mean	26.71	2.6
																																									SEM	3.40	0.2

Localized Articular Cartilage and Subchondral Cortical Bone Thickness: Six slides representing each quadrant were stained with Safranin O and analyzed for articular cartilage and subchondral cortical bone thickness using Osteomeasure.

				Cartilage-Left			Cartilage-Right			Sub Bone-Left			Sub Bone Right		
Duration	Mouse #	Limb	Starting Slide	Post	Trans	Ant	Post	Trans	Ant	Post	Trans	Ant	Post	Trans	Ant
	A01	Left	1	578.0	471.6	430.3	422.3	629.7	696.5	258.8	194	124.1	190.3	208.1	145.4
	A02	Left	7	434.6	496.7	592.1	361.7	544.1	665.9	383.1	82.8	302.4	247.4	214.7	392.6
	A03	Left	19	416.9	483.5	540.0	369.0	466.4	569.8	223.9	217.6	290.2	287.5	269	246.3
	A04	Left	1	425.5	501.5	477.8	511.2	531.9	582.4	184.7	151.7	509.2	239.1	272.5	312.3
	A05	Left	1	492.4	478.3	526.5	406.2	546.7	617.3	190.3	352	394.2	316.4	323.7	584
	A06	Left	19	446.9	427.2	546.5	448.5	617.9	562.8	240.7	216.2	282.1	220.8	565.1	212.2

A07	Left	1	468.2	501.8	472.3	443.0	619.7	682.6	357.5	359.9	148.3	290	558.5	215.7
B08	Left	13	447.0	553.5	508.1	483.5	602.5	654.7	244.8	263.2	546.7	191.6	535.2	416.8
B09	Left	1	378.5	531.6	492.5	450.6	571.2	645.1	246.4	310.2	381.1	207.7	464.8	156.5
B10	Left	1	379.4	505.3	598.5	368.1	449.3	572.4	220.6	247.5	391.3	254.4	790.5	919.4
B11	Left	1	475.5	501.9	604.2	404.0	576.6	704.3	218.7	321.4	661.5	264.9	328.9	606.7
B12	Left	1	525.0	489.0	512.3	415.5	559.5	596.1	227.1	146.5	281.5	168.8	441	343.9
B13	Left	1	428.5	467.5	539.3	384.9	564.2	566.0	302.4	187.6	605.5	227.2	481	409.7
B14	Left	1	449.5	490.9	487.2	433.0	577.4	512.6	235.1	272.6	351.8	315.9	298.8	121.9
C15	Left	1	568.4	536.5	532.1	486.9	584.1	665.5	286.5	183.1	352.3	169.8	551.8	532.2
C16	Left	7	525.7	583.3	527.8	376.6	604.2	628.9	253.9	299.7	362.7	264.1	814.2	593.7
C17	Left	1	597.6	559.8	517.9	491.0	579.7	523.8	255.2	424.2	385	239	490.3	257.1
C18	Left	1	398.2	559.3	538.7	458.4	544.8	592.9	213.8	280.5	464.3	305.6	659	555.8
C19	Left	1	493.0	575.1	524.3	480.3	745.7	629.9	213.5	437.3	575.6	287.2	903.6	550.1
C20	Left	1	437.8	635.2	560.5	564.8	550	534.7	245.9	622.7	392.8	470.4	461.9	379.3
C21	Left	1	640.2	607.5	550.9	442.4	678.8	553.7	294.2	233.4	487.4	185	644.8	602.9
A01	Right	7	559.5	675.6	615.3	647.3	530.2	488.1	282.3	638.5	592.8	287.1	351	456.3
A02	Right	19	399.7	601.1	650.4	514.8	723.4	478.2	499.4	550.7	700.5	198	357.2	260
A03	Right	13	591.0	625.9	512.7	578.7	592.3	511.4	609.7	721.4	263.9	393.8	553	568.3
A04	Right	13	541.3	591.6	587.6	562.8	617.3	428.0	247.8	542.6	440.2	300.1	373.5	318.2
A05	Right	7	513.7	576.2	595.9	604.2	590.5	376.9	252.9	514.4	380.7	231.8	246.5	178.1
A06	Right	7	421.5	615.4	532.0	666.0	558.1	482.7	330.8	506.7	526.2	190.7	438.8	430.1
A07	Right	1	565.9	617.7	662.3	562.7	669.6	629.6	442.5	666.9	574.3	300.1	283.2	486.8
B08	Right	7	506.6	574.7	575.5	605.2	503.7	456.7	526.3	405.3	555.5	411.4	579.3	413.3
B09	Right	1	506.1	552.7	612.8	489.1	582.2	506.1	408.8	586.6	524.4	297.4	298.4	235.5
B10	Right	1	518.1	589.5	609.5	513.6	554.5	509.5	218.7	488.8	445.6	241.6	414.9	415.8
B11	Right	1	539.2	616.4	530.7	634.6	572.3	449.7	307.8	455.5	544.8	272.2	574.9	272.8
B12	Right	1	451.4	549.8	554.4	574.7	542.1	507.2	332.1	662.9	509	301.2	235.3	574.2
B13	Right	1	577.1	695.8	647.1	617.9	629.1	513.6	391.3	439.3	379.6	193.6	367.6	193.3
B14	Right	1	441.9	623.6	568.7	476.5	543.7	522.1	151.3	272.1	163.2	172.2	342.4	245.2
C15	Right	1	506.9	657.9	610.5	599.2	636.1	485.2	311.1	572.5	468.1	184	308.5	515.6
C16	Right	1	603.3	612.4	555.7	527.4	594.3	469.2	209.5	471.7	558.4	165.4	278.1	310.1
C17	Right	1	459.5	521.7	385.6	648.0	489.6	549.2	384.3	718.6	649.2	213.6	259	504.8
C18	Right	1	527.1	612.3	535.5	627.2	650.9	443.1	437.6	375.9	318	253	300.8	358.7
C19	Right	1	411.0	578.3	473.2	575.3	655.3	420.5	322.2	572.9	476.6	303.3	289.1	284.6
C20	Right	1	485.3	625.7	436.7	539.1	523.6	584.4	213.9	307.3	319.4	239.7	297.5	607.5
C21	Right	7	411.8	652.3	518.4	526.1	585.8	542.0	329.1	732.8	333.7	196	441.7	414.1

Epiphyseal Bone MicroCT Data: Indices of cancellous bone architecture proximal to the growth plate in mice loaded at multiple experimental time points

SampName	Load	Time	BV/TV	Tb.Th [mm]	Tb.Sp [mm]	TMD [mg HA/ccm]
e154	Left	2-week	0.2382	0.0504	0.1963	966.128
e154	Right	2-week	0.2831	0.0536	0.1791	976.09
e154	Left	2-week	0.2955	0.0559	0.1744	948.092
e154	Right	2-week	0.328	0.0576	0.1799	993.995
e154	Left	2-week	0.2685	0.0537	0.1893	956.882
e154	Right	2-week	0.3097	0.0577	0.1877	996.274
e154	Left	2-week	0.3094	0.0597	0.2002	951.022
e154	Right	2-week	0.2924	0.0577	0.2085	985.205
e154	Left	2-week	0.3169	0.0579	0.1922	972.509
e154	Right	2-week	0.2827	0.0535	0.185	974.983
e154	Left	2-week	0.2549	0.0569	0.1951	953.757
e154	Right	2-week	0.2627	0.0567	0.2329	979.215
e154	Left	2-week	0.2649	0.0539	0.1931	978.694
e154	Right	2-week	0.288	0.0577	0.1982	993.149
e154	Left	1-week	0.2756	0.0519	0.174	975.308
e154	Right	1-week	0.3247	0.0608	0.1864	1004.0224
e154	Left	1-week	0.2497	0.0503	0.1858	966.714
e154	Right	1-week	0.2857	0.0551	0.1943	976.806
e154	Left	1-week	0.2592	0.0519	0.1912	967.756
e154	Right	1-week	0.2733	0.0549	0.2019	974.787
e154	Left	1-week	0.2726	0.0558	0.1988	968.537
e154	Right	1-week	0.3038	0.0579	0.1868	998.813
e154	Left	1-week	0.1888	0.0463	0.223	957.012
e154	Right	1-week	0.2416	0.051	0.2171	965.021
e154	Left	1-week	0.2341	0.0505	0.1944	978.108

e154	Right	1-week	0.301	0.0553	0.1729	986.963
e154	Left	1-week	0.2342	0.0499	0.1889	982.405
e154	Right	1-week	0.2676	0.053	0.195	987.875
e154	Left	0-day	0.3038	0.0593	0.1939	996.665
e154	Right	0-day	0.3169	0.0577	0.175	992.497
e154	Left	0-day	0.2624	0.055	0.1995	979.41
e154	Right	0-day	0.2518	0.0539	0.2053	977.066
e154	Left	0-day	0.3214	0.0586	0.1734	996.339
e154	Right	0-day	0.3267	0.0591	0.1929	994.581
e154	Left	0-day	0.2849	0.0568	0.194	984.033
e154	Right	0-day	0.2662	0.055	0.2072	984.749
e154	Left	0-day	0.2657	0.0574	0.2048	984.098
e154	Right	0-day	0.2395	0.0522	0.2002	978.238
e154	Left	0-day	0.2707	0.0541	0.1903	980.517
e154	Right	0-day	0.278	0.0541	0.2034	990.739
e154	Left	0-day	0.3028	0.0561	0.1839	998.618
e154	Right	0-day	0.3114	0.0557	0.1795	1000.441

Metaphyseal Cancellous Bone MicroCT Data: Indices of cancellous bone architecture distal to the growth plate in mice at multiple experimental time points

SampName	Load	Time	VOX-BV/TV	Tb.Th [mm]	Tb.Sp [mm]	TMD [mg HA/ccm]
e154	Left	2-week	0.1211	0.0405	0.2152	877.839
e154	Right	2-week	0.1458	0.044	0.1992	889.298
e154	Left	2-week	0.1202	0.0453	0.271	870.286
e154	Right	2-week	0.1403	0.0474	0.2338	911.826
e154	Left	2-week	0.1088	0.0428	0.2561	878.034
e154	Right	2-week	0.1129	0.0441	0.2386	909.677
e154	Left	2-week	0.142	0.0449	0.2237	869.895

e154	Right	2-week	0.1448	0.0439	0.2182	906.747
e154	Left	2-week	0.1215	0.0393	0.2068	872.825
e154	Right	2-week	0.1537	0.0441	0.1802	906.552
e154	Left	2-week	0.1267	0.047	0.2294	865.923
e154	Right	2-week	0.1306	0.0476	0.2183	886.889
e154	Left	2-week	0.1082	0.0398	0.239	878.359
e154	Right	2-week	0.1235	0.0437	0.2105	908.115
e154	Left	1-week	0.1377	0.0465	0.2156	911.826
e154	Right	1-week	0.1386	0.0448	0.2171	923.09
e154	Left	1-week	0.1328	0.0401	0.1982	888.972
e154	Right	1-week	0.1431	0.0407	0.1926	904.989
e154	Left	1-week	0.1159	0.0425	0.2384	861.561
e154	Right	1-week	0.1224	0.0455	0.2318	891.381
e154	Left	1-week	0.1425	0.0421	0.208	887.019
e154	Right	1-week	0.1266	0.0425	0.2104	890.991
e154	Left	1-week	0.1019	0.0352	0.2173	871.718
e154	Right	1-week	0.1254	0.0418	0.2223	890.73
e154	Left	1-week	0.1142	0.0381	0.2161	899.455
e154	Right	1-week	0.1458	0.0444	0.2029	915.212
e154	Left	1-week	0.0852	0.0377	0.2227	876.146
e154	Right	1-week	0.0897	0.04	0.2354	896.134
e154	Left	0-day	0.1463	0.0415	0.2059	907.529
e154	Right	0-day	0.1609	0.0427	0.2056	907.594
e154	Left	0-day	0.1004	0.0458	0.2389	884.35
e154	Right	0-day	0.1028	0.0436	0.2396	877.578
e154	Left	0-day	0.1499	0.0483	0.2343	918.272
e154	Right	0-day	0.1226	0.0491	0.2692	916.384
e154	Left	0-day	0.149	0.0464	0.1967	907.529
e154	Right	0-day	0.1241	0.041	0.2041	891.447
e154	Left	0-day	0.1236	0.0474	0.2389	910.328

e154	Right	0-day	0.1127	0.0467	0.2337	889.168
e154	Left	0-day	0.1252	0.0467	0.2738	903.557
e154	Right	0-day	0.1354	0.0472	0.2481	918.728
e154	Left	0-day	0.1391	0.0484	0.2135	940.995
e154	Right	0-day	0.1497	0.0441	0.2083	927.518

Number of Chondrocytes Expressing LC3: Indices of chondrocyte autophagy measured by immunohistochemicalstaining of chondrocytes using LC3 antibody normalized by cartilage area

		Post	Mid	Ant	Post	Mid	Ant	Post	Mid	Ant	Post	Mid	Ant	Overall Average (Medial + Lateral)
Mouse #	**Limb**	**Cart Area [mm]**	**Cart Area [mm]**	**Cart Area [mm]**	**Chon N**	**Chon N**	**Chon N**	**Cart Area [mm]**	**Cart Area [mm]**	**Cart Area [mm]**	**Chon N**	**Chon N**	**Chon N**	**ChonN/CA**
A01	Left	0.0936	0.1022	0.0138	0	0	4	0.0460	0.0715	0.1067	0	0	1	11.524
A02	Left	0.0955	0.1047	0.0930	0	0	0	0.0508	0.0936	0.0955	0	0	0	0.000
A03	Left	0.1002	0.1202	0.1203	0	1	0	0.0384	0.0520	0.0935	0	0	0	1.907
A04	Left	0.1265	0.1212	0.0947	2	1	2	0.0419	0.0443	0.0840	0	0	1	11.705
A05	Left	0.0794	0.0989	0.0891	2	5	2	0.0348	0.0855	0.0777	0	1	3	27.935
A06	Left	0.1033	0.1196	0.0520	10	1	0	0.0404	0.0861	0.0796	0	1	0	24.946
A07	Left	0.0974	0.1007	0.0695	2	2	0	0.0496	0.1034	0.0894	0	1	1	11.765
B08	Left	0.1139	0.1146	0.0289	5	0	1	0.0430	0.0667	0.0844	0	0	0	13.289
B09	Left	0.1002	0.1035	0.0491	10	7	4	0.0655	0.0628	0.0769	1	0	1	50.217
B10	Left	0.1097	0.1260	0.0324	0	2	0	0.0493	0.0776	0.0825	0	0	0	4.188
B11	Left	0.0822	0.0938	0.0535	0	6	2	0.0575	0.0959	0.0909	0	0	0	16.882
B12	Left	0.0815	0.0834	0.0800	0	7	0	0.0549	0.0849	0.0815	0	1	1	19.305
B13	Left	0.0854	0.0946	0.0672	5	9	1	0.0570	0.0623	0.0803	1	1	0	38.055
B14	Left	0.0893	0.0940	0.0353	1	1	0	0.0399	0.0859	0.0793	0	0	0	4.720
C15	Left	0.0921	0.1109	0.0605	4	7	2	0.0799	0.1222	0.0821	2	5	6	47.469
C16	Left	0.1033	0.0926	0.0403	7	11	6	0.0664	0.0993	0.0778	7	7	9	97.963
C17	Left	0.1107	0.1011	0.0493	16	12	10	0.0563	0.0898	0.0729	1	28	6	152.082
C18	Left	0.1418	0.0987	0.0153	17	3	4		0.0574	0.1028		9	16	117.783
C19	Left	0.0925	0.1040	0.0707	3	8	2	0.0602	0.1169	0.0743	3	6	1	44.346

C20	Left	0.0760	0.1052	0.0607	2	4	7	0.1070	0.1077	0.0678	12	4	4	62.927
C21	Left	0.0790	0.0915	0.0721	3	6	3	0.0686	0.0910	0.0831	2	14	4	65.937
A01	Right	0.0727	0.1169	0.0853	2	17	2	0.0850	0.1286	0.0868	22	38	3	146.001
A02	Right	0.0242	0.0929	0.1170	15	0	22	0.1503	0.1253	0.0404	1	0	30	123.620
A03	Right	0.0819	0.1242	0.1013	11	12	17	0.1592	0.1124	0.0597	9	8	11	106.484
A04	Right	0.0594	0.0852	0.1097	2	3	3	0.1443	0.1198	0.0252	8	2	0	33.120
A05	Right	0.0619	0.0951	0.1041	7	1	1	0.1312	0.1115	0.0372	5	6	0	36.965
A06	Right	0.0647	0.1047	0.0879	5	2	5	0.1121	0.1118	0.0486	21	2	4	73.618
A07	Right	0.0117	0.0682	0.1137	1	5	2	0.1268	0.1247	0.0522	31	2	1	84.441
B08	Right	0.0386	0.0624	0.1146	1	1	29	0.1359	0.0837	0.0086	7	2	0	90.131
B09	Right	0.0206	0.0589	0.1006	2	2	8	0.1383	0.0867	0.0231	34	1	2	114.439
B10	Right	0.0667	0.0862	0.0922	10	3	2	0.1099	0.0970	0.0497	26	1	0	83.718
B11	Right	0.0753	0.0924	0.0954	0	3	1	0.1256	0.1072	0.0273	24	1	6	66.895
B12	Right	0.0812	0.1098	0.0770	8	4	5	0.0764	0.1023	0.0856	13	17	2	92.048
B13	Right	0.0586	0.0797	0.0961	1	10	2	0.1384	0.0905	0.0425	17	4	1	69.195
B14	Right	0.0629	0.0783	0.0951	3	11	3	0.1118	0.0810	0.0424	14	13	1	95.437
C15	Right	0.0547	0.0924	0.0936	3	3	2	0.1123	0.0959	0.0511	24	4	1	74.009
C16	Right	0.0611	0.0978	0.0759	3	5	2	0.0773	0.1082	0.0502	8	15	1	72.257
C17	Right	0.1068	0.0896	0.0406	4	4	1	0.1031	0.1158	0.0552	5	4	3	41.087
C18	Right		0.0745	0.1220		14	27	0.1420	0.0826		30	15		204.243
C19	Right	0.0662	0.1017	0.0672	6	3	9	0.1265	0.0942	0.0488	15	0	0	65.403
C20	Right	0.1566	0.0954	0.0129	7	1	2		0.0616	0.0999		5	7	51.595
C21	Right	0.0606	0.1022	0.0863	6	16	5	0.1173	0.1204	0.0601	32	16	1	138.969

Number of Osteoclasts in Epiphyseal Bone: Immunohistochemical staining using Cathepsin K antibody was performed to determine the number of osteoclasts within epiphysis normalized by bone surface

				Post	Mid	Ant	Post	Mid	Ant	Post	Mid	Ant	Average	Overall Average
Duration	Mouse #	Limb	Starting Slide	Bone Area [mm]	Bone Area	Bone Area	OcN	OcN	OcN	OcN/BA	OcN/BA	OcN/BA	OcN/BA	OcN/BA
	A01	Left	1	10.431	12.374	13.047	7	5	5	0.671	0.404	0.383	0.486	0.474170272
	A02	Left	7	5.148	11.320	15.986	3	6	6	0.583	0.530	0.375	0.496	0.462194066
	A03	Left	19	11.346	13.732	14.661	2	3	6	0.176	0.218	0.409	0.268	0.276805464

A04	Left	1	5.875	10.184	13.468	4	2	4	0.681	0.196	0.297	0.391	0.338682255
A05	Left	1	2.224	12.787	11.846	0	6	5	0.000	0.469	0.422	0.297	0.409573597
A06	Left	19	5.274	9.833	13.470	2	5	2	0.379	0.508	0.148	0.345	0.314935281
A07	Left	1	8.029	13.342	16.658	1	3	4	0.125	0.225	0.240	0.197	0.210369646
B08	Left	13	6.231	11.221	10.982	2	4	3	0.321	0.356	0.273	0.317	0.316523586
B09	Left	1	7.182	12.129	14.456	5	6	5	0.696	0.495	0.346	0.512	0.473842418
B10	Left	1	5.440	11.718	13.418	1	6	6	0.184	0.512	0.447	0.381	0.425161725
B11	Left	1	6.907	9.771	13.183	1	6	4	0.145	0.614	0.303	0.354	0.368377165
B12	Left	1	4.285	11.566	12.238	0	8	7	0.000	0.692	0.572	0.421	0.53400927
B13	Left	1	5.436	10.265	14.969	1	7	4	0.184	0.682	0.267	0.378	0.391249063
B14	Left	1	7.738	12.569	13.480	0	5	3	0.000	0.398	0.223	0.207	0.236785168
C15	Left	1	5.025	11.246	14.259	0	1	1	0.000	0.089	0.070	0.053	0.065510408
C16	Left	7	5.336	9.500	12.873	0	2	0	0.000	0.211	0.000	0.070	0.072178714
C17	Left	1	5.653	9.478	15.075	0	0	0	0.000	0.000	0.000	0.000	0
C18	Left	1	6.637	12.081	9.656	0	1	1	0.000	0.083	0.104	0.062	0.070488059
C19	Left	1	6.636	9.270	12.046	0	0	0	0.000	0.000	0.000	0.000	0
C20	Left	1	6.633	12.381	13.572	0	0	0	0.000	0.000	0.000	0.000	0
C21	Left	1	7.192	10.568	12.147	1	0	0	0.139	0.000	0.000	0.046	0.033436317
A01	Right	7	6.487	12.227	13.407	1	3	2	0.154	0.245	0.149	0.183	0.186792523
A02	Right	19	9.734	10.384	11.834	2	2	1	0.205	0.193	0.085	0.161	0.156487176
A03	Right	13	7.343	12.043	14.915	1	0	1	0.136	0.000	0.067	0.068	0.058305978
A04	Right	13	7.409	8.041	12.581	1	3	2	0.135	0.373	0.159	0.222	0.214045677
A05	Right	7	8.513	11.386	12.438	1	2	1	0.117	0.176	0.080	0.125	0.123700756
A06	Right	7	9.110	11.036	14.680	1	2	2	0.110	0.181	0.136	0.142	0.143569246
A07	Right	1	7.811	11.181	12.126	3	1	1	0.384	0.089	0.082	0.185	0.160676641
B08	Right	7	7.334	9.565	9.869	0	1	2	0.000	0.105	0.203	0.102	0.112076212
B09	Right	1	5.461	10.802	11.650	0	1	1	0.000	0.093	0.086	0.059	0.071651972
B10	Right	1	6.710	10.181	9.908	1	1	2	0.149	0.098	0.202	0.150	0.149257073

B11	Right	1	6.351	10.218	12.380	0	1	1	0.000	0.098	0.081	0.060	0.069088447
B12	Right	1	6.120	10.638	10.383	0	3	3	0.000	0.282	0.289	0.190	0.221069386
B13	Right	1	9.290	11.540	13.800	1	2	2	0.108	0.173	0.145	0.142	0.144380981
B14	Right	1	8.035	11.579	12.787	0	1	0	0.000	0.086	0.000	0.029	0.030863531
C15	Right	1	7.852	10.342	11.393	0	0	0	0.000	0.000	0.000	0.000	0
C16	Right	1	5.925	11.161	13.571	0	1	1	0.000	0.090	0.074	0.054	0.065238594
C17	Right	1	4.355	10.437	11.925	0	0	0	0.000	0.000	0.000	0.000	0
C18	Right	1	5.594	11.232	8.808	0	1	0	0.000	0.089	0.000	0.030	0.039011298
C19	Right	1	6.104	10.941	10.886	1	0	1	0.164	0.000	0.092	0.085	0.071606565
C20	Right	1	5.986	10.674	11.533	0	0	0	0.000	0.000	0.000	0.000	0
C21	Right	7	7.201	10.254	14.358	1	0	2	0.139	0.000	0.139	0.093	0.094302258

Appendix C: Chapter 4 Data

Histological Score: Indices of articular cartilage damage measured by Safranin O stain. Each level corresponds to a slide separated at a 90 µm interval. Four boxes in each level correspond to four areas of tibiofemoral articular cartilage.

Knee

Right

Recovery	Mouse #	Starting Slide #	Levels 1	2	3	4	5	6	7	8	9	10	11	12	13	14	15	16	17	18	19	20	Summed score	Highest score
DKK1	1542	1	0.0	0.0	0.0	0.0	0.0	0.0	0.5	0.0	0.0	0.0	0.5										3.0	1.0
Wnt3	1566	1	0.0	0.0	0.0	0.0	0.0	0.0	0.0	0.0	0.5	0.0	0.5	0.0	0.5								5.0	0.5
Wnt3	1568	1	0.0	0.0	0.0	0.0	0.0	0.0	0.0	0.0	0.0	0.0	0.0	0.5	0.0								3.5	0.5
DKK1	1605	1	0.0	0.0	0.0	0.0	0.0	0.0	0.0	0.0	0.5	0.0	0.5	0.0									4.0	1.0
WT	1614	1	0.0	0.0	0.0	0.0	0.0	0.0	0.0	0.0	0.0	0.0	0.5	0.5	0.0	0.0							6.0	1.0
DKK1	1625	1	0.0	0.0	0.0	0.0	0.0	0.0	0.0	0.0	0.0	0.0	0.0	0.0	0.0	0.0							3.5	1.0
DKK1	1629	7	0.0	0.0	0.0	0.0	0.0	0.0	0.0	0.0	0.0	0.0	0.5	0.5	0.5								6.5	0.5
DKK1	1630	1	0.5	0.5	0.0	0.0	0.0	0.0	0.0	0.0	0.0	0.0	0.0	0.0	0.5	0.0	0.0	0.0					3.0	0.5
DKK1	1641	1	0.0	0.0	0.0	0.0	0.0	0.0	0.0	0.0	0.0	0.0	0.0	0.0	0.5								3.0	0.5
DKK1	1642	1	0.0	0.0	0.0	0.0	0.0	0.0	0.0	0.0	0.0	0.0	0.0	0.0	0.0	0.5							3.5	0.5
WT	1646	1	0.0	0.0	0.0	0.0	0.0	0.0	0.0	0.0	0.0	0.0	0.0	0.0	0.0	0.5							10.0	3.0
WT	1647	7	0.0	0.0	0.5	0.0	0.0	0.0	0.0	0.0	0.0	0.0	0.0	0.0	0.0								3.5	0.5
WT	1648	1	0.0	0.0	0.0																		0.0	0.0
Wnt3	1649	1	0.0	0.0	0.0	0.0	0.0	0.0	0.0	0.0	0.0	0.0	0.0	0.0	0.0								7.0	0.5
Wnt3	1650	1	0.0	0.0	0.0	0.0	0.0	0.0	0.0	0.0	0.0	0.0	0.0	0.0	0.5								7.0	1.0
Wnt3	1651	1	0.0	0.0	0.0	0.0	0.0	0.0	0.0	0.0	0.0	0.0	0.0	0.0	0.0	0.0	0.0	0.0	0.0	0.0	0.0	0.5	16.0	2.0
WT	1656	1	0.0	0.0	0.0	0.0	0.0	0.0	0.0	0.0	0.0	0.0	0.0	0.0	0.0	0.0	0.0	0.0					6.0	1.0
WT	1657	7	0.0	0.0	0.0	0.0	0.0	0.0	0.0	0.0	0.0	0.0	0.0	0.0	0.0	0.0	0.0						6.0	1.0
WT	1658	7	0.0	0.0	0.0	0.0	0.0	0.0	0.0	0.0	0.0	0.0	0.0	0.0	0.0	0.0	0.0						4.5	0.5
WT	1659	1	0.0	0.0	0.0	0.0	0.0	0.0	0.0	0.0	0.0	0.0	0.0	0.0	0.0	0.0	0.0						5.5	1.0
Wnt3	1660	1	0.0	0.0	0.0	0.0	0.0	0.0	0.0	0.0	0.0	0.0	0.0	0.0	0.0	0.0	0.0						9.0	1.0
Wnt3	1661	1	0.0	0.0	0.0	0.0	0.0	0.0	0.0	0.0	0.0	0.0	0.0	0.0	0.0	0.0	0.0	0.0					7.5	1.0
																						Mean	5.50	0.88
																						SEM	0.72	0.14

Left

Duration	Mouse #	Starting Slide #	1	2	3	4	5	6	7	8	9	10	11	12	13	14	15	16	17	18	19	20	Summed score	Highest score
DKK1	1542	1	0.0	0.0	0.0	2.0	0.0	0.0	0.0	0.0	0.0	0.0	0.5	0.0									9.0	2.0
Wnt3	1566	1	0.0	0.0	0.0	0.0	0.0	0.0	0.0	0.0	0.0	0.0	0.0	0.0	0.0	0.0	0.0	0.0	0.0	0.0	0.0	0.0	3.5	0.5
Wnt3	1568	1	0.0	0.0	0.0	0.0	0.0	0.0	0.0	0.0	0.0	0.0	0.5	0.0	0.0	0.0	0.0	0.0	0.0	0.0	0.0	0.0	5.5	1.0
DKK1	1605	1	0.0	0.0	0.0	0.0	0.0	0.0	0.0	0.0	0.0	0.0	0.0	0.0	0.0	0.0	0.0	0.0	0.0	0.0	0.0	0.0	9.0	1.0

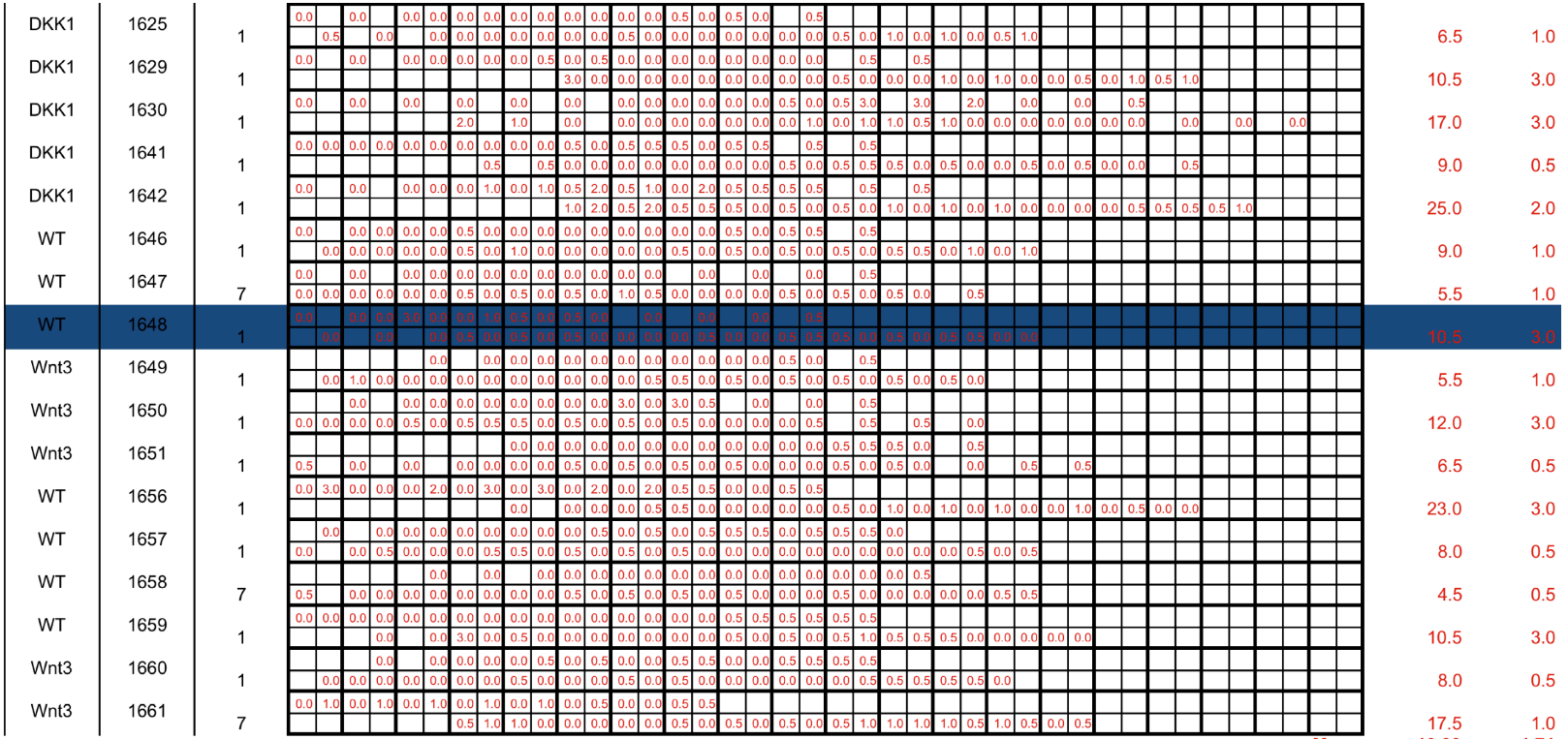

Localized Articular Cartilage and Subchondral Cortical Bone Thickness: Six slides representing each quadrant were stained with Safranin O and analyzed for articular cartilage and subchondral cortical bone thickness using Osteomeasure.

			Cartilage-Left			Cartilage-Right			Sub Bone-Left			Sub Bone Right		
Mouse #	Limb	Starting Slide	Post	Trans	Ant	Post	Trans	Ant	Post	Trans	Ant	Post	Trans	Ant
1542	Left	1	449.2	510.5	588.1	518.3	723.3	745.2	359.6	102.7	141.3	345.0	317.8	390.6
1566	Left	1	715.8	545.1	636.4	595.4	722.0	682.7	197.0	285.5	225.2	226.4	408.0	177.9
1568	Left	1	634.4	681.3	629.3	513.8	746.1	767.8	238.2	238.4	532.2	324.6	291.4	265.9
1605	Left	1	392.6	566.5	683.6	483.9	691.2	721.6	246.2	150.4	180.6	320.0	261.0	481.6

1614	Left	1	623.9	549.2	688.2	477.3	665.4	783.1	222.0	196.6	272.4	267.7	456.5	343.8
1625	Left	1	451.6	655.9	700.4	426.4	677.2	779.9	331.2	268.0	295.2	427.9	388.6	342.3
1629	Left	1	565.7	769.1	608.6	511.5	664.8	743.7	240.9	331.0	742.4	358.4	349.1	343.6
1630	Left	1	597.9	796.4	664.9	474.3	781.7	685.8	545.4	125.4	316.6	498.3	608.1	869.2
1641	Left	1	549.3	814.5	538.1	548.3	618.0	738.9	437.6	233.2	487.4	390.2	503.5	308.3
1642	Left	1	495.1	709.1	736.3	538.1	699.9	760.6	222.2	636.8	178.0	360.7	342.0	524.7
1646	Left	1	491.8	667.2	560.7	555.4	715.3	712.2	398.9	205.7	303.2	385.0	372.9	293.9
1647	Left	7	750.0	594.8	429.6	840.8	705.7	626.1	223.9	371.9	133.8	410.9	282.5	402.8
1648	Left	1												
1649	Left	1	580.8	691.8	534.3	737.2	733.3	700.7	406.6	153.9	292.9	296.8	772.8	418.3
1650	Left	1	820.3	764.5	585.4	705.0	695.3	693.8	393.3	296.9	442.3	289.8	456.8	534.0
1651	Left	1	917.1	932.4	681.1	715.1	899.2	778.8	499.5	160.1	414.3	335.7	518.3	699.0
1656	Left	1	414.9	595.6	635.3	453.2	711.5	829.4	447.5	195.3	278.3	424.6	287.9	306.3
1657	Left	1	889.3	601.0	407.4	852.2	885.1	555.3	291.1	357.3	138.9	419.0	273.7	203.1
1658	Left	7	799.9	723.5	437.3	813.8	757.1	657.7	269.5	171.0	210.9	166.5	305.0	296.7
1659	Left	1	430.7	624.2	589.8	458.8	738.8	690.4	244.8	309.4	211.2	266.0	266.6	242.2
1660	Left	1	727.0	597.6	453.9	710.7	735.8	626.8	406.3	394.6	330.7	228.3	492.7	402.3
1661	Left	7	402.9	465.7	570.6	460.0	620.5	656.9	361.9	252.8	417.4	476.1	307.8	251.9
1542	Right	1	851.9	666.8	525.1	817.5	724.7	504.6	272.5	518.3	496.5	411.2	371.5	370.1
1566	Right	1	760.5	757.9	778.1	680.5	601.5	478.2	258.4	244.0	495.5	285.6	366.3	365.9
1568	Right	1	608.7	742.6	812.6	591.2	713.0	652.7	241.6	286.7	398.3	172.1	175.9	339.7
1605	Right	1	914.7	896.9	720.0	844.7	839.8	605.6	447.0	396.1	657.1	218.5	383.2	356.2
1614	Right	1	577.3	760.7	755.1	682.1	661.8	463.5	361.1	187.0	528.3	122.0	118.1	229.2
1625	Right	1	846.6	722.2	814.6	776.1	635.6	390.1	350.7	675.6	604.7	339.6	533.5	202.3
1629	Right	7	675.5	752.6	689.4	741.4	799.4	765.0	552.0	789.5	682.2	294.4	371.2	570.6
1630	Right	1	696.1	874.6	760.0	904.6	759.6	452.8	578.7	888.0	774.1	420.3	490.5	358.8
1641	Right	1	620.5	680.2	610.7	597.3	732.0	625.2	464.9	577.5	639.1	281.7	406.3	323.0
1642	Right	1	617.7	747.4	751.5	701.5	685.8	570.6	367.9	638.0	835.4	276.6	598.9	490.6
1646	Right	1	667.8	753.2	698.3	670.3	668.9	565.6	402.7	423.9	569.2	269.8	278.6	578.2
1647	Right	7	856.7	665.9	706.5	713.1	703.8	443.3	160.2	530.9	626.1	130.4	330.4	481.5
1648	Right	1												
1649	Right	1	524.9	742.2	709.6	549.3	668.8	613.4	381.6	432.9	556.3	385.0	249.4	533.2
1650	Right	1	725.0	806.8	655.9	885.5	808.6	581.9	492.4	413.1	874.1	272.9	333.8	557.4
1651	Right	1	712.0	837.4	578.9	769.7	709.9	358.2	539.3	659.2	733.6	273.0	286.3	309.8
1656	Right	1	672.5	755.5	732.6	600.2	619.6	486.2	345.8	446.4	364.4	344.1	325.3	165.5
1657	Right	7	690.5	787.4	809.5	657.8	694.0	469.1	683.2	590.7	228.2	290.3	323.8	248.1
1658	Right	7	809.0	720.3	754.2	575.6	696.4	603.2	333.1	463.3	488.5	461.0	212.5	278.8

1659	Right	1	608.5	689.7	795.7	729.3	563.2	386.1	481.6	304.3	340.5	175.5	512.9	251.0
1660	Right	1	623.4	811.4	819.3	544.2	573.5	526.6	364.5	435.3	623.3	366.2	637.9	444.7
1661	Right	1	649.6	783.5	763.6	652.5	551.8	366.3	185.1	313.7	294.5	382.9	417.8	458.3

Metaphyseal Cancellous Bone MicroCT Data: Indices of cancellous bone architecture distal to the growth plate in WT, Wnt3, and Dkk1 KO mice loaded for two weeks

Gene	Load	Sample	BV/TV	Tb.Th [mm]	Tb.Sp [mm]	TMD [mg HA/ccm]
Wnt3	Load	1660L	0.1384	0.0408	0.1769	946.595
Wnt3	Control	1660R	0.1335	0.0402	0.1853	932.271
WT	Load	1659L	0.0928	0.0469	0.2962	924.718
WT	Control	1659R	0.0841	0.0391	0.3006	950.046
Dkk1	Load	1542L	0.101	0.0513	0.2614	925.629
Dkk1	Control	1542R	0.0955	0.0367	0.2401	938.847
Wnt3	Load	1566L	0.1332	0.0442	0.1791	936.373
Wnt3	Control	1566R	0.0923	0.0389	0.2358	947.506
Wnt3	Load	1568L	0.0569	0.0408	0.282	920.876
Wnt3	Control	1568R	0.0775	0.039	0.2578	968.081
Dkk1	Load	1605L	0.1067	0.0526	0.2634	914.626
Dkk1	Control	1605R	0.0725	0.0376	0.2519	942.363
Wnt3	Load	1650L	0.1443	0.0516	0.209	956.752
Wnt3	Control	1650R	0.1248	0.043	0.197	946.465
Wnt3	Load	1651R	0.1397	0.0452	0.2293	942.428
Wnt3	Control	1651L	0.1654	0.0487	0.2006	942.688
WT	Load	1614L	0.0708	0.0464	0.3271	918.663
WT	Control	1614R	0.0709	0.0405	0.3189	935.396
Dkk1	Load	1625L	0.1198	0.0475	0.2034	939.498
Dkk1	Control	1625R	0.0966	0.0367	0.2019	949.525
Dkk1	Load	1641L	0.1908	0.0516	0.1581	947.376
Dkk1	Control	1641R	0.1714	0.0472	0.1632	960.008

Dkk1	Load	1642L	0.1248	0.053	0.2127	934.484
Dkk1	Control	1642R	0.0984	0.04	0.2149	949.329
WT	Load	1646L	0.0867	0.0506	0.5258	928.82
WT	Control	1646R	0.0863	0.0438	0.4366	932.661
WT	Load	1647L	0.159	0.0491	0.2168	923.155
WT	Control	1647R	0.1486	0.0432	0.1984	942.363
WT	Load	1648L	0.1093	0.0523	0.2582	940.54
WT	Control	1648R	0.0956	0.0421	0.3035	948.939
Wnt3	Load	1649L	0.1555	0.0499	0.1828	947.376
Wnt3	Control	1649R	0.12	0.043	0.2075	952.325
Dkk1	Load	1629L	0.1967	0.0488	0.1532	933.117
Dkk1	Control	1629R	0.1742	0.0426	0.1564	942.037
Dkk1	Load	1630L	0.1561	0.0501	0.1812	936.438
Dkk1	Control	1630R	0.1457	0.0413	0.1759	930.903
WT	Load	1656L	0.1182	0.0475	0.1949	906.682
WT	Control	1656R	0.1006	0.0403	0.2017	943.144
WT	Load	1657L	0.1371	0.0489	0.2151	953.171
WT	Control	1657R	0.1192	0.0446	0.2605	950.827
WT	Load	1658L	0.1449	0.0485	0.1897	965.867
WT	Control	1658R	0.107	0.0387	0.1945	954.278
Wnt3	Load	1661L	0.1032	0.0473	0.2534	936.373
Wnt3	Control	1661R	0.1221	0.0429	0.2498	959.747

Epiphyseal Bone MicroCT Data: Indices of cancellous bone architecture proximal to the growth plate in WT, Wnt3, and Dkk1 KO mice loaded for two weeks

Gene	Load	Sample	BV/TV	Tb.Th [mm]	Tb.Sp [mm]	TMD [mg HA/ccm]
WT	Load	1659L	0.3327	0.0563	0.1465	1000.506
WT	Control	1659R	0.3602	0.055	0.1479	993.083

Wnt3	Load	1660L	0.2467	0.0509	0.1576	958.836
Wnt3	Control	1660R	0.2897	0.0487	0.164	987.419
Dkk1	Load	1542L	0.2864	0.0613	0.1729	984.6848
Dkk1	Control	1542R	0.2752	0.0538	0.1666	1013.398
Wnt3	Load	1566L	0.2668	0.0515	0.1607	973.03
Wnt3	Control	1566R	0.3277	0.0549	0.152	993.409
Wnt3	Load	1568L	0.2254	0.0523	0.1926	978.369
Wnt3	Control	1568R	0.3142	0.0552	0.1735	1006.692
Dkk1	Load	1605L	0.3453	0.07	0.1815	983.5128
Dkk1	Control	1605R	0.3153	0.0575	0.1712	990.479
Wnt3	Load	1650L	0.3565	0.0631	0.1651	1014.9609
Wnt3	Control	1650R	0.3468	0.0586	0.1658	1015.351
Wnt3	Load	1651R	0.3548	0.0624	0.1775	1005.7153
Wnt3	Control	1651L	0.3521	0.0635	0.1665	1010.273
WT	Load	1614L	0.3041	0.0545	0.1672	977.131
WT	Control	1614R	0.313	0.0556	0.1654	979.866
Dkk1	Load	1625L	0.3465	0.0707	0.1595	998.7485
Dkk1	Control	1625R	0.3347	0.0614	0.1591	1014.8958
Dkk1	Load	1641L	0.3582	0.0615	0.1491	992.563
Dkk1	Control	1641R	0.391	0.0659	0.151	1025.4436
Dkk1	Load	1642L	0.3845	0.0696	0.1583	1012.8123
Dkk1	Control	1642R	0.3421	0.0657	0.159	1014.1144
WT	Load	1646L	0.2386	0.0536	0.1921	971.141
WT	Control	1646R	0.2759	0.056	0.1945	986.117
WT	Load	1647L	0.3129	0.0569	0.1525	998.488
WT	Control	1647R	0.3486	0.0579	0.1622	1007.603
WT	Load	1648L	0.2829	0.0544	0.1789	993.93
WT	Control	1648R	0.3153	0.0531	0.1792	999.074
Wnt3	Load	1649L	0.3626	0.0608	0.1469	1017.4351
Wnt3	Control	1649R	0.3685	0.0587	0.1587	1009.166

Dkk1	Load	1629L	0.4032	0.0712	0.1484	995.3627
Dkk1	Control	1629R	0.4338	0.0671	0.1408	1026.1598
Dkk1	Load	1630L	0.362	0.0659	0.1499	983.9684
Dkk1	Control	1630R	0.3592	0.0636	0.156	995.9488
WT	Load	1656L	0.2657	0.0559	0.17	968.342
WT	Control	1656R	0.319	0.057	0.1581	998.748
WT	Load	1657L	0.3522	0.0583	0.1538	1009.947
WT	Control	1657R	0.3423	0.055	0.1564	1005.129
WT	Load	1658L	0.3249	0.0547	0.1463	1005.064
WT	Control	1658R	0.3247	0.0519	0.1504	1008.189
Wnt3	Load	1661L	0.2743	0.0536	0.1657	981.559
Wnt3	Control	1661R	0.3633	0.0576	0.1558	1018.346

Number of Chondrocytes Expressing MMP-13: Indices of cartilage catabolic activity measured by immunohistochemicalstaining of chondrocytes using MMP-13 antibody normalized by cartilage area

															Overall Average (Medial + Lateral)
			Post	Mid	Ant	Post	Mid	Ant	Post	Mid	Ant	Post	Mid	Ant	
Gene	Mouse #	Limb	Cart Area	Cart Area	Cart Area	Chon N	Chon N	Chon N	Cart Area	Cart Area	Cart Area	Chon N	Chon N	Chon N	ChonN/CA
Dkk1	1542	Left	0.0600	0.0967	0.0945	2	3	2	0.1116	0.1004	0.1009	7	5	3	39.001
Wnt3	1566	Left	0.1101	0.1276	0.1300	4	0	2	0.1015	0.1166	0.0884	8	4	1	28.185
Wnt3	1568	Left	0.1048	0.1453	0.0969	0	9	7	0.0808	0.1277	0.1050	2	17	6	62.077
Dkk1	1605	Left	0.0582	0.1094	0.1188	0	1	7	0.0557	0.1063	0.0812	0	2	1	20.772
WT	1614	Left	0.0819	0.1090	0.1268	5	6	20	0.0761	0.1062	0.1011	0	5	10	76.499
Dkk1	1625	Left	0.0619	0.0932	0.1423	2	4	1	0.1243	0.1123	0.0783	9	6	5	44.098
Dkk1	1629	Left	0.0851	0.1362	0.1244	2	14	3	0.0743	0.1262	0.0863	1	8	2	47.432
Dkk1	1630	Left	0.1407	0.1267	0.0818	7	4	4	0.0452	0.0865	0.0850	1	4	0	35.348
Dkk1	1641	Left	0.0859	0.1248	0.0958	2	2	3	0.1061	0.1042	0.0915	4	0	4	24.658
Dkk1	1642	Left	0.0829	0.1034	0.0636	3	0	0	0.0772	0.1004	0.0981	2	2	5	22.829
WT	1646	Left	0.0978	0.0928	0.1291	1	5	5	0.0780	0.0944	0.0848	5	5	3	41.605
WT	1647	Left	0.1299	0.0863	0.0545	26	2	0	0.1359	0.0976	0.0943	8	7	1	73.509
Wnt3	1649	Left	0.1067	0.1427	0.0919	0	3	0	0.1423	0.1030	0.0927	0	4	0	10.304
Wnt3	1650	Left	0.1483	0.1417	0.1001	0	0	3	0.0965	0.1355	0.1068	3	0	5	15.088
Wnt3	1651	Left	0.1490	0.1155	0.0261	5	1	0	0.1323	0.1311	0.1076	0	1	1	12.092
WT	1656	Left	0.0790	0.1045	0.1112	0	5	16	0.0721	0.1373	0.0890	0	5	15	69.118
WT	1657	Left	0.1896	0.1074	0.0615	36	5	5	0.1586	0.1106	0.1215	12	5	8	94.763
WT	1658	Left	0.1422	0.1109	0.0713	0	0	2	0.1135	0.0923	0.1052	0	2	6	15.741
WT	1659	Left	0.0579	0.1349	0.1100	1	0	8	0.0917	0.0993	0.0842	5	0	3	29.417
Wnt3	1660	Left	0.1561	0.1071	0.0837	0	3	0	0.1368	0.0944	0.0864	4	1	0	12.040
Wnt3	1661	Left	0.0597	0.0816	0.1165	1	2	8	0.0905	0.1243	0.0775	0	2	5	32.725
Dkk1	1542	Right	0.0837	0.0714	0.0731	0	10	0	0.1351	0.0777	0.0544	0	13	0	46.423
Wnt3	1566	Right	0.1140	0.1040	0.0907	0	1	0	0.1214	0.1047	0.0537	0	0	0	1.700
Wnt3	1568	Right	0.0613	0.1313	0.0910	0	0	5	0.1147	0.1373	0.0995	0	0	3	12.595
Dkk1	1605	Right	0.1195	0.1469	0.0811	7	0	0	0.1569	0.1085	0.0729	23	0	4	49.575
WT	1614	Right	0.0729	0.1103	0.0947	3	2	2	0.1244	0.1273	0.0679	2	5	9	38.501
Dkk1	1625	Right	0.0712	0.1216	0.1101	13	0	0	0.1471	0.0966	0.0554	30	0	0	71.428
Dkk1	1629	Right	0.0761	0.1239	0.1057	2	0	1	0.1387	0.1407	0.0671	2	0	10	23.003
Dkk1	1630	Right	0.0708	0.0757	0.0860	1	8	2	0.1382	0.1260	0.0422	4	14	5	63.081
Dkk1	1641	Right	0.1032	0.0993	0.0824	5	0	0	0.1191	0.1081	0.0706	24	0	0	49.761

Dkk1	1642	Right	0.0962	0.0868	0.0897	3	2	0	0.1084	0.1088	0.0752	0	0	3	14.158
WT	1646	Right	0.0806	0.1114	0.0955	0	0	0	0.1269	0.1197	0.0854	1	0	1	3.228
WT	1647	Right	0.1296	0.0928	0.1003	7	10	0	0.1355	0.1119	0.0800	25	8	1	78.456
Wnt3	1649	Right	0.0669	0.1292	0.0999	0	0	12	0.1181	0.1342	0.1095	0	0	19	47.129
Wnt3	1650	Right	0.0947	0.1398	0.0943	0	0	8	0.1597	0.1468	0.0852	1	0	12	29.148
Wnt3	1651	Right		0.1293	0.1221		0	0	0.1993	0.0615	0.0616	0	0	0	0.000
WT	1656	Right	0.0598	0.1349	0.0940	4	6	1	0.1501	0.1093	0.0653	19	8	3	66.843
WT	1657	Right	0.1400	0.0978	0.1085	3	0	1	0.1293	0.1417	0.0962	1	4	5	19.621
WT	1658	Right	0.0811	0.0992	0.0910	0	0	1	0.1501	0.1351	0.0698	0	6	0	11.177
WT	1659	Right	0.0921	0.0966	0.1191	0	0	0	0.1467	0.1141	0.0741	0	0	0	0.000
Wnt3	1660	Right	0.0867	0.0958	0.1043	1	1	0	0.1257	0.1042	0.0607	0	5	0	12.126
Wnt3	1661	Right	0.0562	0.1104	0.0887	1	11	3	0.1497	0.1121	0.0510	7	7	4	58.080

Number of Chondrocytes Expressing β-catenin: Indices of Wnt signaling activity measured by immunohistochemicalstaining of chondrocytes using β-catenin antibody normalized by cartilage area

Gene	Mouse #	Limb	Post Cart Area [	Mid Cart Area	Ant Cart Area	Post Chon N	Mid Chon N	Ant Chon N	Post Cart Area	Mid Cart Area	Ant Cart Area	Post Chon N	Mid Chon N	Ant Chon N	Overall Average (Medial + Lateral) ChonN/CA
Dkk1	1542	Left	0.0739	0.0858	0.0846	0	2	2	0.1150	0.1309	0.0784	0	0	0	7.034
Wnt3	1566	Left	0.1052	0.1152	0.1212	0	3	0	0.1133	0.0999	0.0987	1	7	1	18.362
Wnt3	1568	Left	0.1178	0.1241	0.1396	0	0	0	0.0962	0.0940	0.1013	0	1	0	1.486
Dkk1	1605	Left	0.0974	0.0964	0.1112	0	4	0	0.0790	0.0924	0.0871	1	6	0	19.519
WT	1614	Left	0.0728	0.0903	0.1130	1	0	0	0.0698	0.1050	0.1092	0	0	2	5.356
Dkk1	1625	Left	0.0741	0.0975	0.1225	0	1	3	0.1289	0.1138	0.0827	0	3	1	12.916
Dkk1	1629	Left	0.0846	0.0766	0.1276	0	3	0	0.0898	0.0938	0.0720	0	0	0	5.511
Dkk1	1630	Left	0.1127	0.1148	0.1005	0	0	0	0.0392	0.1006	0.0913	0	1	0	1.789
Dkk1	1641	Left	0.0795	0.1057	0.0979	0	0	0	0.0894	0.1001	0.0858	0	0	0	0.000
Dkk1	1642	Left	0.0925	0.1054	0.0752	0	0	0	0.0643	0.1177	0.0863	0	0	0	0.000
WT	1646	Left	0.0848	0.0955	0.1057	0	0	0	0.0800	0.0798	0.0870	0	7	0	13.136
WT	1647	Left	0.1197	0.0748	0.0497	0	0	0	0.0921	0.0966	0.0927	3	0	0	5.709
Wnt3	1649	Left	0.1062	0.1232	0.0948	0	0	0	0.0946	0.0873	0.0844	4	0	1	8.468
Wnt3	1650	Left	0.1351	0.1137	0.0449	0	0	0	0.0940	0.1317	0.0871	0	0	4	6.595
Wnt3	1651	Left	0.1590	0.1143	0.0417	0	0	0	0.0969	0.1217	0.1067	0	0	0	0.000
WT	1656	Left	0.0629	0.0810	0.0610	0	2	0	0.0658	0.1055	0.0869	0	6	7	32.387
WT	1657	Left	0.1494	0.1009	0.0655	2	1	0	0.1301	0.0987	0.1192	1	3	4	16.574
WT	1658	Left	0.1453	0.0940	0.1030	0	0	0	0.1314	0.1066	0.0834	0	0	2	3.014
WT	1659	Left	0.0122	0.1007	0.1202	0	2	0	0.0745	0.1259	0.0763	0	13	0	29.424
Wnt3	1660	Left	0.1421	0.1126	0.0354	0	0	0	0.1271	0.0882	0.0825	0	7	0	11.908
Wnt3	1661	Left	0.0361	0.0813	0.1042	0	0	0	0.0847	0.1328	0.0752	0	6	0	11.664
Dkk1	1542	Right	0.0639	0.1305	0.0754	1	0	0	0.1272	0.1278	0.0600	5	1	0	11.971
Wnt3	1566	Right	0.1169	0.1062	0.1251	0	0	0	0.1394	0.1209	0.0750	5	0	0	7.315
Wnt3	1568	Right	0.0766	0.1297	0.0985	2	0	0	0.1107	0.1197	0.1041	0	0	0	3.129
Dkk1	1605	Right	0.0880	0.1399	0.0752	0	1	0	0.1302	0.1453	0.0745	4	0	0	7.656
WT	1614	Right	0.0825	0.1159	0.0702	1	0	0	0.1198	0.1379	0.0497	7	0	0	13.891
Dkk1	1625	Right	0.0582	0.1083	0.1052	0	0	0	0.1540	0.1041	0.0433	9	0	0	15.704
Dkk1	1629	Right	0.0815	0.1171	0.1195	0	0	0	0.1297	0.1403	0.1530	0	0	0	0.000
Dkk1	1630	Right	0.0731	0.1163	0.0905	0	0	0	0.1546	0.0901	0.0493	0	0	0	0.000

Dkk1	1641	Right	0.0961	0.0886	0.0840	0	0	0	0.1174	0.0982	0.0622	0	0	0	0.000
Dkk1	1642	Right	0.1036	0.1109	0.0967	0	0	0	0.1141	0.1118	0.0786	0	0	0	0.000
WT	1646	Right	0.0955	0.0852	0.0873	0	0	0	0.1393	0.1334	0.1016	0	0	0	0.000
WT	1647	Right	0.0966	0.0874	0.0766	1	0	0	0.1256	0.1202	0.0943	0	0	0	1.665
Wnt3	1649	Right	0.0681	0.1161	0.0862	0	0	6	0.1209	0.1350	0.1091	0	0	0	9.443
Wnt3	1650	Right	0.0756	0.1056	0.0920	0	0	0	0.1620	0.1256	0.0652	0	0	0	0.000
Wnt3	1651	Right		0.0867	0.1025		0	0	0.1769	0.1313	0.0495	0	0	0	0.000
WT	1656	Right	0.0395	0.1128	0.0832	0	9	0	0.1281	0.0938	0.0456	1	0	0	19.884
WT	1657	Right	0.1029	0.0928	0.0950	0	0	0	0.1130	0.1367	0.1129	0	0	0	0.000
WT	1658	Right	0.0585	0.0884	0.0869	0	1	0	0.1277	0.1182	0.0721	0	0	0	1.812
WT	1659	Right	0.0867	0.1023	0.0934	0	2	1	0.1128	0.1045	0.0767	0	0	0	5.204
Wnt3	1660	Right	0.0683	0.1148	0.0935	0	5	0	0.1088	0.1178	0.0504	0	4	0	16.258
Wnt3	1661	Right	0.0307	0.1122	0.0796	0	0	0	0.1105	0.1187	0.0528	0	0	0	0.000